PROPERTIES

OF

DIATOMIC OPEN–SHELL

MOLECULES

BY THE

MOLECULAR–BEAM

ELECTRIC–RESONANCE

SPECTROSCOPY

w. l. meerts
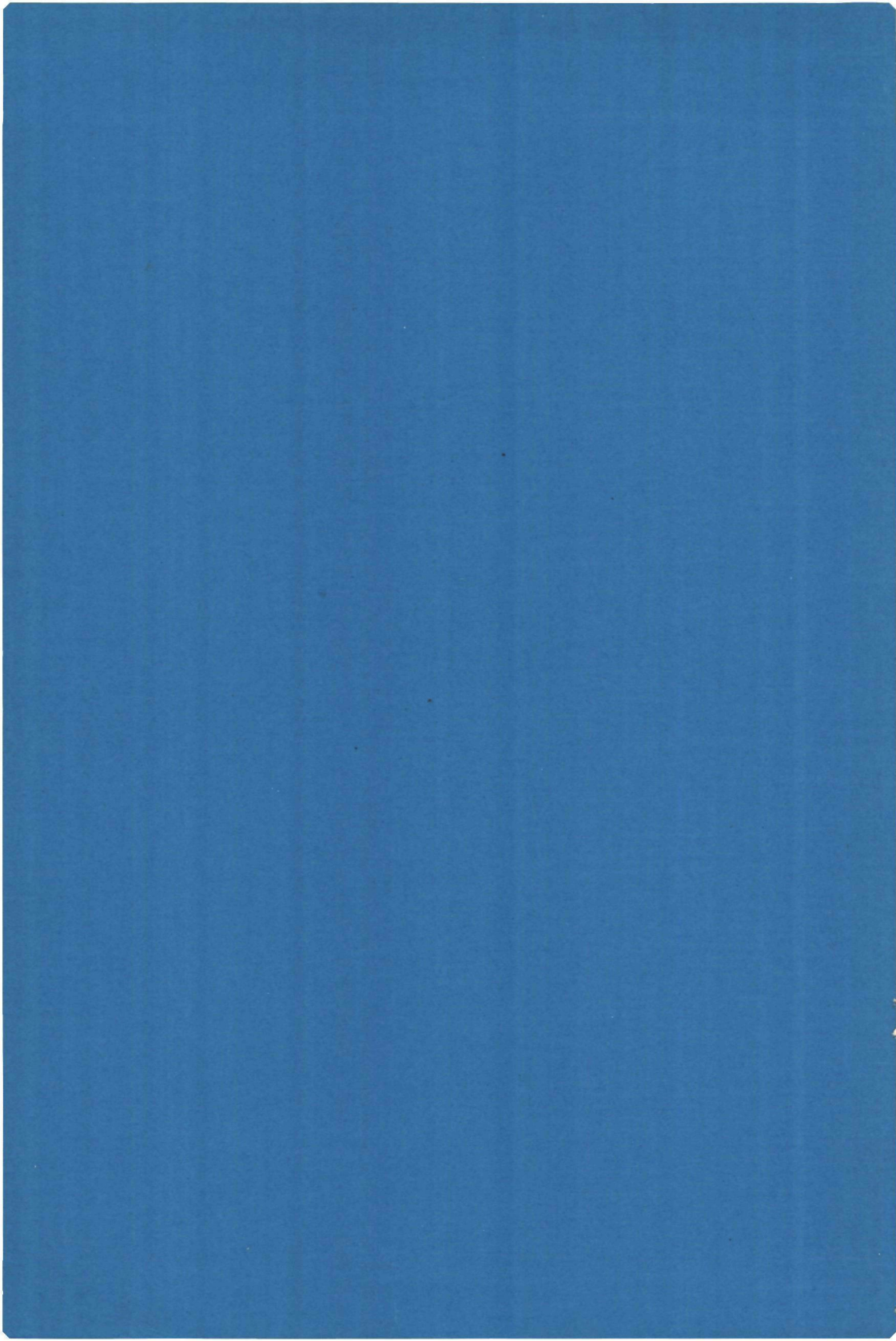
PROPERTIES OF DIATOMIC OPEN-SHELL MOLECULES

BY

THE MOLECULAR-BEAM ELECTRIC-RESONANCE

SPECTROSCOPY

PROPERTIES OF DIATOMIC OPEN-SHELL MOLECULES BY THE MOLECULAR-BEAM ELECTRIC-RESONANCE SPECTROSCOPY

DOOR
WILHELMUS LEONARDUS MEERTS
GEBOREN TE 'S GRAVENHAGE

1975

4

Voor mijn ouders
Voor Hanneke,
Frank en Jeroen

5

CONTENTS

1. Introduction.

The power of the molecular beam electric resonance
(MBER) spectroscopy in the investigation of structure and
properties of molecules is well established. It is a method
which has yielded the finest details about molecular hyperfine
structure, the most accurate values for molecular electric
dipole moments and rotational moments, and the most reliable
information about the internal interactions between nuclei and
electrons. The molecules investigated range from simple alkali
halides to polyatomic species bound by weak van der Waals forces
usually with a closed shell configuration ($^1\Sigma$) of the electronic
ground state. A review of the MBER investigations performed
until about 1973 is given by Zorn and English (ZOR 73).
The first investigation by MBER of molecules in a non-$^1\Sigma$ state
has been performed on the metastable state $a^3\Pi$ of carbon
monoxide (FRE 65, STE 70). Only one diatomic radical,[1] the
stable molecule NO, had been investigated before this study was
started (NEU 70). In 1972 Freund et al (FRE 72) measured the
spectrum of LiO produced by heating Li_2O in an iridium tube
source to 1800 ^oK. Both NO and LiO have a $^2\Pi$ ground electronic
state.

Free radicals possess all an open-shell configuration
of the electronic ground state, which implies an unpaired
electron spin or a net electron orbital angular momentum or
both. Consequently they are suitable for electron paramagnetic
resonance (EPR) investigations. A large number of EPR measure-
ments have been performed since about 1950. The most important
for the present investigation are the measurements on NO by
Beringer et al (BER 50, BER 54), on OH by Radford (RAD 61,
RAD 62), and on SH by Radford (RAD 63), Tanimoto and Uehara

---

1) In this work all diatomic molecules with a non-$^1\Sigma$ ground
   electronic state are called radicals.

(TAN 73) and Brown and Thistlethwaite (BRO 72). Investigations
by the EPR and/or microwave absorption spectroscopy has been
performed on gaseous diatomic radicals NS, NF, SF, SO, CF, FO,
ClO, BrO and IO. Very few measurements have been done on radi-
cals containing heavy atoms. A complet review about the investi-
gations of free radicals can be found in the monograph of
Carrington (CAR 74), and in the work of Winnewisser et al (WIN 72)
and of Carrington et al (CAR 70).

In the present investigation the MBER technique has
been used to investigate the spectra of the radicals ^{14}NO, ^{15}NO,
OH, OD, SH and SD. The work was undertaken to investigate the
feasibility of the MBER techniques for the investigation of
spectra of radicals. The production of strong enough beams of the
short lived OH and SH radicals turned out to be one of the main
experimental problems. A fruitless attempt was also undertaken
to produce beams of SF and CN radicals to perform a measurement
of their MBER spectra.

High resolution spectra of all the investigated mole-
cules were obtained from the present MBER study. These spectra
may be of help for the interpretation of observed spectra from
interstellar radio sources, and to increase the chance of detec-
ting the presence of those radicals in interstellar space. The
highly accurate measurements (0.1 - 5 kHz) of the position of
the energy levels in the molecules as obtained from the MBER
spectra provide a test of the theory describing the interactions
between nuclei and electrons in diatomic molecules with an open
shell configuration. It is known that the spectra of molecules in
a $^1\Sigma$ state can well be explained by the existing theories to
within the present experimental accurcy of the MBER technique
(70 - 100 Hz). However the theory of the spectra of molecules in
an open shell configuration was not so well developed. In all
experiments in the past low resolution spectra were obtained
and the theory of Van Vleck (VLE 29), improved by Mulliken
and Christy (MUL 31) and by Almy and Horsfall (ALM 37) was

10

capable of explaining the observed spectra. This theory in-
cludes only the fine structure and Λ-doubling effects. The
observations of hyperfine structure in the spectra of radicals
(BER 50) made it necessary to extend the theory. This was first
done systematically by Frosh and Foley (FRO 52) in a treatement
which includes only first order effects in both fine and hyper-
fine structure. This approximation is capable to explain most of
the low resolution EPR and microwave absorption measurements.
However also in the EPR and microwave absorption investigations
a need was felt to take into account higher order contributions
to the energy (DOU 55, CAR 68). For high resolution MBER obser-
vations of spectra of radicals a further refinement of the
theory was required. Freed (FRE 66) applied a degenerate pertu-
bation theory to the $^3\Pi$ state. The MBER measurements on CO
in the $a^3\Pi$ state were used as a test for the theory (STE 70,
GAM 71). A development of the theory of the spectrum of a
molecule in a $^2\Pi$ state based on the degenerate perturbation
theory is given in this thesis.

        The ground electronic state of the investigated mole-
cules NO, OH and SH is a $^2\Pi$ state. The $^2\Pi$ state is split by the
spin-orbit interaction to a doublet $^2\Pi_{1/2}$ and $^2\Pi_{3/2}$. This
splitting is about 130, 140 and 380 cm^{-1} for NO, OH and SH,
respectively. Each of these levels is doubly degenerate if
rotational effects are neglected.
The rotation of the molecule breaks the symmetry of the elec-
tronic charge distribution around the molecular axis, which
splits every rotational state both in the $^2\Pi_{1/2}$ level and in
the $^2\Pi_{3/2}$ level into a doublet, called Λ-splitting. The smallest
known Λ-splitting occurs in NO: 0.7 MHz in the J = 3/2, $^2\Pi_{3/2}$
state, and increases in all $^2\Pi$ molecules with increasing
rotational state, but for the lower rotational states investi-
gated in this work is usually below 10 GHz. The nuclear spin(s)
splits levels additionally into a number of sublevels (hyper-
fine Λ-splitting). The hyperfine Λ-splitting varies between
1 and about 100 MHz for NO, OH and SH, and can be obtained very
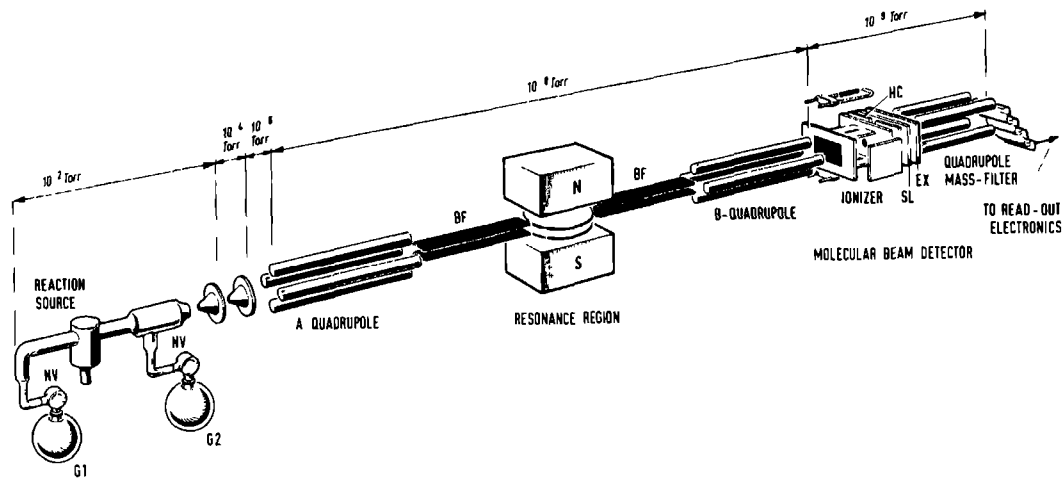
Fig. 1 Schematic diagram of the spectrometer (modification of the version of de Leeuw (LEE 71a)). (G 1) gas reservoir primary gas, (G 2) gas reservoir secondary gas, (NV) needle valve, (BF) buffer field, (HC) horizontal corrector, (SL) second lens, (EX) exit aperture.

accurately by the MBER techniques from transitions within one
rotational state (Δ J=0 transitions). The fine and hyperfine
structure properties of the molecules could be obtained from the
analysis of the observed hyperfine Λ-doubling spectra, and
are used as a test of the ab-initio calculations of the electro-
nic charge distribution in the molecule.

In the following sections a short description of the
MBER method is given followed by a description of the employed
sources which were used for the production of the radicals. The
thesis is a series of five papers covering the experimental
results of the investigated molecules. In the paper on NO also
a developement of the degenerate perturbation theory for $^2\Pi$
states is given.

2. The molecular beam electric resonance spectrometer.

2.1.1. General principles.

A general outline of a MBER spectrometer is shown in Fig.1.
The principal components are the source, two state selecting
A- and B- fields , a transition region (C-field), and a molecular
beam detector. The molecules in the beam, produced in the source,
are selected by the A-field in a desired quantum state.
The A-field acts as a polarizer. The beam enters the transi-
tion region (C-field) in which its state may be changed and the
beam then passes through the B-field quantum state selector
(analyzer) to the detector, whose output is proportionally to the
number of molecules reaching it. If a transition is induced in
the C-field from a state in which the molecules are transmitted
by the A- as well as the B-field to a quantum state in which
the molecules are rejected from the beam by the B-field, the
number of molecules reaching the detector decreases.

In contrast to the operation of an absorption spectrometer
or a beam maser spectrometer it is the flux of molecules, rather
than the intensity of radiation, which is measured.

13

The change in the flux of molecules does not depend on the frequency of the induced transitions. With the MBER method transitions in a very wide frequency range can be observed, from radio frequencies to, in principle, the sub - millimeter wave region. This is one of the powerful features of the MBER method, the other is its high resolving power. If the electric field strength of the inducing radio frequency or microwave field is perpendicular to the beam path, the line width is only determined by the transit time of the molecules through the transition region and is usually 3 to 10 kHz for a 20 cm long C-field.

The disadvantage of the MBER method is the requirement of state selection, and its lower sensitivity as compared with the EPR- and the absorption spectroscopy.

2.1.2. The molecular beam electric resonance machine.

The molecular beam electric resonance spectrometer used in the present experiments was essentially the same as used by de Leeuw (LEE 71a, LEE 73). Hence only the features relevant to the present investigations will be discussed.

The beam was detected by an electron bombardment ionizer designed by Stolte (STO 72) followed by a commercial electric quadrupole mass selector (EAI QUAD 250). The overall efficiency of the detection system was of the order 2×10^{-3}.

Two types of C-field were used in the present experiment: (1) a 20 cm long field for high precision Stark measurements at frequencies below about 2 GHz, and (2) a short (about 8 cm) transition field for measurements at frequencies above about 2 GHz. The long field consisted of two optically flat quartz plates coated with a thin gold layer (LEE 71a). The latter field was not suitable to induce transitions above 2 GHz. The requirement of high resolution and high DC-field homogeneity for Stark measurements were incompatible at high frequencies. The main difficulty was to provide a uniphase excitation over the entire C-field. First order Doppler effects, seen as a shift or

14

broadening of the spectral line, may arise if the microwave
field is not perpendicular to the direction of the molecular
velocity. To avoid some of these problems the smaller transi-
tion field constructed of two copper plates 8 x 4 cm^2 and
separated by 1 cm was used for transitions at frequencies to
about 9 GHz. The microwave field was excited by an open-ended
coaxial cable (SMA type) mounted close to the beam. Unfortu-
nately this structure did not operate in a single mode and the
lines were split. However, it was a great improvement compared
to the long C-field, because the microwave field was better
located between the copper plates. The transition frequencies
beyond 3 GHz could be measured with an accuracy of 5 kHz or less.
The accuracy below 3 GHz was much higher because the lines were
unsplit at these frequencies.

The sources that were used in this investigation are
described in Sect. 2.2.

2.1.3. State selection of molecules in a $^2\Pi$ state.

The state selecting is done with inhomogeneous electric
A- and B-fields, which are strong enough to produce significant
deflection of the molecular beam. The force acting on a polar
molecule in an inhomogeneous electric field is given by

$$(2.1) \qquad \vec{F} = -\ \text{grad}\ W = -\ \frac{\partial W}{\partial E}\ \text{grad}\ E$$

where E the electric field strength and W the Stark energy of
the molecule. The trajectory of a molecule in an inhomogeneous
field depends strongly on $\partial W/\partial E$ i.e. on the effective dipole
moment μ_{eff}. This moment is a strong function of the quantum
state of the molecule and of the electric field. If an elec-
tric quadrupole field is used the force on the molecules is
directed perpendicular to the axis of the molecular beam,
because the electric field has an axial symmetry and

(2.2)
$$\text{grad } E = C_o \frac{\vec{r}}{r}$$

with C_o a constant depending on the geometry of the selector
and $\vec{r}$ is the radius vector perpendicular to the beam axis.
Molecules in a quantum state with $\mu_{eff} > o$ (positive Stark
effect) are transmitted through the quadrupole field, while
molecules in a state with $\mu_{eff} < o$ (negative Stark effect) are
rejected from the beam.

Diatomic molecules in a $^2\Pi$ electronic ground state
have almost ideal properties for state selection with elec-
tric quadrupole fields. If the hyperfine structure is neglec-
ted the $^2\Pi_{1/2}$ and the $^2\Pi_{3/2}$ level each split into two closely
lying states with different symmetry. The upper Λ-doublet state
has a positive Stark effect while the lower state has a nega-
tive Stark effect. In the C-field the transitions from the
upper to the lower Λ-doublet within one rotational state
$(\Delta J = 0)$ are induced.

2.2. The source

2.2.1. General features.

Three types of beam sources have been used: (1) a simple
nozzle source for beams of stable NO molecules, (2) a high tem-
perature thermal dissociation source for the production of CN
under thermodynamical equilibrium conditions and (3) a gas reac-
tion source for the production of short lived radicals like
OH, SH, SF, etc.

The reaction source shown schematically in Fig. 3 was
mounted in the source chamber pumped by a 500 m^3/h mechanical
pump system and separated from the resonance part of the machine
by two buffer chambers: B1, pumped by a 2000 l/sec diffusion
pump, and B2 pumped by a 250 l/sec diffusion pump. The beam was
formed by a 2 mm diameter conical diaphragm between the source
chamber and the buffer chamber B1. The distance between this dia-
phragm and the end of the reaction tube could be varied during

the experiment, and was usually 5 to 20 mm. Between B1 and B2
a 4 mm diameter conical diaphragm was placed.

The nozzle or the high temperature source were mounted
in the first buffer chamber B1, which served then as a source
chamber. The beam was then formed by a 0.7 - 1 mm diameter
skimmer between B1 and B2.

2.2.2. The nozzle source.

The nozzle source was a simple gas container with a
hole (nozzle) through which the gas was expanding into the
source chamber. The temperature of the source could be regu-
lated between 80 and 300 ^{0}K. The choice of the nozzle dia-
meter was determined by the electronic level in which the ob-
served transitions originate. For NO the $^2\Pi_{3/2}$ level lies about
123 cm^{-1} above the $^2\Pi_{1/2}$ level. In a nozzle source the gas is
isentropically expanding and the energy of the internal degrees
of freedom of the molecules is converted to the lowest energy
levels. Consequently the $^2\Pi_{1/2}$ level is populated at the expense
of the $^2\Pi_{3/2}$ level. Two different source diameters have been
used: 0.5 mm for transitions originating in the $^2\Pi_{3/2}$ level and
0.1 mm for transitions in the $^2\Pi_{1/2}$ level. The intensities of
two transitions, one in the $^2\Pi_{1/2}$ and one in the $^2\Pi_{3/2}$ level,
were observed with both nozzles in order to determine the op-
timum conditions for observation of a transition originating in
the $^2\Pi_{1/2}$ or in the $^2\Pi_{3/2}$ level. The measurements were per-
formed at room temperature. It was found that for both nozzles
the intensity of the transition in the $^2\Pi_{1/2}$ level increased
when the nozzle pressure was increased up to a maximum pressure
determined by the pumping capacity. At this pressure the line
intensity with the 0.1 mm nozzle was about 3 times higher than
with the 0.5 mm nozzle. The maximum intensity of the transitions
in the $^2\Pi_{3/2}$ level obtained with the 0.5 mm nozzle was a factor
2.5 higher than with the 0.1 mm nozzle. These results are in
agreement with the expectations. By cooling the source to about
130 ^{0}K the intensities of the transitions of the $^2\Pi_{1/2}$ level

17

again increased by about a factor of 3. For measurements of the transitions in the $^2\Pi_{3/2}$ level the 0.5 mm nozzle was used yielding signal to noise ratio of at least 5 at RC = 1s.
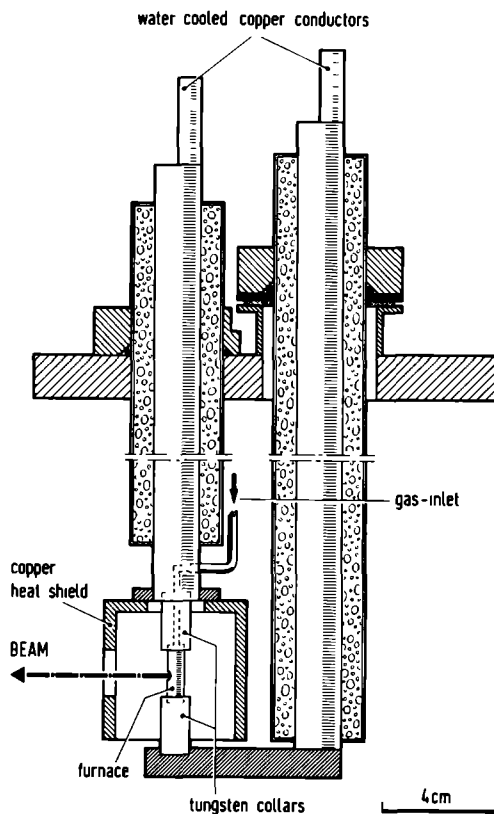
Fig. 2 High temperature dissociation source

2.2.3. The high temperature dissociation source.

The high temperature source was simular to the one used by Hendrie (HEN 54) for thermal dissociation of the N_2 gas. The source shown in Fig. 2 was essentially an effusive source consisting of a tantalum or tungsten tube with a small hole (dia-

meter 0.3 - 0.8 mm) in the middle. The wall thickness was of the order of 0.4 to 0.6 mm, the outer diameter of the tube 5 mm and its length 20 mm. The tube fitted tightly into two tantalum collars 10 mm in diameter and 20 mm long. These collars were connected to two water cooled current leads. The construction was kept as simple as possible and no radiation shields were mounted. The tube was directly heated by an alternating current of 500-800 A. The heat radiation from the furnace (about 2 kW) was collected on a 5 mm thick cylindrical copper shield, mounted on one of the water cooled current leads.

The source tubes were made of solid material, the tantalum tubes by simply drilling, the tungsten tubes by the spark erosion techniques.

The highest temperature that could be reached with these tubes was 2800 ^{O}K and 3400 ^{O}K for a tantalum and tungsten tube; respectively. The latter tubes turned out to be much less elastic at these high temperature, and often broke spontaneously probably due to internal stresses. The tantalum tubes were much more reliable.

2.2.4. The reaction source.

For the formation of a beam of short living radicals a reaction source was used shown in Fig. 3, which is a modification of the design used in EPR experiments (CAR 67). The source consisted of a quartz tube of 10 mm inner diameter from which the gas could freely flow into the source chamber.

In the present experiment usually atoms reacted with a secondary gas. The highly reactive atoms like H- or F-atoms or atoms in a metastable state like for example Ar*, were obtained from an electrode-less (microwave) discharge in a primary gas (H_2O, CF_4, Ar) flowing through a circular cavity. The cavity was the type 5 cavity described by Fehsenfeld et al (FEH 65) resonating at 2.45 GHz. The microwave power was obtained from an Electro Medical Supplies microwave powergenerator

19

REACTION SOURCE MBER

beam chopper

secundary
reaction gas

source chamber

1st buffer
chamber

primary gas

A - field

2nd buffer chamber

microwave
discharge cavity

5×10^{-2} Torr

$< 10^{-4}$ Torr

$< 2 \times 10^{-6}$ Torr

20 cm

ROOTS PUMP
500 m³/h

DIFFUSION PUMP
2000 l/s

DIFFUSION PUMP
250 l/s
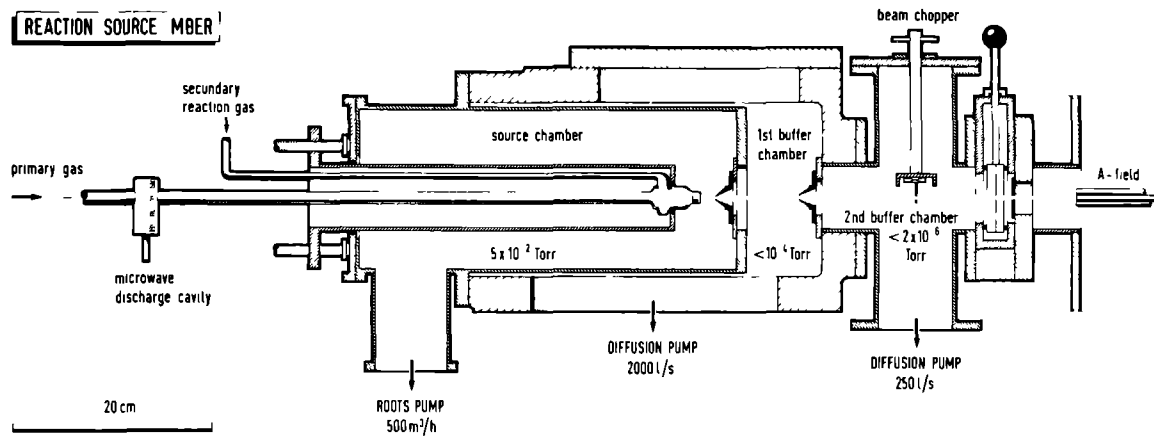
Fig. 3

Mk.2., regulated from 10 to 200 W. At about 10 mm from the end
of the quartz tube a secondary gas (NO_2, H_2S, OCS) entered the
tube through a concentric ring of small holes, and reacted with
the discharge products.

No attempt was made to measure accurately either the gas
pressure or the flow rate. Such measurements were very difficult
because only manometers of the McLeod type are applicable for an
accurate absolute pressure measurement in the range 0.5 to 3 Torr.
These manometers cannot be used for condensable gases, like water.
The primary as well as the secondary gas flow was controlled by
two needle valves and the normal procedure was to optimize the
flow rates for the maximum MBER signal. The setting of the gas
flows was a gamble when no transitions could be observed. The
pressure in the source chamber was monitored with a thermotron
gauge. A rough value for the flow rates could be obtained by weig-
hing the gas cylinder before and after running the source for a
certain time, usually a few days. However, this method was only
applicable to small cylinders, because an accurate weighing
(0.5 g.) could only be performed for cylinders below 3 kg.

No special treatement of the internal wall of the quartz
system was necessary. However, it has proved advantageous to wash
the system every two or three weeks of operation with a 20%
hydrogen fluoride solution in water. This was a standard procedure
in the experiments. The frequency of this cleaning is determined
by the gases that are used. Especially when carbon compounds
were used a more frequent cleaning was necessary.

3. Production of radicals in the gas phase.

3.1. Introduction

The primary goal of the production of free radicals was
obtaining strong beams for MBER measurements, and the signal to
noise ratio of the observed transitions was all that mattered.
However, in order to get some information about the number of
radicals formed in the reactions, an attempt was made to measure

the absolute concentrations. This is important for prospects of
of MBER investigations on other not yet investigated radicals
and of possible application of other molecular beam techniques
(for example, the beam-maser technique) to the radicals inves-
tigated in this thesis. For the measurements the reaction source
described in the previous section and the detector of the MBER
machine was employed. Only in one experiment the high tempera-
ture source was used (Sect.3.6.3). The beam was modulated by a
mechanical beam chopper at about 30 Hz, and phase sensitive de-
tection was applied to facilitate the determination of the com-
position of the beam. However, the detector was an electron
bombardement ionizer and it was rather hard to determine the
absolute number of molecules in the beam from the observed in-
tensities of the ion fragments. The relative composition could
be obtained from the intensities of MBER transitions of the
radicals, but the unknown ionization efficiencies for the various
molecular species were still involved.

        The determination of the intensity of a beam composed
of a single gas was rather easy. The detector could in this
case be calibrated by admitting a calibrating gas into the de-
tector chamber. Nitrogen gas has been used as a calibrant, and
it was found that the sensitivity of the detector was about
$3(3) \times 10^{-2}$ A/Torr. Calculations (MEE 74) showed that this number
was reliable to within a factor of 2 to 4.

        In the following by "the number of molecules or radicals"
is meant the number of molecules flowing through the reaction tube.
Only a small part of these molecules reach the detector: about
2 out of 10^8 molecules, the rest is pumped by the pumps of the
source chamber and of the two buffer chambers. The flow rates
of the primary and secondary gases could be obtained by a com-
parison with the calibrating gas (N_2) in combination with weig-
hing.

3.2. Dissociation of a single gas.

        The absolute number of molecules flowing through the dis-

22

charge tube could easily be obtained. The discharge products in a homonuclear diatomic gas like H_2, O_2 and N_2 were determined from the decrease of the relative intensity of the detected ion peaks at m/e = 2, 32, and 28, respectively. It was found that at a discharge power of 150 W the degree of dissociations for H_2, O_2, and N_2 was roughly constant over a large region of pressures (0.01 to 3 Torr). The degree of dissociation (ω) is defined as the relative decrease of the number of ions when the discharge is turned on, detected at the maximum possible value of m/e for the investigated molecule (for H_2, O_2 and N_2 this value is 2, 32 and 28, respectively). For N_2 the degree of dissociation was rather sensitive to the position of the microwave discharge cavity. The discharge region had to be about 2 cm from the end of the tube. For all the other investigated gases the degree of dissociation was not very sensitive to this distance, and for an easy handling of the discharge cavity this distance was taken 30 to 40 cm. The optimum results for a discharge in H_2, O_2 and N_2 were α= 16%, 13% and 3%, respectively. These molecules dissociated into their atoms and the number of atoms with the discharge on was 2α times the number of molecules with the discharge off.

For polyatomic molecules, like for example H_2O and CF_4, the composition of the fragments in the beam after the discharge was more complex due to possible recombinations in the tube. The composition of the discharge fragments of water will be discussed in the next section. The observed degree of dissociation in H_2O and CF_4 was 85% and 80%, respectively.

3.3.1. Production of the OH radical.

The OH radicals can be produced in a number of different reactions. Dousmanis et al (DOU 55) and Radford (RAD 61) obtained them simply in a high frequency discharge in water. The most efficient production is a reaction of atomic hydrogen with NO_2:

(3.1) $$H + NO_2 \rightarrow OH + NO$$

This reaction has been investigated by Del Greco and Kaufman (DEL 62). For investigations on OH in excited vibrational states a better reaction is a reaction of atomic hydrogen with ozon (MCK 55, LEE 71b, LEE 74, CLO 71), or of atomic hydrogen with F_2O (CHU 70). The present investigation was only performed in the ground vibrational state of OH and because of the rather simple experimental requirements the reaction (3.1) was prefered. The pressures and flows of H_2O and NO_2 were optimized on one of the known hyperfine Λ-doubling transitions of OH.

The hydrogen atoms were obtained from a microwave discharge either in H_2 or in H_2O. At the optimum conditions for the OH production the flow of H_2 molecules through the reaction tube was 15×10^{18} mol/s, which gave 5×10^{18} at/s of H-atoms in the discharge (Sect. 3.2). The discharge in water produced a higher OH yield and the number of H-atoms formed in the discharge of water under optimum conditions was 6×10^{18} at/s. The water dissociated in the discharge mainly into atomic hydrogen and molecular oxygen:

(3.2) $$H_2O \rightarrow 2\ H + \tfrac{1}{2}\ O_2$$

The H-atoms partly recombine to H_2. From the observed peak intensities in the beam at different masses and from absolute measurements with pure H_2 and O_2 gases it was found that the composition of the gas mixture after the discharge in water was (original water flow 17×10^{18} mol/s)

$$1 \times 10^{18} \text{ mol/s } H_2O$$
$$8 \times 10^{18} \text{ mol/s } O_2$$
$$6 \times 10^{18} \text{ at/s } H$$
$$13 \times 10^{18} \text{ mol/s } H_2$$

To obtain the number of NO molecules formed in the reaction of atomic hydrogen with NO_2 the intensity of one of the hyperfine Λ-doubling transitions of NO was measured and compared with the intensity of the same transition as obtained from a beam of pure

NO gas. From the known absolute flow rate of the pure NO beam and the measured intensity ratio the number of NO molecules produced in the reaction (3.1) of 6×10^{18} mol/s was obtained. It was concluded from the decrease in peak intensity at m/e= 46 (NO_2^+ ion) when the water discharge was turned on, that about 80% of the NO_2 has been consumed in the reaction.

The NO molecule is a stable radical, while the OH radical is unstable and recombines very rapidly. If we assume that the number of OH radicals produced in the reaction (3.1) was the same as the number of the produced NO molecules (6×10^{18} mol/s) and that the linear flow velocity of the gas in the tube is of the order of 20 m/s, then the density of OH radicals was 4×10^{15} mol/cm^3.

The decay of the OH radicals has been investigated by ter Meulen (MEU 70). He found that the most rapid recombination reaction is

(3.3) $$2 \; OH \rightarrow H_2O + \tfrac{1}{2} \; O_2$$

and that after about 0.5 ms (the time needed for the OH radicals to reach the end of the quartz tube, about 1 cm from the reaction zone) the number of OH radicals was decreased by a factor of 2. From these results and an investigation of the observed mass spectrum of the beam we conclude that the composition of the various gases in the reaction tube is:

3×10^{18} mol/s OH

6×10^{18} mol/s NO

2×10^{18} mol/s NO_2

3×10^{18} mol/s H_2O of which about 65% originates in the re-combination of the OH radi-cals

9×10^{18} mol/s O_2 of which about 10% comes from the recombination

25

$$13 \times 10^{18} \text{ mol/s } H_2$$

All these values were obtained under optimum conditions for the formation of the OH radical. The estimated number of OH radicals is between 2 and 4×10^{18} mol/s through the quartz tube at a total gas flow of 36×10^{18} mol/s, so a concentration of 5 to 10%. The uncertainty stems from the approximations and estimations accepted in the calculations.

3.3.2. Production of the OD radical.

The production of the OD radical is very similar to that of the OH radical. From Eq. (3.1) it is clear that a replacement of the hydrogen atoms by deuterium atoms will result in a formation of OD radicals. The deuterium atoms were obtained from a microwave discharge in heavy water, D_2O. From an intensity comparison with the results for OH it was found that the OD production was as efficient as of OH. This is, of course, not unexpected.

3.4.1. Production of the SH radical.

The $A^2\Sigma \leftarrow X^2\Pi$ band spectra of SH and SD have been measured by Ramsay (RAM 52). The radicals were produced by flash photolysis of H_2S and D_2S.

The most efficient reaction for the production of SH radicals was proposed by McDonald (MCD 63):

$$(3.4) \qquad H + H_2S \rightarrow SH + H_2$$

Carrington and Levy (CAR 67) investigated by EPR spectroscopy the production of SH radicals in a reaction of atomic nitrogen with H_2S:

$$(3.5) \qquad N + H_2S \rightarrow SH + NS$$

The measured spectra were identified as originating from the radicals NS and SH.

26

The higher efficiency of the reaction (3.4) over the reaction (3.5) is probably due to the fact that much more H-atoms than N-atoms are available in the primary gas, because of the higher degree of dissociation of H_2 as compared to N_2 (see also Sect. 3.2.).

The atomic hydrogen was obtained from a microwave discharge in water as in the case of the OH production. As secondary gas H_2S was used. A replacement of H_2O by D_2O as primary gas had hardly any effect on the yield of the SH radicals, as could unambiguously be concluded from an intensity measurement of one of the hyperfine Λ-doubling transitions of SH. This is explained by the assumption that the highly reactive H-atom (D-atom) strips off one H-atom from the H_2S molecule. The reaction between atomic deuterium and H_2S is:

(3.6) $$D + H_2S \rightarrow SH + HD$$

Also very weak MBER spectra of SD were observed but this SD is probably formed in a secondary reaction in which the hydrogen atom in SH is replaced by a deuterium atom:

(3.7) $$SH + D \rightarrow SD + H$$

A determination of the number of SH radicals produced in the present experiment was even more difficult than for OH (Sect.3.3.1.), because it was found that only a very small fraction of the H_2S molecules has been consumed in the reaction (3.5). Only the relative number of SH and OH radicals could be obtained. From an investigation of the beam and line intensities at optimum conditions for the formation of the radicals, it was found that about 8 times more OH radicals than SH radicals were detected. In order to obtain the absolute number of SH radicals this has to be corrected for the difference in the ionization efficiencies of the detector for OH and SH. Unfortunately, the ionization efficiencies for these radicals are not known. If the efficiencies are assumed to be equal the calculated flow of SH radicals through the reaction tube is between 2 and 5×10^{17} mol/s. The total flow of the water molecules at optimum condi-

tions for the SH production was the same as for the formation of OH, and the measured flow of H_2S was 34×10^{18} mol/s. From these results it follows that the composition of the gas mixture in the tube was:

$$0.2 \text{ to } 0.5 \times 10^{18} \text{ mol/s SH}$$

$$1 \quad \times 10^{18} \text{ mol/s } H_2O$$

$$8 \quad \times 10^{18} \text{ mol/s } O_2$$

$$12 \quad \times 10^{18} \text{ mol/s } H_2$$

$$31 \quad \times 10^{18} \text{ mol/s } H_2S$$

and $\qquad\qquad 3 \quad \times 10^{18}$ at /s S (see below).

The total gas flow was about 60×10^{18} mol/s, so a SH concentration of 0.4 to 1.0%.

Practically no H-atoms were detected in the beam, which implies that all the H-atoms formed in the discharge (6×10^{18} mol/s) have been consumed in the reaction with H_2S. However the number of observed SH radicals was an order of magnitude smaller than the number of OH radicals under optimum conditions which indicates a very fast recombination of the SH radicals, at least in the present source. A possible recombination by

$$(3.8) \qquad\qquad 2 \text{ SH} \rightarrow H_2S + S$$

was confirmed by a rather strong deposit of solid sulphur, which was found everywhere in the source chamber.

3.4.2. Production of the SD radical.

The SD radical was obtained in the reaction (3.4) by replacing H_2S by D_2S. To obtain a higher yield of SD the hydrogen atoms should also be replaced by deuterium atoms. For the D_2S a 98% enriched sample was used. As this sample had to be recovered it was desirable to replace H_2O by D_2O to reduce contamination of D_2S by H_2S. During the measurements the D_2S and D_2O gases were trapped in a liquid nitrogen trap. The D_2S was separated from the D_2O by repeated destillation between two cold traps. At every run about 10% of the used D_2S was lost, mainly due to the

28

recombination of the SD to D_2S and sulphur probably by (3.8).

3.5. Production of the SF radical.

In order to get an impression of the possibilities for a production of other types of radicals of the group SF, CF, NS, FO, ClO, BrO and IO an attempt was made to produce SF and to measure its MBER spectrum. It was known from EPR (CAR 69) and microwave absorption (AMA 73) measurements on SF, that the best results could be expected from a reaction of atomic fluorine with OCS. This is a rather complex reaction and a mass spectrometric investigation confirmed that not only SF is formed. The fluorine atoms were obtained from a microwave discharge in CF_4, which was found to be the best source of atomic fluorine. As secondary gas OCS was used. The flow rates of the CF_4 gas and the OCS gas were optimized for a maximum detected ion intensity at m/e = 51 (SF^+). The flow rate of the CF_4 gas obtained by weighing of the gas cylinder was 1.2×10^{18} mol/s through the tube. The gas flow of the OCS was approximately the same. To give an impression of the complexibility of the observed mass spectrum a spectrum is shown in Fig.4 for the flow rates of 1.2×10^{18} mol/s for CF_4 and OCS. The following observations were made.

The ion intensity at m/e = 51 was almost independent of the microwave power for an input power over 100 W. In the experiment a quartz tube was used, also in the discharge region. This gave rise to a large concentration of probably SiF_4, which explains the ion peaks associated with Si-atoms, especially the SiF_3^+ peak was quite intense. The quartz tube was strongly etched by the F-atoms so that after about 8 hours a hole was burned in the tube at the discharge region. When the quartz tube in the discharge region was replaced by an about 20 cm long Al_2O_3 tube, the SiF_3^+ ion peak was reduced by a factor of 20. The residual SiF_3^+ peak comes from the reaction of F-atoms with the rest of the reaction source, which was made of quartz.

An attempt was made to estimate the number of produced

SF radicals. Only on basis of the mass spectrum this was prac
tically impossible in view of large number of molecules that
were formed. In principle some information about the origin of
ion peaks may be obtained from the focusing behaviour of the
peaks when the electric field is applied to the quadrupoles. Un-
fortunately the effects of the applied field were either very
small or ambiguous. The only significant result was that the
ion peaks m/e = 70 (SF_2^+) and m/e = 51 (SF^+) were strongly rela-
ted. An upper limit for the number of produced SF radicals
could be obtained by assuming that all the detected signal at
m/e = 51 originated the SF radical and by comparing this inten-
sity with the intensity of the detected beam. In addition the
(unknown) ionization efficiencies of SH and SF had to be assumed
to be equal. The total number of SF radicals through the quartz
tube was calculated to be 6 x 10^{16} mol/s. Of course this is an
upper limit and it is possible that the actual number is much
smaller.
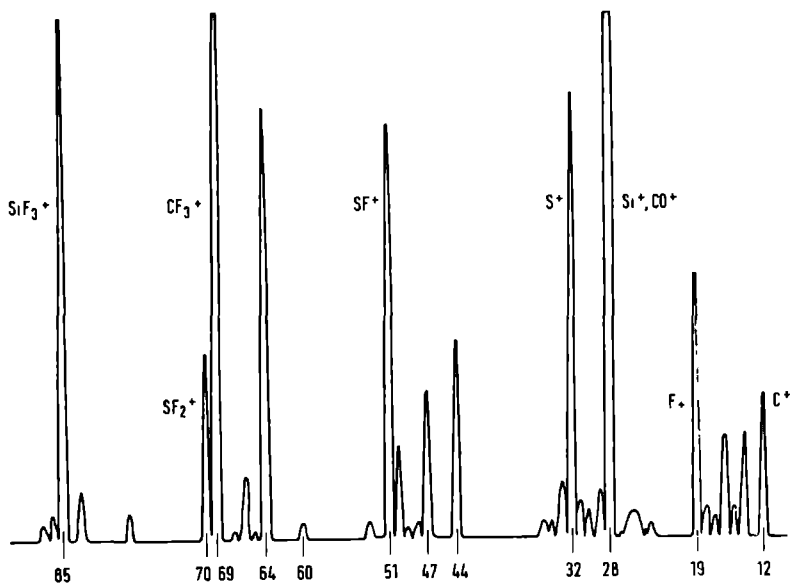
Fig. 4 Mass spectrum of the molecular fragments in the beam
of the reaction between atomic fluorine and OCS.

30

Summarizing it can be concluded that the number of SF radicals formed in the reaction between atomic fluorine and OCS is almost an order of magnitude below the number of produced SH radicals. An explanation has to be sought in a lower efficiency of the production of SF from the reaction of atomic fluorine with OCS due to formation of many molecular fragments and in a larger number of secondary reactions between the SF radicals mutually and between SF and the other reaction fragments.
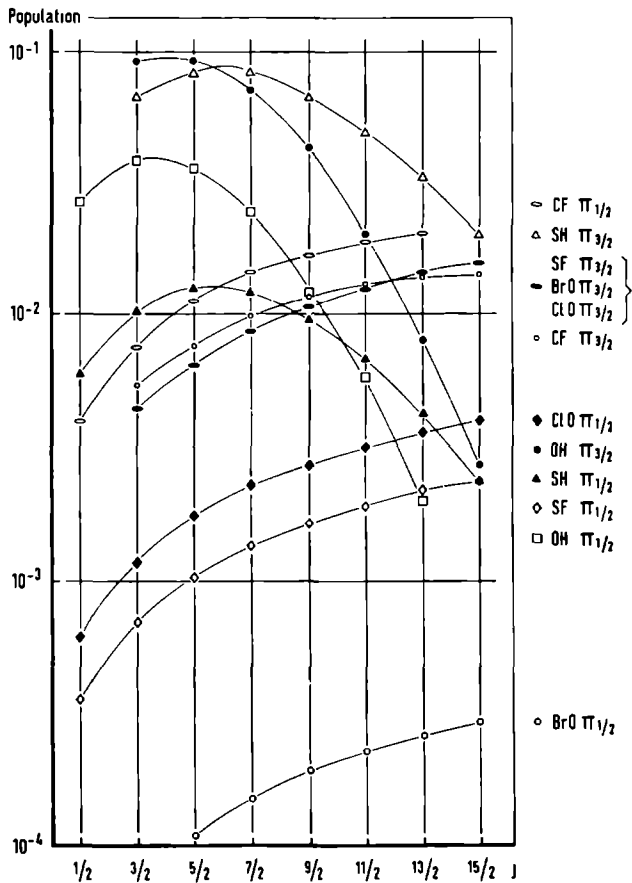
Fig. 5 Population of the lower rotational states of the $\Pi_{1/2}$ and $\Pi_{3/2}$ levels of OH, SH, CF, SF, ClO and BrO at T = 300 $^\circ$K.

Which of these processes plays the most important role, could
not be determined from the present experiments.

We calculated the expected maximum signal to noise ratio
of about 3 at RC = 1 s for a transition of SF originating in the
J = 13/2 state of the $^2\Pi_{3/2}$ level using the estimated number of
produced SF radicals, the known intensity of transitions of SH
and the rotational population as obtained from fig. 5.
Using the available data for the spin-orbit coupling constant
and the rotational constant of SF a rough estimate of the $\Delta F = 0$
transistion frequencies of the J = 13/2, $^2\Pi_{3/2}$ state of SF is
about 1300 kHz. A search with the MBER spectrometer in this region
indicated the presence of a transition, but the signal to noise
was smaller than unity at a RC = 1 s. By applying averaging
techniques an MBER measurement of the $\Delta F = 0$ transitions looks
feasible because only a small frequency region has to be searched.
But to resolve the total spectrum a large number of $\Delta F = \pm 1$
transitions ought to be investigated. As the hyperfine structure
constants of SF are not well known a search over a large fre-
quency region is necessary, which is pratically impossible at
signal to noise ratios of the order of unity. The possibilities
of observation of transitions originating in the $^2\Pi_{1/2}$ level are
even much less favourable as can be seen from Fig. 5 and the in-
vestigation was postponed until a way of more efficient detec-
tion and/or production of SF is found.

3.6. Production of the CN radical.

3.6.1. Introduction.

At the start of the present investigation only little
information about the ground electronic state of CN was known.
Due to its composition of carbon and nitrogen it was expected
that the CN radical would be present in interstellar space. So
a knowledge of accurate transition frequencies and spectrum was
desirable. The CN radical is also interesting from theoretical
point of view, because its ground electronic state is a $^2\Sigma$ state

with an unpaired spin angular momentum. All the radicals discussed so far have a $^2\Pi$ electronic ground state.

Evenson _et el_ (EVE 64) investigated the CN radical by microwave/optical double resonance. The CN radical was formed in the reaction of the discharge product of molecular nitrogen with CH_2Cl_2 and other organic compounds. The CN radical was produced in its excited metastable $A^2\Pi$ state. The v = 10 vibrational level of this state lies very close to the v = 0 level of the next excited electronic state, the $B^2\Sigma^+$ state. The fluorescence which accompanies the reaction of active nitrogen with CH_2Cl_2 is due to emission from the $B^2\Sigma^+$ state to the $X^2\Sigma^+$ ground state. Evenson _et al_ showed that the fluorescence intensity was changed when microwave transitions between the $A^2\Pi$ and $B^2\Sigma^+$ states were induced. Recently Meakin and Harris (MEA 72) and Cook and Levy (COO 73) reinvestigated the CN radical by employing a somewhat refined technique and obtained more accurate information about the fine and hyperfine structure of the $A^2\Pi$ and $B^2\Sigma^+$ states.

However, for the ground electronic state only the rotational constant, the electric dipole moment (THO 68) and some rather inaccurate information on the hyperfine structure obtained from EPR spectroscopy in inert matrices (EAS 70) was known. The aim of the present study was the production of a molecular beam of CN radicals for a MBER investigation. Three production methods have been tried:

(1) a reaction method similar to the one used by Evenson _et al_, (2) dissociation in a microwave discharge of a gas containing the CN group, and (3) a high temperature dissociation reaction under thermodynamic equilibrium conditions. Unfortunately all three methods failed to produce a beam of CN radicals sufficiently strong for a MBER experiment. Recently Penzias _et al_ (PEN 74) determined the hyperfine structure of the CN radical from an astronomical observation. The N = 1 to 0 rotational emission line was observed in the Orion nebula and the rotational constant, the hyperfine structure as well as the ρ-doubling were determined.

3.6.2. Reaction between atomic N and organic compounds.

The CN radical was produced by Evenson et al (EVE 64) in a diffuse flame reaction between active nitrogen and methylene chloride. In the present study an attempt was made to produce the CN radical in the reaction-type source (section 2.2.4.). The active nitrogen was obtained from a microwave discharge in N_2. As secondary gas CH_2Cl_2 and CCl_4 was used. From a mass spectrometric investigation of the reaction products it was found that a large number of different fragments were formed. The most abundant ones containing a CN group could be identified as ClCN and C_2N_2. It was barely possible to determine the number of CN radicals from the observed mass spectrum. This was due to the fact that all the molecules in the beam containing a CN group contribute to the signal at m/e = 26. Moreover the signal to noise ratio of the total intensity at m/e = 26 peak (CN^+) was about 20 at RC = 1 s, and this was much to low for a MBER study even if all the detected ions at m/e = 26 originated from the CN radical.

The very low concentration of CN radicals (estimated to be smaller than 3×10^{16} mol/s flowing through the reaction tube) was probably caused by the low concentration of the N-atoms which is a consequence of the low degree of dissociation of N_2 and the complex nature of the reaction between the N-atoms and, for example, CH_2Cl_2. The direct formation of CN is rather unlikely in this type of reaction which produces a variety of molecular fragments. In addition the CN is expected to be very unstable.

3.6.3. Dissociation of molecules containing a CN group.

In the first experiment an attempt was made to produce CN by dissociation in a microwave discharge of C_2N_2 gas flowing through the reaction tube. Immediately after the start of the discharge a black deposit on the inside of the tube in the discharge region was seen, even at low discharge power (30 W).

The detected beam intensity at m/e = 26 and 52 decreased very strongly. When the discharge power was increased to 50 W no beam was detected at all, all the C_2N_2 probably polimerizing to a solid $(CN)_n$, coating the wall of the tube. At a discharge power of 20 W some signal was dected at m/e = 26, which could be refocused by applying voltages on the quadrupole field rods. From this it was concluded that some CN radicals were formed, but the signal to noise ratio of the total beam at m/e = 26 was still far too low (50 at RC = 1 s) for a MBER study. Moreover the tube broke spontaneously after about 30 minutes of operation probably because it was etched by the $(CN)_n$ deposit in the discharge region.

        The second attempt was performed using a reaction of excited metastable Ar^{*} with C_2N_2. The Ar^{*} was obtained from a microwave discharge in a primary gas flow of Ar. No or hardly any CN radicals were found in the beam. It was also tried to replace the Ar^{*} by H-atoms obtained from a microwave discharge in water but without any success.

3.6.4. Thermal dissociation of C_2N_2.

        In this experiment the high temperature source described in Sect. 2.2.3. was used. A gas or a gas mixture was heated up to about 3000 ^{o}K and it was hoped that by an equilibrium reaction at this temperature C_2N_2 would dissociate into CN. At the low flow rates of the gas(es) the gas mixture inside the furnace could be considered to be in thermodynamic equilibrium. From a mass spectrometric investigation it was found that the C_2N_2 was removed from the beam at a temperature of the furnace above 1200 ^{o}K and that the beam only consisted of N_2 gas. This observation can be understood from the following equilibrium reactions

(3.9) $C_2N_2 \rightleftharpoons 2\ CN$

(3.10) $C_2N_2 \rightleftharpoons 2\ C(g) + N_2$

(3.11) $\frac{1}{2}N_2 + C(g) \rightleftharpoons CN$
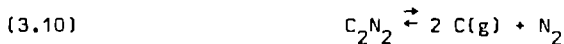
The reactions (3.9) and (3.11) can be combined to one reaction

(3.12) $$C_2N_2 \rightleftarrows 2\ CN \rightleftarrows 2\ C(g) + N_2$$

which is equivalent to (3.10).

Which one of these equilibrium reactions plays the dominant role is determined by the equilibrium constants K of each reaction. However in this particular case there was another complication: all the components in the three reactions are permanent gases, except carbon, which is a solid with a rather low vapor pressure (10^{-2} Torr at 3000 $^\circ$K). This implies that the partial pressure of the carbon component is always determined by the vapor pressure at that temperature. The consequence is, that when the C_2N_2 starts to dissociate by the reaction (3.10) at a temperature below 3000 $^\circ$K the carbon gas which is formed, condenses almost completely, and is removed from the equilibrium. This results in a complete dissociation of C_2N_2 into carbon and N_2. The carbon component has a partial pressure which was too low to detect and only N_2 was found in the beam at temperatures between 1200 and 3000 $^\circ$K.

The above discussion explains the experimental observations. The question remains, however, if it is possible to produce a beam of CN radicals at higher temperatures. An answer has to be sought in the equilibrium reaction (3.11). The thermodynamic quantities which determine the equilibrium of the reaction (3.11) were obtained by Berkowitz (BER 62):

(3.13) $$\log K = \frac{12.868}{T} - 2.899$$

where

(3.14) $$K = \frac{P_{CN}}{P_C \sqrt{P_{N_2}}}\ ,$$

and P_{CN}, P_C and P_{N_2} are the partial pressures in units of one atmosphere of CN, C(g) and N_2, respectively. For the partial pressure of C(g) the vapor pressure of carbon at the given temperature has to be used, and the pressure of the N_2 gas can be chosen arbitrary, because extra N_2 gas can be added, if necessary.

36

Table 3.1. The equilibrium $C(g) + \frac{1}{2} N_2 \rightleftarrows CN$

$T(^oK)$	K	$P_C^{a)}$	P_{N_2}	P_{CN}
3000	5.9	10^{-2} T	1 T	0.002 T
3250	1.2	10^{-1}	1	0.004
3500	0.59	1	1	0.02
3750	0.34	10	10	0.34

a) Vapor pressure at the given temperature.

Table 3.1. gives the results at a number of temperatures. It is seen from this Table that a temperature of at least 3500 ^oK is required for a reasonable amount of CN radicals. Enormous problems arise at such a high temperature, because almost all materials melt. There remains one possibility, "burning" of graphite in a N_2 atmosphere by leading N_2 through a heated graphite pipe. However at the temperature of 3500 ^oK, a massive pipe (length 20 mm, diameter 5 mm) is burnt within one minute.

The main conclusion of these experiments is, that it is practically impossible to produce any diatomic radical containing carbon (for example CN or CP) for MBER purposes in a furnace at thermodynamic equilibrium at reasonably low temperatures.

References.

ALM 37 G.M. Almy and R.B. Horsfall, Phys.Rev. 51 (1937) 491.

AMA 73 T. Amano and E. Hirota, J.Mol.Spectrosc. 45 (1973) 417.

BER 50 R. Beringer and J.G. Castle, Phys.Rev. 78 (1950) 581.

BER 54 R. Beringer, E.B. Rawson and A.F. Henry, Phys.Rev. 94
        (1954) 343.

BER 62 J. Berkowitz, J.Chem.Phys. 36 (1962) 2533.

BRO 72 J.M. Brown and P.J. Thistlethwaite, Mol.Phys. 23 (1972)
        635.

CAR 67 A. Carrington and D.H. Levy, J.Phys.Chem. 71 (1967) 2.

CAR 68 A. Carrington, B.J. Howard, D.H. Levy and J.C. Robertson,
        Mol.Phys. 15 (1968) 187.

CAR 69 A. Carrington, G.N. Currie, D.H. Levy and T.A. Miller,
        J.Chem.Phys. 50 (1969) 2726.

CAR 70 A. Carrington, D.H. Levy and T.A. Miller, Advances in
        Chemical Physics, vol XVIII, Interscience Publishers, New
        York, London, Sydney, Toronto (1970).

CAR 74 A. Carrington, Microwave Spectroscopy of Free Radicals,
        Academic Press, London, New York (1974).

CHU 70 A. Churg and D.H. Levy, Astrophys.J. 162 (1970) L161.

CLO 71 P.N. Clough, A.H. Curban and B.A. Thrush, Proc.Roy.Soc.A,
        323 (1971) 541.

COO 73 T.J. Cook and D.H. Levy, J.Chem.Phys. 58 (1973) 3547.

DEL 62 F.P. Del Greco and F. Kaufman, Discussions Faraday Soc.
        33 (1962) 128.

DOU 55 G.C. Dousmanis, T.M. Sanders Jr. and C.H. Townes,
        Phys.Rev. 100 (1955) 1735.

EAS 70 W.C. Easley and W. Weltner Jr., J.Chem.Phys 52 (1970) 197.

EVE 64 K.M. Evenson, J.L. Dunn and H.P. Broida, Phys.Rev. 136
        (1964) A 1566.

FEH 65 F.C. Fehsenfeld, K.M. Evenson and H.P. Broida, Rev.Sci.
        Instrum. 36 (1965) 294.

FRE 65 R.S. Freund and W. Klemperer, J.Chem.Phys. 43 (1965) 2422.

FRE 66 K.F. Freed, J.Chem.Phys. 45 (1966) 4214.

FRE 72 S.M. Freund, E. Herbst, R.P. Mariella Jr. and W. Klemperer,
        J.Chem.Phys. 56 (1972) 1467.

FRO 52   R.A. Frosh and H.M. Foley, Phys.Rev. 88 (1952) 729.

GAM 71   R.H. Gammon, R.C. Stern, M.E. Lesk, B.J. Wicke and W. Klem-
         perer, J.Chem.Phys. 54 (1971) 2136.
         R.H. Gammon, R.C. Stern and W. Klemperer, J.Chem.Phys.
         54 (1971) 2151.

HEN 54   J.M. Hendrie, J.Chem.Phys. 22 (1954) 1503.

LEE 71a F.H. de Leeuw, Ph.D. Thesis, Katholieke Universiteit,
         Nijmegen (1971).

LEE 71b K.P. Lee, W.G. Tam, R. Larouche and G.A. Woonton, Can.J.
         Phys. 49 (1971) 2207.

LEE 73   F.H. de Leeuw and A. Dymanus, J.Mol.Spectrosc. 48 (1973)
         427.

LEE 74   K.P. Lee and W.G. Tam, Chem.Phys. 4 (1974) 434.

MCD 63   C.C. McDonald, J.Chem.Phys. 39 (1963) 2587.

MCK 55   J.D. McKinley Jr., D. Garvin and M.J. Boudart, J.Chem.Phys.
         23 (1955) 784.

MEA 72   P. Meakin, D.O. Harris, J.Mol.Spectrosc. 44 (1972) 219.

MEE 74   W.L. Meerts, Quarterly Report No. 43, Atomic and Mole-
         cular Research Group, Katholieke Universiteit, Nijmegen (1974).

MEU 70   J.J. ter Meulen, ibid. No. 28 (1970).

MUL 31   R.S. Mulliken and A. Christy, Phys.Rev. 38 (1931) 87.

NEU 70   R.M. Neumann. Astrophys.J. 161 (1970) 779.

PEN 74   A.A. Penzias, R.W. Wilson and K.B. Jefferts, Phys.Rev.
         Letters 32 (1974) 701.

RAD 61   H.E. Radford, Phys.Rev. 122 (1961) 114.

RAD 62   H.E. Radford, Phys.Rev. 126 (1962) 1035.

RAD 63   H.E. Radford and M. Linzer, Phys.Rev.Letters 10 (1963) 443.

RAM 52   D.A. Ramsay, J.Chem.Phys. 20 (1952) 1920.

STE 70   R.C. Stern, R.H. Gammon, M.E. Lesk, R.S. Freund and W.A.
         Klemperer, J.Chem.Phys. 52 (1970) 3467.

STO 72   S. Stolte, Ph.D. Thesis, Katholieke Universiteit, Nijmegen
         (1972).

TAN 73   M. Tanimoto and H. Uehara, Mol.Phys. 25 (1973) 1193

THO 68   R. Thomson and F.W. Dalby, Can.J.Phys. 46 (1968) 2815.

VLE 29   J.H. Van Vleck, Phys.Rev. 33 (1929) 467.

WIN 72   G. Winnewisser, M. Winnewisser and B.P. Winnewisser,
         Physical Chemistry, Series One, vol 3, Spectroscopy, p 241,
         London, Baltimore (1972).

ZOR 73   J.C. Zorn and T.C. English, Advances in Atomic and Molecu-
         lar Physics, vol 9, Academic Press, New York, London (1973).

The Hyperfine Λ-Doubling Spectrum of $^{14}N^{16}O$ and $^{15}N^{16}O$

W. L. MEERTS AND A. DYMANUS

Department of Physics, University of Nijmegen, Nijmegen, The Netherlands

The molecular beam electric resonance method was used for the investigation of the hyperfine Λ-doubling transitions $\Delta J = 0$, $\Delta F = 0, \pm 1$ for a number of J values of both the $^2\Pi_{1/2}$ and the $^2\Pi_{3/2}$ states of the molecules $^{14}N^{16}O$ and $^{15}N^{16}O$. The observed spectrum is explained using the degenerate perturbation theory introduced by Freed (*1*). This theory is adapted for a $^2\Pi$ molecule and includes contributions up to third order in fine and hyperfine structure. The agreement between observed and calculated values is satisfactory.

I. INTRODUCTION

The microwave spectrum of NO was measured previously by Gallagher and Johnson (*2*), Favero *et al.* (*3*), and by Brown and Radford (*4*). The Λ-splitting constants and the hyperfine structure constants were determined from these measurements. Recently Neumann (*5*) measured the hyperfine Λ-doubling spectrum of $^{14}N^{16}O$ with the molecular beam electric resonance method and obtained accurate frequencies of the $\Delta J = 0$ transitions and values of the molecular coupling constants. For theoretical interpretation of the spectrum Neumann used the degenerate perturbation theory (DPT) discussed by Freed (*1*) with fine-structure contributions up to fourth order and hyperfine structure contributions up to second order. The agreement between experimental and theoretical results looked very satisfactory.

The present investigation on NO was intended both as a first step and as a test case in a program on hyperfine structure of open-shell molecules using the molecular beam electric resonance method. In addition to reproducing the measurements of Neumann (*5*) we were able to measure a large number of transitions in higher J states of the $^2\Pi_{1/2}$ and $^2\Pi_{3/2}$ states of both ^{14}NO and ^{15}NO. These transitions extend over a region from about 0.7 MHz to about 1.5 GHz. Especially the high-frequency transitions might be of interest to radioastronomers. When fitting the present measurements in ^{14}NO it was discovered that the frequencies predicted by Neumann (*5*) for the $^2\Pi_{1/2}$ state deviated from our experimental values by even as much as 250 kHz. It was not possible to explain these deviations within the scope of the theory used by Neumann. Consequently we decided to extend the theory by including hyperfine-structure contributions

320

up to third order This yields new contributions to the energy, which have a J dependence which differs from that present in the theory used by previous investigations (2–5) The new contributions result in a much better agreement between theoretical and experimental frequencies for both molecules

II THEORY

II 1 *Hamiltonian*

The complete Hamiltonian for a diatomic molecule can be written formally as

$$\mathbf{H} = \mathbf{H}_0 + \lambda\mathbf{V} + \lambda^2\mathbf{V}', \tag{1}$$

where $\mathbf{H}_0$ is the nonrelativistic Hamiltonian for electronic energies in the Born–Oppenheimer approximation, $\mathbf{V}$ contains the spin–orbit and gyroscopic terms which give rise to the Λ splitting, and $\mathbf{V}'$ describes the hyperfine contributions. For $\mathbf{V}$ we used

$$\mathbf{V} = B(\mathbf{J}^2 - \mathbf{L}_z^2 + \mathbf{S}^2) + A\mathbf{L}_z\mathbf{S}_z - 2B\mathbf{J}\cdot\mathbf{S}$$
$$+ (B + \tfrac{1}{2}A)(\mathbf{L}_+\mathbf{S}_- + \mathbf{L}_-\mathbf{S}_+) - B(\mathbf{J}_+\mathbf{L}_- + \mathbf{J}_-\mathbf{L}_+). \tag{2}$$

The Hamiltonian $\mathbf{V}$ of Eq. (2) is in accordance with that of Van Vleck (6), but differs slightly from the one used by Freed (1). For the hyperfine Hamiltonian $\mathbf{V}'$ we used the expression given by Freed (1) This rather complex expression will not be reproduced here

With the Hamiltonian (1) the spectrum of a $^2\Pi$ state is calculated using the degenerate perturbation theory (DPT) described by Freed (1) The contributions of the fine and hyperfine interactions to the energy are taken into account up to third order In the final expressions for state energies we separate terms with different dependence on the rotational quantum number J, as only these terms can be determined from the experimental data. The results show that the fine structure effects up to third order describe, within experimental accuracy, the J dependence of the contributions to the Λ splitting The hyperfine contributions up to third order have to be considered in order to obtain an acceptable agreement with experimental results, but the fourth-order contributions are below the experimental accuracy and are neglected (see also Section V) In the calculations the interactions of excited $^2\Sigma$, $^2\Pi$, and $^2\Delta$ states with the ground $X^2\Pi$ state are considered

II 2. *Wavefunctions, Symmetry and Energy Matrix*

The ground electronic state of NO is a $^2\Pi$ state. Application of DPT with the Hamiltonian (1) makes it necessary to solve a 4×4 secular equation (1). However, the Hamiltonian (1) is invariant under reflections of the coordinates and spins of all particles in a plane containing the nuclei Consequently, if wavefunctions are used with the proper symmetry (called Kronig symmetry) with

respect to these reflections (see also Appendix A), the secular determinant factors in two 2×2 determinants.

The coupling scheme of the angular momenta in the NO molecule is nearly a Hund case (a) ($7, 8$). Wavefunctions, including the rotation of the nuclear frame, are formally written as $| \, ^2\Gamma^\pm_{|\Omega|} \, J \, \rangle$, where $\Gamma \equiv \Sigma^s, \Pi, \Delta, \cdots$, and Ω is the projection of the total angular momentum J on the molecular axis. These wavefunctions are defined by

$$| \, ^2\Gamma^\pm_{|\Omega|} \, J \, \rangle = (1/\sqrt{2}) \, [| \, J \Lambda \Sigma \Omega \rangle \pm (-1)^s \, | \, J - \Lambda - \Sigma - \Omega \, \rangle] \qquad (3)$$

with $\Omega = \Lambda + \Sigma$. The functions on the right-hand side of Eq. (3) are given by Freed (1). Their Kronig symmetry is $\pm \, (-1)^{J-1/2}$ (see also Appendix A). The phase factor $(-1)^s$ has significance only if $\Gamma \equiv \Sigma^s$, $s = \pm$, in which case $(-1)^s = 1$ for $s = +$, and $(-1)^s = -1$ for $s = -$.

The matrix elements of the fine- and hyperfine-structure Hamiltonian for a $^2\Pi$ state on the basis defined in Eq. (3) are calculated using the results of Freed (1). The nuclear spin $\mathbf{I}$ of the nitrogen atom is coupled with the rotational angular momentum $\mathbf{J}$ to $\mathbf{F}$ in the conventional way: $\mathbf{J} + \mathbf{I} = \mathbf{F}$. The results are given in Tables I and II.[1] Only matrix elements, which are important for further calculations are tabulated. The matrix is Hermitian.

In $\mathbf{V}$ should also be included the term $\gamma \, \mathbf{N \cdot S}$. This term is discussed extensively by Freed (1). Its contributions to the energy are of the order of 100 MHz. However, in first order (see Section II. 3) this term does not contribute to the Λ splitting. The matrix elements of $\gamma \, \mathbf{N \cdot S}$ can easily be calculated using the formulas of Ref. (1). They have exactly the same J dependence as $\mathbf{V}$ of Table I, and give only a correction to ζ_t and θ_t, which are an order of magnitude smaller than those from $\mathbf{V}$. It is clear that these terms can be absorbed in $\mathbf{V}$ for further calculations, if we are only interested in terms with a different J dependence. This has been done without changing the definitions of these constants used in Table I.

In Tables I and II (and in the following) the symbols $^2\Sigma^\pm$ (i), $^2\Pi^\pm$ (l), and $^2\Delta^\pm$ (k) indicate a $^2\Sigma$, $^2\Pi$, and $^2\Delta$ excited electronic state, respectively; the index in the brackets numbers the state. Table III defines the quantities used in Tables I and II, where G, D, K, and Q are the molecular constants defined by Freed (1). The indices correspond to the Λ values of the initial and final states, respectively.

II. 3. *Fine Structure*

Because we measured Λ-doubling transitions from a Kronig $+$ to a Kronig $-$ state within one J state, only contributions to the Λ splitting are of interest, i.e., contributions different for states with an opposite symmetry. From Table I it is seen that only the $^2\Sigma^s$ states give a contribution to the Λ splitting.

[1] A factor $\sqrt{[I(2I + 1)(I + 1)]}$ is missing in the 4th equation of Table V of Ref. (1).

Table I   Matrix elements of V.

The upper and the lower sign in the matrix refer to the (+) and (-) sign of the wavefunctions, respectively. Only matrix elements which are important for further calculations are given.

	$X^2\Pi^{\pm}_{\frac{1}{2}}$	$X^2\Pi^{\pm}_{3/2}$	$^2\Sigma^{s\pm}_{\frac{1}{2}}(i)$
$X^2\Pi^{\pm}_{\frac{1}{2}}$	$-\frac{1}{2}A_{\Pi}+B_{\Pi}{}^{a}(J+\frac{1}{2})^2$		
$X^2\Pi^{\pm}_{3/2}$	$B_{\Pi}z$	$\frac{1}{2}A_{\Pi}+B_{\Pi}(x-^7/4)$	
$^2\Sigma^{s\pm}_{\frac{1}{2}}(i)$	$\theta_i\pm(-1)^s\zeta_i(J+\frac{1}{2})$	$\zeta_i z$	$B_{\Sigma}(J+\frac{1}{2})^2\pm(-1)^s B_{\Sigma}(J+\frac{1}{2})$
$^2\Pi^{\pm}_{\frac{1}{2}}(1)$	$-\frac{1}{2}\bar{A}_{\Pi}(1)+\bar{B}_{\Pi}(1)(J+\frac{1}{2})^2$	$\bar{B}_{\Pi}(1)z$	
$^2\Pi^{\pm}_{3/2}(1)$	$\bar{B}_{\Pi}(1)z$	$\frac{1}{2}\bar{A}_{\Pi}(1)+\bar{B}_{\Pi}(1)(x-^7/4)$	
$^2\Delta^{\pm}_{3/2}(k)$	$\eta_1(k)z$	$\eta_2(k)$	
$^2\Delta^{\pm}_{5/2}(k)$	0	$\eta_1(k)$ w	

^{a} For B_{Π} we substituted $B_{\Pi}-J(J+1)D_{\Pi}$, where D_{Π} is the centrifugal distortion constant.

Table II   Matrix elements of the hyperfine structure hamiltonian (V').

	$X^2\Pi^\pm_{\frac{1}{2}}$	$X^2\Pi^\pm_{3/2}$
$X^2\Pi^\pm_{\frac{1}{2}}$	$y\{\frac{1}{2}(G_{11}-\frac{1}{6}\sqrt{6}K_{11}-\frac{1}{3}\sqrt{6}D_{11})+C_{RS}x\ \pm D_{1-1}(J+\frac{1}{2})\}$ $+4Q_{11}(\frac{3}{4}-x)u$	
$X^2\Pi^\pm_{3/2}$	$\frac{1}{6}\sqrt{6}(D_{11}-K_{11})zy\ \pm Q_{1-1}\sqrt{6}(2J+1)zu$	$y\{\frac{3}{2}(G_{11}+\frac{1}{6}\sqrt{6}K_{11}+\frac{1}{3}\sqrt{6}D_{11})+C_{RS}x\}+4Q_{11}(\frac{27}{4}-x)u$
$^2\Sigma^{s\pm}_{\frac{1}{2}}(i)$	$y\{D_i\pm(-1)^s(G_i+D_i)(J+\frac{1}{2})\}$	$-(G_i+D_i)zy + Q_izu$
$^2\Pi^\pm_{\frac{1}{2}}(1)$	$y\{\gamma_1(1)\pm(J+\frac{1}{2})\gamma_2(1)\}+\gamma_3(1)u(\frac{3}{4}-x)$	$\gamma_4(1)zy \pm \gamma_5(1)zu(J+\frac{1}{2})$
$^2\Pi^\pm_{3/2}(1)$	$\gamma_4(1)zy \pm \gamma_5(1)zu(J+\frac{1}{2})$	$\gamma_6(1)y + \gamma_3(1)u(\frac{27}{4} - x)$
$^2\Delta^\pm_{3/2}(k)$	$yz(G_\Delta(k)-D_\Delta(k)) + uzQ_\Delta(k)$	$- 3D_\Delta(k)y$
$^2\Delta^\pm_{5/2}(k)$	0	$yw(G_\Delta(k)+D_\Delta(k)) + 2uwQ_\Delta(k)$

Table III   Definition of the quantities used in Table I

and II.

---

x $= J(J+1)$

y $= \dfrac{F(F+1) - J(J+1) - I(I+1)}{2J(J+1)}$

z $= \sqrt{(J-\frac{1}{2})(J+3/2)}$

u $= \dfrac{\frac{3}{4}C(C-1) - J(J+1)\, I(I+1)}{2I(2I-1)\, J(J+1)(2J-1)(2J+3)}$

C $= I(I+1) + J(J+1) - F(F+1)$

w $= \sqrt{(J-3/2)(J+5/2)}$

A_Π spin-orbit coupling constant of the $X^2\Pi$ state

B_Π rotational constant of the $X^2\Pi$ state

B_Σ rotational constant of the $^2\Sigma$ state

C_{RS} Describes the nuclear spin-rotation interaction

θ_i $= <^2\Sigma(i)||(B+\frac{1}{2}A)L_-||X^2\Pi>$

ζ_i $= <^2\Sigma(i)||BL_-||X^2\Pi>$

$\bar{A}_\Pi(1)$ $= <^2\Pi(1)||A||X^2\Pi>$

$\bar{B}_\Pi(1)$ $= <^2\Pi(1)||B||X^2\Pi>$

$\eta_1(k)$ $= <X^2\Pi||BL_-||^2\Delta(k)>$

$\eta_2(k)$ $= <X^2\Pi||(B+\frac{1}{2}A)L_-||^2\Delta(k)> - A^{\frac{11}{22}}_{21} /\sqrt{3}$

G_i $= G_{10(i)}/\sqrt{2}$

D_i $= \frac{1}{2} D_{10(i)}$

Q_i $= 4\sqrt{6}\, Q_{10(1)}$

$\gamma_1(1)$ $= \frac{1}{2}(G_{11(1)} - \frac{1}{6}\sqrt{6}\, K_{11(1)} - \frac{1}{3}\sqrt{6}\, D_{11(1)})$

Table III   (continued)

$$\gamma_2(1) = D_{1-1(1)}$$

$$\gamma_3(1) = 4Q_{11(1)}$$

$$\gamma_4(1) = (D_{11(1)} - K_{11(1)})/\sqrt{6}$$

$$\gamma_5(1) = 2\sqrt{6}\, Q_{1-1(1)}$$

$$\gamma_6(1) = 3/2(G_{11(1)} + \tfrac{1}{\sqrt{6}} K_{11(1)} + \tfrac{1}{3}\sqrt{6}\, D_{11(1)})$$

$$G_\Delta(k) = G_{12(k)}/\sqrt{2}$$

$$D_\Delta(k) = \tfrac{1}{2} D_{12(k)}$$

$$Q_\Delta(k) = 4\sqrt{6}\, Q_{12(k)}$$

The n-th ($n = 1, 2, 3$)-order perturbation Hamiltonian $\mathbf{V}^{(n)}$ is defined by Freed (1, Eq (3 2))

$$\mathbf{V}^{(1)} = \mathbf{V}, \tag{4}$$

$$\mathbf{V}^{(2)} = \sum_i \frac{\mathbf{V} \mid {}^2\Sigma^{s\pm}_{1/2}(i)\rangle\langle {}^2\Sigma^{s\pm}_{1/2}(i) \mid \mathbf{V}}{(\Pi\Sigma_i{}^s)}, \tag{5}$$

$$\mathbf{V}^{(3)} = \mathbf{V}_1^{(3)} + \mathbf{V}_2^{(3)}, \tag{6}$$

$$\mathbf{V}_1^{(3)} = \sum_{i\,j} \frac{\mathbf{V} \mid {}^2\Sigma^{s\pm}_{1/2}(i)\rangle\langle {}^2\Sigma^{s\pm}_{1/2}(i) \mid \mathbf{V} \mid {}^2\Sigma^{s\pm}_{1/2}(j)\rangle\langle {}^2\Sigma^{s\pm}_{1/2}(j) \mid \mathbf{V}}{(\Pi\Sigma_j{}^s)(\Pi\Sigma_i{}^s)}, \tag{7}$$

$$\mathbf{V}_2^{(3)} = -\sum_{i\,\alpha} \frac{\mathbf{V} \mid {}^2\Sigma^{s\pm}_{1/2}(i)\rangle\langle {}^2\Sigma^{s\pm}_{1/2}(i) \mid \mathbf{V} \mid \psi_\alpha{}^\pm\rangle\langle\psi_\alpha{}^\pm \mid \mathbf{V}}{(\Pi\Sigma_i{}^s)^2} \tag{8}$$

Herein $\mid \psi_\alpha{}^\pm\rangle$ is one of the $X^2\Pi^\perp$ states, and $(\Pi\,\Sigma_i{}^s) = E_{X^2\Pi} - E_{^2\Sigma^s(i)}$, the energy difference between the $X^2\Pi$ and the i-th excited $^2\Sigma^s$ state

Now we make the following approximation

$$\langle {}^2\Sigma^{s\pm}_{1/2}(i) \mid \mathbf{V} \mid {}^2\Sigma^{s\pm}_{1/2}(j)\rangle = B_\Sigma(J + \tfrac{1}{2})^2 \pm (-1)^s B_\Sigma(J + \tfrac{1}{2}),$$

where B_Σ is an effective rotational constant of the Σ states With this approximation $\mathbf{V}_1^{(3)}$ becomes

$$\mathbf{V}_1^{(3)} = \sum_i \frac{\mathbf{V} \mid {}^2\Sigma^{s\pm}_{1/2}(i)\rangle\langle {}^2\Sigma^{s\pm}_{1/2}(i) \mid \mathbf{V}}{(\Pi\Sigma_i{}^s)^2} [B_\Sigma(J + \tfrac{1}{2})^2 \pm (-1)^s B_\Sigma(J + \tfrac{1}{2})] \tag{9}$$

In the Tables IV, V, and VI, are tabulated the first , the second , and the third-

Table IV   First order energy contributions due to fine structure.

$$\langle {}^2\Pi_{\frac{1}{2}}^{\pm}|\underline{V}^{(1)}|{}^2\Pi_{\frac{1}{2}}^{\pm}\rangle = -\tfrac{1}{2}A_{\Pi} + B_{\Pi}(J+\tfrac{1}{2})^2$$

$$\langle {}^2\Pi_{3/2}^{\pm}|\underline{V}^{(1)}|{}^2\Pi_{3/2}^{\pm}\rangle = \tfrac{1}{2}A_{\Pi} + B_{\Pi}(J(J+1) - {}^7/4)$$

$$\langle {}^2\Pi_{3/2}^{\pm}|\underline{V}^{(1)}|{}^2\Pi_{\frac{1}{2}}^{\pm}\rangle = B_{\Pi}\,z$$

Table V   Second order energy conditions due to fine structure.

$$\langle {}^2\Pi_{\frac{1}{2}}^{\pm}|\underline{V}^{(2)}|{}^2\Pi_{\frac{1}{2}}^{\pm}\rangle = A_2^{(2)}(J+\tfrac{1}{2})^2 \pm (2J+1)\bar{A}_1^{(2)} + A_3^{(2)}$$

$$\langle {}^2\Pi_{3/2}^{\pm}|\underline{V}^{(2)}|{}^2\Pi_{3/2}^{\pm}\rangle = A_2^{(2)}(J-\tfrac{1}{2})(J+\tfrac{3}{2})$$

$$\langle {}^2\Pi_{3/2}^{\pm}|\underline{V}^{(2)}|{}^2\Pi_{\frac{1}{2}}^{\pm}\rangle = z\,A_1^{(2)} \pm \bar{A}_2^{(2)}z\,(J+\tfrac{1}{2})$$

order contributions to the energy due to the fine structure, respectively, while in Table VII are defined the quantities used in Tables IV–VI. The ($+$) and ($-$) signs in Table VII indicate that the sums extend only over Σ' states with $s = +$ and $s = -$, respectively. The fine-structure contributions from Tables IV–VI are collected in Table VIII according to their J dependence.

II. 4. *Hyperfine Contributions*

The hyperfine structure gives contributions to the energy in second and third order. The second-order hyperfine Hamiltonian is $\mathbf{V}'$, the third order consists of three parts. These parts describe the interaction with the excited Σ, Π, and Δ states. The interaction Hamiltonian can be written formally as

$$\mathbf{V}_{hf}^{(3)} = \mathbf{V}_{hf}^{(3)}(\Sigma) + \mathbf{V}_{hf}^{(3)}(\Pi) + \mathbf{V}_{hf}^{(3)}(\Delta), \tag{10}$$

Table VI   Third order energy contribution due to fine structure.

$$\langle ^2\Pi^{\pm}_{\frac{1}{2}} | V^{(3)} | ^2\Pi^{\pm}_{\frac{1}{2}} \rangle = \tfrac{1}{2} A^{(3)}_2 A_\Pi (J+\tfrac{1}{2})^2 + A^{(3)}_2 (B_\Sigma - B_\Pi)(J+\tfrac{1}{2})^4 \pm \bar{A}^{(3)}_2 B_\Sigma (J+\tfrac{1}{2})^3 \pm A_\Pi \bar{A}^{(3)}_1 (J+\tfrac{1}{2})$$

$$\pm 2\bar{A}^{(3)}_1 (B_\Sigma - B_\Pi)(J+\tfrac{1}{2})^3 + 2 A^{(3)}_1 B_\Sigma (J+\tfrac{1}{2})^2 + \tfrac{1}{2} A^{(3)}_3 A_\Pi + A^{(3)}_3 (B_\Sigma - B_\Pi)(J+\tfrac{1}{2})^2$$

$$\pm \bar{A}^{(3)}_3 B_\Sigma (J+\tfrac{1}{2}) - A^{(3)}_1 B_\Pi z^2 \mp \bar{A}^{(3)}_2 B_\Pi z^2 (J+\tfrac{1}{2})$$

$$\langle ^2\Pi^{\pm}_{3/2} | V^{(3)} | ^2\Pi^{\pm}_{3/2} \rangle = -\tfrac{1}{2}(A_\Pi - 4B_\Pi) A^{(3)}_2 z^2 + A^{(3)}_2 (B_\Sigma - B_\Pi)(J+\tfrac{1}{2})^2 z^2 \pm \bar{A}^{(3)}_2 (B_\Sigma - B_\Pi)(J+\tfrac{1}{2}) z^2$$

$$- A^{(3)}_1 B_\Pi z^2$$

$$\langle ^2\Pi^{\pm}_{\frac{1}{2}} | V^{(3)} | ^2\Pi^{\pm}_{3/2} \rangle = -\tfrac{1}{2} z \{ A^{(3)}_2 B_\Pi (J+\tfrac{1}{2})^2 \pm B_\Pi \bar{A}^{(3)}_1 (2J+1) + A^{(3)}_3 B_\Pi + A^{(3)}_2 B_\Pi z^2$$

$$+ 2(-B_\Pi + B_\Pi (J+\tfrac{1}{2})^2)(A^{(3)}_1 \pm \bar{A}^{(3)}_2 (J+\tfrac{1}{2})) \}$$

$$+ B_\Sigma (J+\tfrac{1}{2})^2 z \{ A^{(3)}_1 \pm \bar{A}^{(3)}_2 (J+\tfrac{1}{2}) \} \pm B_\Sigma \bar{A}^{(3)}_1 (J+\tfrac{1}{2}) z$$

$$+ B_\Sigma A^{(3)}_2 (J+\tfrac{1}{2})^2 z.$$

Table VII Definitions of the molecular constants used in

Table V and VI.

$$A_k^{(n)} \quad = \quad A_k^{(n)+} + A_k^{(n)-}$$

$$\bar{A}_k^{(n)} \quad = \quad A^{(n)+} - A_k^{(n)-} \qquad\qquad n = 2, 3$$

$$A_1^{(n)\pm} \quad = \quad \sum_{\Sigma^\pm} \frac{\zeta_i \theta_i}{(\Pi\Sigma_i^\pm)^{n-1}} \quad a \qquad\qquad k = 1, 2, 3$$

$$A_2^{(n)\pm} \quad = \quad \sum_{\Sigma^\pm} \frac{\zeta_i \zeta_i}{(\Pi\Sigma_i^\pm)^{n-1}}$$

$$A_3^{(n)\pm} \quad = \quad \sum_{\Sigma^\pm} \frac{\theta_i \theta_i}{(\Pi\Sigma_i^\pm)^{n-1}}$$

---

a The sums extend for the (+)sign only over Σ^+ states, for

the (-)sign only over the Σ^- states.

with

$$V_{hf}^{(3)}(\Sigma) = \sum_i \left\{ \frac{V \mid {}^2\Sigma_{1/2}^{s\pm}(i)\rangle\langle {}^2\Sigma_{1/2}^{s\pm}(i) \mid V'}{(\Pi\Sigma_i{}^s)} + \frac{V' \mid {}^2\Sigma_{1/2}^{s\pm}(i)\rangle\langle {}^2\Sigma_{1/2}^{s\pm}(i) \mid V}{(\Pi\Sigma_i{}^s)} \right\}, \quad (11)$$

$$V_{hf}^{(3)}(\Pi) = \sum_l \left\{ \frac{V \mid {}^2\Pi_{1/2}^{\pm}(l)\rangle\langle {}^2\Pi_{1/2}^{\pm}(l) \mid V'}{(\Pi\Pi_l)} + \frac{V' \mid {}^2\Pi_{1/2}^{\pm}(l)\rangle\langle {}^2\Pi_{1/2}^{\pm}(l) \mid V}{(\Pi\Pi_l)} \right.$$
$$\left. + \frac{V \mid {}^2\Pi_{3/2}^{\pm}(l)\rangle\langle {}^2\Pi_{3/2}^{\pm}(l) \mid V'}{(\Pi\Pi_l)} + \frac{V' \mid {}^2\Pi_{3/2}^{\pm}(l)\rangle\langle {}^2\Pi_{3/2}^{\pm}(l) \mid V}{(\Pi\Pi_l)} \right\}, \quad (12)$$

and

$$V_{hf}^{(3)}(\Delta) = \sum_k \left\{ \frac{V \mid {}^2\Delta_{3/2}^{\pm}(k)\rangle\langle {}^2\Delta_{3/2}^{\pm}(k) \mid V'}{(\Pi\Delta_k)} + \frac{V' \mid {}^2\Delta_{3/2}^{\pm}(k)\rangle\langle {}^2\Delta_{3/2}^{\pm}(k) \mid V}{(\Pi\Delta_k)} \right.$$
$$\left. + \frac{V \mid {}^2\Delta_{5/2}^{\pm}(k)\rangle\langle {}^2\Delta_{5/2}^{\pm}(k) \mid V'}{(\Pi\Delta_k)} + \frac{V' \mid {}^2\Delta_{5/2}^{\pm}(k)\rangle\langle {}^2\Delta_{5/2}^{\pm}(k) \mid V}{(\Pi\Delta_k)} \right\}. \quad (13)$$

Table VIII Collected contributions to the fine structure

up to third order $(\underline{V}^{(1)}+\underline{V}^{(2)}+\underline{V}^{(3)} = H_F)$.

$\langle {}^2\Pi_{\frac{1}{2}}^{\pm} | \underline{H}_F | {}^2\Pi_{\frac{1}{2}}^{\pm} \rangle \quad = $

$-\tfrac{1}{2}\alpha_1 + \alpha_2 (J+\tfrac{1}{2})^2 + \alpha_{10}(J+\tfrac{1}{2})^4 \pm \alpha_3 (2J+1) \pm \alpha_4 (J+\tfrac{1}{2})^3 \pm \alpha_5 (J+\tfrac{1}{2})z^2$

$\langle {}^2\Pi_{3/2}^{\pm} | \underline{H}_F | {}^2\Pi_{3/2}^{\pm} \rangle = \tfrac{1}{2}A_\Pi + B_\Pi(J(J+1)-\tfrac{7}{4}) + \alpha_9 z^2 + \alpha_{10}(J+\tfrac{1}{2})^2 z^2 \pm \alpha_8(J+\tfrac{1}{2})z^2$

$\langle {}^2\Pi_{\frac{1}{2}}^{\pm} | \underline{H}_F | {}^2\Pi_{3/2}^{\pm} \rangle \quad = \alpha_6 z + \alpha_{11} z(J+\tfrac{1}{2})^2 \pm \alpha_7 z(J+\tfrac{1}{2}) \pm \alpha_8 z(J+\tfrac{1}{2})^3$

With $\alpha_1 \quad = A_\Pi - A_3^{(3)} A_\Pi - 2A_3^{(2)} + 2A_1^{(3)} B_\Pi$

$\alpha_2 \quad = B_\Pi + A_2^{(2)} + \tfrac{1}{2}A_\Pi A_2^{(3)} + (A_1^{(3)}+A_3^{(3)})(B_\Sigma - B_\Pi) + A_1^{(3)} B_\Sigma$

$\alpha_3 \quad = \bar{A}_1^{(2)} + \tfrac{1}{2}\bar{A}_1^{(3)} A_\Pi + \tfrac{1}{2}\bar{A}_3^{(3)} B_\Sigma$

$\alpha_4 \quad = \bar{A}_2^{(3)} B_\Sigma + 2\bar{A}_1^{(3)}(B_\Sigma - B_\Pi)$

$\alpha_5 \quad = - \bar{A}_2^{(3)} B_\Pi$

$\alpha_6 \quad = B_\Pi + A_1^{(2)} + B_\Sigma (A_1^{(3)} + \tfrac{1}{2}A_2^{(3)} - \tfrac{1}{2}A_3^{(3)})$

$\alpha_7 \quad = \bar{A}_2^{(2)} + \bar{A}_1^{(3)}(B_\Sigma - B_\Pi) + \bar{A}_2^{(3)} B_\Pi$

$\alpha_8 \quad = \bar{A}_2^{(3)}(B_\Sigma - B_\Pi)$

$\alpha_9 \quad = A_2^{(2)} - \tfrac{1}{2}A_2^{(3)}(A_\Pi - 4B_\Pi) - A_1^{(3)} B_\Pi$

$\alpha_{10} = A_2^{(3)}(B_\Sigma - B_\Pi)$

$\alpha_{11} = (A_1^{(3)} + A_2^{(3)})(B_\Sigma - B_\Pi)$

Table IX Energy contributions due to the hyperfine structure up to third order.

$$({V}_{-hf}^{(2)} + {V}_{-hf}^{(3)} = {H}_{-hf}).$$

$$\langle {}^2\Pi_{\frac{1}{2}}^{\pm}|\underline{H}_{-hf}|{}^2\Pi_{\frac{1}{2}}^{\pm}\rangle = y\{\beta_1 + \beta_5(J+\tfrac{1}{2})^2 + \beta_9 z^2 + C_{RS}x \pm \beta_2(J+\tfrac{1}{2}) \pm \beta_{10}(J+\tfrac{1}{2})^3\} +$$

$$+ u\{\phi_1(\tfrac{3}{4}-x) + \phi_4(\tfrac{3}{4}-x)(J+\tfrac{1}{2})^2 \pm \phi_5 z^2(J+\tfrac{1}{2})\}$$

$$\langle {}^2\Pi_{3/2}^{\pm}|\underline{H}_{-hf}|{}^2\Pi_{3/2}^{\pm}\rangle = y\{\beta_3 + \beta_6 z^2 + \beta_7(J+\tfrac{1}{2})^2 + \beta_8 w^2 + C_{RS}x\} +$$

$$+ u\{\phi_2(\tfrac{27}{4} - x) + \phi_4(\tfrac{27}{4} - x)(J+\tfrac{1}{2})^2 + \phi_6 z^2 \pm \phi_5 z^2(J+\tfrac{1}{2})\}$$

$$\langle {}^2\Pi_{3/2}^{\pm}|\underline{H}_{-hf}|{}^2\Pi_{\frac{1}{2}}^{\pm}\rangle = zy\{\beta_4 + \beta_{11}z^2 \pm \beta_{12}(J+\tfrac{1}{2})\} +$$

$$+ zu\{\pm \phi_3(J+\tfrac{1}{2}) + \phi_7 - \phi_4 w^2 \pm \phi_5 z^2(J+\tfrac{1}{2})\}$$

Table X   Definition of the molecular constants from Table IX.

$$\beta_1 = \tfrac{1}{2}(G_{11}- \tfrac{1}{6}\sqrt{6}K_{11}- \tfrac{1}{3}\sqrt{6}D_{11})+2\sum_i \frac{D_i\Theta_i}{(\Pi\Sigma_i^s)} - \sum_l \frac{\gamma_1(1)\bar{A}_\Pi(1)}{(\Pi\ \Pi_1)}$$

$$\beta_2 = D_{1-1}+2\sum_i (-1)^s \frac{D_i\zeta_i+\Theta_i(G_i+D_i)}{(\Pi\ \Sigma_i^s)} - \sum_l \frac{\gamma_2(1)\bar{A}_\Pi(1)}{(\Pi\ \Pi_1)}$$

$$\beta_3 = \tfrac{3}{2}(G_{11}+ \tfrac{1}{6}\sqrt{6}K_{11}+ \tfrac{1}{3}\sqrt{6}D_{11})-6\sum_k \frac{n_2(k)D_\Delta(k)}{(\Pi\ \Delta_k)} +$$
$$+ 2\sum_l \frac{(\tfrac{1}{2}\bar{A}_\Pi(1)-2\bar{B}_\Pi(1))\gamma_6(1)}{(\Pi\ \Pi_1)}$$

$$\beta_4 = \tfrac{1}{6}\sqrt{6}(D_{11}-K_{11})+\sum_i \frac{D_i\zeta_i-\Theta_i(G_i+D_i)}{(\Pi\ \Sigma_i^s)} -3\sum_k \frac{D_\Delta(k)n_1(k)}{(\Pi\ \Delta_k)} +$$
$$+\sum_k \frac{n_2(k)\{G_\Delta(k)-D_\Delta(k)\}}{(\Pi\ \Delta_k)} +\sum_l \frac{\bar{B}_\Pi(1)\{\gamma_1(1)+\gamma_6(1)\}}{(\Pi\ \Pi_1)}$$

$$\beta_5 = 2\sum_i \frac{\zeta_i(G_i+D_i)}{(\Pi\ \Sigma_i^s)} +\sum_l \frac{\gamma_1(1)\bar{B}_\Pi(1)}{(\Pi\ \Pi_1)}$$

$$\beta_6 = -2\sum_i \frac{(G_i+D_i)\zeta_i}{(\Pi\ \Sigma_i^s)} + 2\sum_l \frac{\gamma_4(1)\bar{B}_\Pi(1)}{(\Pi\ \Pi_1)}$$

$$\beta_7 = 2\sum_l \frac{\bar{B}_\Pi(1)\gamma_6(1)}{(\Pi\ \Pi_1)}$$

$$\beta_8 = 2\sum_k \frac{n_1(k)\{G_\Delta(k)+D_\Delta(k)\}}{(\Pi\ \Delta_k)}$$

Table X (continued)

$$\beta_9 = 2\sum_k \frac{\eta_1(k)\left[G_\Delta(k)-D_\Delta(k)\right]}{(\Pi\ \Delta_k)} + 2\sum_l \frac{\gamma_4(l)\bar{B}_\Pi(l)}{(\Pi\ \Pi_l)}$$

$$\beta_{10} = 2\sum_l \frac{\gamma_2(l)\bar{B}_\Pi(l)}{(\Pi\ \Pi_l)}$$

$$\beta_{11} = 2\sum_l \frac{\gamma_4(l)\bar{B}_\Pi(l)}{(\Pi\ \Pi_l)}$$

$$\beta_{12} = \sum_i (-1)^s \frac{\zeta_i(D_i+G_i)}{(\Pi\ \Sigma_i^s)} + \sum_l \frac{\bar{B}_\Pi(l)\gamma_2(l)}{(\Pi\ \Pi_l)}$$

$$\phi_1 = 4Q_{11} - \sum_l \frac{\gamma_3(l)\bar{A}_\Pi(l)}{(\Pi\ \Pi_l)} - 2\sum_k \frac{\eta_1(k)Q_\Delta(k)}{(\Pi\ \Delta_k)}$$

$$\phi_2 = 4Q_{11} + 2\sum_l \frac{(\tfrac{1}{2}\bar{A}_\Pi(l)-2\bar{B}_\Pi(l))\gamma_3(l)}{(\Pi\ \Pi_l)} - \sum_k \frac{\eta_1(k)Q_\Delta(k)}{(\Pi\ \Delta_k)}$$

$$\phi_3 = 2\sqrt{6}\ Q_{1-1} + \sum_i (-1)^s \frac{Q_i\zeta_i}{(\Pi\ \Sigma_i^s)}$$

$$\phi_4 = 2\sum_l \frac{\gamma_3(l)\bar{B}_\Pi(l)}{(\Pi\ \Pi_l)}$$

$$\phi_5 = 2\sum_l \frac{\gamma_5(l)\bar{B}_\Pi(l)}{(\Pi\ \Pi_l)}$$

Table X (continued)

$$\phi_6 = 2\sum_i \frac{Q_i \varsigma_i}{(\Pi \, \Sigma_i^s)} + \sum_k \frac{\eta_1(k) Q_\Delta(k)}{(\Pi \, \Delta_k)}$$

$$\phi_7 = \sum_i \frac{Q_i \theta_i}{(\Pi \, \Sigma_i^s)} + \sum_k \frac{\eta_2(k) Q_\Delta(k)}{(\Pi \, \Delta_k)}$$

The second- and third-order hyperfine contributions due to the fine structure are easily calculated using Eqs. (11)–(13), and Tables I and II. The result is given in Table IX, while in Table X are defined the relations between the molecular constants of Tables IX and III.

Experimentally we can separate only terms with a different J dependence. This reduces the equations of Table IX to those of Table XI. The equations given in Tables VIII and XI are the final results. The molecular constants defined in these equations should describe the hyperfine Λ-doubling spectrum up to third order in energy. The theory outlined above is used to analyze the experimental spectrum. The constants are adjusted by a least-squares method to fit the experimental data.

III. EXPERIMENTAL RESULTS

The experiments were performed using the molecular beam electric resonance method. The experimental setup has been described in detail elsewhere (9). For the measurements on $^{15}N^{16}O$ we used an enriched (95 %) sample. The gas was recovered after every run of about 4 hr. The loss was approximately 1.5 % per run. The measured frequencies involved the electric dipole transitions from a +Kronig symmetry level to a −Kronig symmetry level, within one J state.

The NO molecule in its $^2\Pi$ state has a very strong Zeeman effect, and the transitions of the $^2\Pi_{3/2}$ state are strongly split by the earth's magnetic field. These splittings decrease with increasing J value. The $\Delta F = 0$ transitions are seen as triplets. The frequencies of the central lines of these triplets are, within experimental accuracy, those of the zero field transitions. The $\Delta F = \pm 1$ transitions appear as broad doublets (^{14}NO) or triplets (^{15}NO) symmetrically located about the zero field frequencies. We were able to minimize the magnetic field to ~ 5 mG. The full line widths were 10–20 kHz for $J = \frac{3}{2}$ and $\frac{5}{2}$ of $^2\Pi_{1/2}$, and less than 10 kHz for the other transitions.

Table XI Hyperfine structure contributions up to third order after collecting terms with the same J dependence.

$$\langle {}^2\Pi_{\frac{1}{2}}^{\pm} | \underline{H}_{hf} | {}^2\Pi_{\frac{1}{2}}^{\pm} \rangle = y\{(x_1 + z^2 x_5) \pm (J+\tfrac{1}{2})(x_2 + z^2 x_6)\} +$$

$$+ u\{(\tfrac{3}{4}-x)(\zeta_1 + \zeta_4 J(J+1)) \pm \zeta_5 z^2 (J+\tfrac{1}{2})\}$$

$$\langle {}^2\Pi_{3/2}^{\pm} | \underline{H}_{hf} | {}^2\Pi_{3/2}^{\pm} \rangle = y\{x_3 + z^2 x_7\} +$$

$$+ u\{(\tfrac{27}{4}-x)(\zeta_2 + \zeta_4 J(J+1)) + (\zeta_7 \pm \zeta_5 (J+\tfrac{1}{2})) z^2\}$$

$$\langle {}^2\Pi_{\frac{1}{2}}^{\pm} | \underline{H}_{hf} | {}^2\Pi_{3/2}^{\pm} \rangle = zy\{(x_4 + z^2 x_8) \pm x_9 (J+\tfrac{1}{2})\} +$$

$$+ zu\{\pm(\zeta_3 + \zeta_5 J(J+1))(J+\tfrac{1}{2}) + (\zeta_6 - \zeta_4 J(J+1))\}$$

with

$x_1 = \beta_1 + \beta_5 + \tfrac{3}{4} C_{RS}$		$\zeta_1 = \phi_1 + \tfrac{1}{4}\phi_4$	
$x_2 = \beta_2 + \beta_{10}$		$\zeta_2 = \phi_2 + \tfrac{1}{4}\phi_4$	
$x_3 = \beta_3 + \beta_7 - 3\beta_8 + \tfrac{3}{4} C_{RS}$		$\zeta_3 = \phi_3 - \tfrac{3}{4}\phi_5$	
$x_4 = \beta_4$		$\zeta_4 = \phi_4$	
$x_5 = \beta_5 + \beta_9 + C_{RS}$		$\zeta_5 = \phi_5$	
$x_6 = \beta_{10}$		$\zeta_6 = \phi_7 + \tfrac{15}{4}\phi_4$	
$x_7 = \beta_6 + \beta_7 + \beta_8 + C_{RS}$		$\zeta_7 = \phi_6$	
$x_8 = \beta_{11}$			
$x_9 = \beta_{12}$			

The observed transition frequencies at zero electric and magnetic fields and their uncertainties are given in Table XII for ${}^{14}N^{16}O$, and in Table XIII for ${}^{15}N^{16}O$.

As can be seen from Table XII the experimental results of Neumann (5) on

Table XII Observed and predicted hyperfine Λ-doubling transitions for $^{14}N^{16}O$.

J	Ω	F_+	F_-[a]	This work	previous measurements (5)	Calculated frequencies
				Observed frequencies (MHz)		
0.5	0.5	0.5	0.5	205.9510(2)	205.951(1)	205.9582
		1.5	1.5	431.1905(2)	431.191(1)	431.1587
		1.5	0.5	411.2056(2)	411.206(1)	411.1886
		0.5	1.5	225.9357(2)	225.936(1)	225.9282
1.5	0.5	0.5	0.5	560.8538(2)		560.8529
		1.5	1.5	651.5425(2)	651.543(1)	651.5275
		2.5	2.5	801.1963(2)		801.2179
		1.5	2.5	758.9106(2)		758.9379
		2.5	1.5	693.8282(2)		693.8076
		0.5	1.5	624.6494(2)		624.6259
		1.5	0.5	587.7467(2)		587.7545
2.5	0.5	1.5	1.5	929.259 (4)		929.2441
		3.5	3.5	1160.7768(3)		1160.8073
		3.5	2.5	1114.677(15)		1114.7102
		2.5	3.5	1072.596(12)		1072.6308
		2.5	1.5	991.7338(2)		991.7351
		1.5	2.5	964.023 (2)		964.0428
3.5	0.5	4.5	4.5	1514.768 (1)		1514.7580
		4.5	3.5	1434.588 (1)		1434.6099
		3.5	4.5	1467.511 (1)		1467.4984
		3.5	2.5	1325.299 (1)		1325.2872
		2.5	3.5	1348.459 (4)		1348.4151
1.5	1.5	1.5	1.5	0.612 (1)	0.612(1)	0.6118
		2.5	2.5	1.029 (1)	1.029(1)	1.0288
		1.5	2.5	74.931 (3)	74.930(1)	74.9212
		2.5	1.5	73.286 (3)	73.289(1)	73.2806
		0.5	1.5	46.464 (3)	46.470(5)	46.4567

336

Table XII   (continued)

				Observed frequencies (MHz)		Calculated frequencies
J	Ω	F_+	F_- [a]	This work	previous measurement (5)	
2.5	1.5	2.5	1.5	3.121 (1)	3.121(1)	3.1203
		3.5	3.5	3.923 (1)	3.923(1)	3.9226
		3.5	2.5	47.211 (1)	47.212(1)	47.2122
		2.5	3.5	40.172 (6)		40.1693
		2.5	1.5	34.390(30)		34.3715
3.5	1.5	3.5	4.5	39.221 (2)		39.2310
		2.5	3.5	31.550 (4)		31.5415
4.5	1.5	5.5	4.5	40.512 (1)		40.5129
		4.5	3.5	35.045 (2)		35.0452
5.5	1.5	4.5	4.5	31.124 (1)	31.124(1)	31.1251
		5.5	5.5	30.265 (1)	30.265(1)	30.2649
		6.5	6.5	32.425 (1)	32.425(1)	32.4242
		5.5	6.5	48.786 (1)		48.7861
		6.5	5.5	13.905 (1)		13.9029
6.5	1.5	5.5	5.5	49.405 (1)	49.405(1)	49.4056
		6.5	6.5	48.578 (1)	48.577(1)	48.5772
		7.5	7.5	51.260 (1)	51.260(1)	51.2598
		7.5	6.5	63.640 (1)		63.6409
		6.5	7.5	36.196 (1)		36.1960
		6.5	5.5	59.742 (1)		59.7421
		5.5	6.5	38.243 (1)		38.2406
7.5	1.5	6.5	6.5	73.540 (1)	73.540(1)	73.5397
		7.5	7.5	72.786 (1)	72.786(1)	72.7853
		8.5	8.5	76.025 (1)	76.025(1)	76.0240
		7.5	8.5	85.255 (1)		85.2563
		8.5	7.5	63.552 (1)		63.5530
		6.5	7.5	81.547 (1)		81.5468
		7.5	6.5	64.778 (1)		64.7783

337

Table XII (continued)

J	Ω	F_+	F_- [a]	This work	previous measurements	Calculated frequencies
8.5	1.5	7.5	7.5	104.216 (2)		104.2147
		8.5	8.5	103.575 (2)		103.5746
		9.5	9.5	107.400 (1)		107.3400
		9.5	8.5	114.024 (1)		114.0220
		8.5	9.5	96.951 (1)		96.9526
		8.5	7.5	110.306 (1)		110.3057
		7.5	8.5	97.483 (1)		97.4836

Column header spanning: **Observed frequencies (MHz)**

[a] $F_\pm$ F-state with Kronig symmetry ±.

$^{14}N^{16}O$ agree very well with ours. However, his predicted frequencies (5), especially for the $^2\Pi_{1/2}$ state, show a great discrepancy with our experimental results.

IV. ANALYSIS OF THE SPECTRUM

From Table VIII it follows that the Λ splitting is determined by the constants α_3, α_1, α_5, α_7, and α_8. We make the following approximations for the other molecular constants from Table VIII:

$$\alpha_1 = A_{II}; \quad \alpha_2 = B_{II} + \alpha_7; \quad \alpha_6 = B_{II} + \alpha_3; \quad \alpha_9 = \alpha_7; \quad \alpha_{10} = \alpha_{11} = 0.$$

This is a permitted approximation, because terms which do not contribute directly to the Λ splitting must be at least of the order of 10 MHz to give higher-order effects on the energy within the present experimental accuracy (about 1 kHz). From Table VIII it follows that $\alpha_8 = \alpha_5(B_{II}-B_2)/B_{II}$. As A_{II} and B_{II} are known from other experiments the Λ splitting is described up to third order by four constants α_3, α_1, α_5, and α_7.

IV. 1. $^{15}N^{16}O$.

The absence of the contributions from electric quadrupole interaction in $^{15}N^{16}O$ ($I = 1/2$) simplifies the spectrum considerably. Nine hyperfine structure constants, all χ, have to be determined for this molecule.

We calculated the coefficient matrix, which describes the dependence of the calculated frequencies on the various constants. The rank of this matrix was

Table XIII   Observed and calculated hyperfine Λ-doubling
transitions for $^{15}N^{16}O$.

J	Ω	F_+	F_-	Observed frequencies (MHz)	Calculated frequencies (MHz)
0.5	0.5	0	0		501.1979
		0	1	482.6212(2)	482.6189
		1	0	309.2256(2)	309.2217
		1	1	290.6565(2)	290.6426
1.5	0.5	1	1	790.9748(3)	790.9651
		2	1	742.8364(3)	742.8346
		1	2	670.7076(3)	670.7201
		2	2	622.5690(3)	622.5896
2.5	0.5	2	2	1121.1513(3)	1121.1691
		2	3		1064.6944
		3	2	1015.4147(5)	1015.3914
		3	3	958.9183(3)	958.9167
3.5	0.5	3	3	1454.9160(5)	1454.9013
		4	3		1394.6320
		3	4		1355.0719
		4	4		1294.8026
1.5	1.5	2	1	84.589 (2)	84.5877
		1	2		82.9340
		1	1		0.8732
		2	2	0.780 (5)	0.7804
2.5	1.5	2	3	55.738 (3)	55.7429
		3	2		49.1965
		2	2	3.393 (3)	3.3923
		3	3	3.154 (1)	3.1542
3.5	1.5	4	3		45.5804
		3	4		29.3107
		3	3		8.3544
		4	4		7.9152
4.5	1.5	4	5		44.5249
		4	4		16.5308
		5	5		15.8352
		5	4		12.1591
5.5	1.5	6	5	50.2509(5)	50.2511
		5	5	28.6642(5)	28.6634
		6	6	27.6570(5)	27.6578
		5	6	6.0702(5)	6.0701
6.5	1.5	6	7	62.2184(5)	62.2183
		6	6	45.4609(5)	45.4604
		7	7	44.0920(5)	44.0927
		7	6	27.3347(5)	27.3349
7.5	1.5	8	7	80.4891(5)	80.4891
		7	7	67.5905(5)	67.5905
		8	8	65.8107(5)	65.8110
		7	8	52.9121(5)	52.9124

Table XIII (continued)

8.5	1.5	8	9	105.3590(5)	105.3590	
		8	8	95.6788(5)	95.6795	'
		9	9	93.4413(5)	93.4403	
		9	8	83.7610(5)	83.7608	

^{a} $F_\pm$ F-state with Kronig symmetry ±.

smaller than the number of constants. Consequently not all constants can be determined independently from the experimental data. It turned out that there is a relation between χ_4, χ_5, and χ_7. From the coefficient matrix it follows, that the effect of χ_4 on the energy can be absorbed in an effective χ_5', and χ_7':

$$\chi_5' = \chi_5 - \alpha\chi_4 , \qquad (14)$$

$$\chi_7' = \chi_7 + \alpha\chi_4 . \qquad (15)$$

The constants χ_5 and χ_7 in Table XI are replaced by χ_5' and χ_7', respectively, whereas the effect of χ_4 in the matrix element $\langle ^2\Pi_{1/2}^\pm \,|\, H_{hf} \,|\, ^2\Pi_{3/2}^\pm \rangle$ of Table XI can be taken as zero in the fitting procedure. The value of α is calculated from the coefficient matrix. The resulting α (Table XIV) is varying very slowly with increasing J. The error in the value of α is set equal to the maximum variation in α with increasing J.

The molecular constants α_3, α_4, α_5, α_7, χ_1, χ_2, χ_3, χ_5', χ_6, χ_7', χ_8, and χ_9 are varied in a least-squares fit of the experimental spectrum. The constant χ_8 was found to be very small, and was subsequently set at zero.

Using Eqs. (14) and (15) we calculated χ_4 and $(\chi_5 + \chi_7)$ from χ_5' and χ_7'. Table XIV lists the values of the molecular constants of the best least-squares fit. The calculated frequencies are given in Table XIII.

IV. 2. $^{14}N^{16}O$

The hyperfine-structure constants χ_1 through χ_9 are determined in the same way as for $^{15}N^{16}O$. The nuclear spin $I = 1$ of ^{14}N introduces a contribution to the hyperfine energy due to the electric quadrupole interaction. This makes it necessary to determine seven additional molecular constants ζ_1 through ζ_7. The electric quadrupole constants adjusted in the least-squares fit of the spectrum of $^{14}N^{16}O$ are ζ_1, ζ_2, ζ_3, and ζ_5. The remaining three constants ζ_4, ζ_6, and ζ_7 were found to be less than 1 kHz without giving any improvement of the fit and are as taken zero. The results are listed in Table XIV. The calculated frequencies are tabulated in Table XII. Table XV lists the molecular constants taken from other sources and used as known in the fit.

Table XIV Molecular constants of $^{14}N^{16}O$ and $^{15}N^{16}O$ obtained in this work (all values are in MHz, except α, which is dimensionless).

constant name	value for $^{14}N^{16}O$	value for $^{15}N^{16}O$
α_3	89.0235(2)	85.8210(2)
α_7	1.4132(4)	1.3149(4)
α_4	$(-1.06(5)) \times 10^{-3}$	$(-1.36(5)) \times 10^{-3}$
α_5	$(-0.10(1)) \times 10^{-3}$	$(-0.10(1)) \times 10^{-3}$
X_1	46.3151(7)	$-65.0240(7)$
X_2	56.3001(5)	$-78.9582(4)$
X_3	113.639 (2)	-159.468 (3)
X_5'	0.6015(7)	$-0.8444(7)$
X_6	$(0.56(6)) \times 10^{-3}$	$(-3.77(6)) \times 10^{-3}$
X_7'	$-0.5837(3)$	0.7888(1)
X_9	$(-5.2 \ (5)) \times 10^{-3}$	$(8.2 \ (5)) \times 10^{-3}$
ζ_1	-1.841 (1)	
ζ_2	-1.862 (1)	
ζ_3	12.115 (40)	
ζ_5	$(-15.4 \ (7)) \times 10^{-3}$	
α	0.02836(2)	0.027334(8)
X_4	-20.896 (25)	29.875 (25)
$X_5 + X_7$	$(17.8 \ (8)) \times 10^{-3}$	$(-55.6 \ (8)) \times 10^{-3}$

Table XV Molecular constants of $^{14}N^{16}O$ and $^{15}N^{16}O$ taken from other sources and used in the present fit.

	value for $^{14}N^{16}O$	value for $^{15}N^{16}O$	Ref.
A_Π	123.160 cm^{-1}	123.160 [a] cm^{-1}	(15)
B_Π	50 838.56 MHz	49 041.34 MHz	(2)
D_Π	0.177 MHz	0.139 MHz	(2)
B_Σ	59 568.76 MHz	57 206 MHz	(7)

[a] We used for $^{15}N^{16}O$ the value of $^{14}N^{16}O$.

V. DISCUSSION

The differences between the experimental frequencies and the frequencies calculated as outlined above (Tables XII and XIII) are approximately an order of magnitude smaller than between the experimental and the predicted frequencies of Neumann (5). The third-order hyperfine-structure contributions give rise to a number of terms with a different J dependence. These contributions are responsible for the better agreement between experiment and theory; they were not included in previous calculations of the spectrum. The additional coupling constants are χ_5 through χ_9, and ζ_5.

However, the fit for the frequencies of the $^2\Pi_{1/2}$ state is not as good as we expected. An obvious thought is that neglect of higher-order contributions from fine and hyperfine structure might be responsible for the remaining discrepancy.

The fourth-order fine structure can be separated into two parts. One part containing terms with a similar J dependence as those of Table VIII and may be absorbed in α_1 through α_{11} without changing anything in the mathematics of the least-squares fit. The other part contains terms with a different J dependence. However, calculations of these contributions and rough estimates similar to those of Ref. (1) showed that they were smaller than the experimental accuracy. So fourth-order fine structure cannot explain the discrepancy.

The fourth-order hyperfine contributions were calculated by Freed (1) for a $^3\Pi$ state. They were calculated by us for a $^2\Pi$ state and included in the least-

Table XVI   Relations between hyperfine constants of Table XI

and conventional constants (neglecting third

order effects).

conventional constants	present constants	Ref.
a	$\frac{1}{3}(3x_1 + x_3)$	(10)
b	$-2x_4$	(10)
c	$2(-x_1+x_4) + \frac{2}{3}x_3$	(10)
d	$2x_2$	(10)
eQq_1	$\frac{1}{2}(\zeta_1 + \zeta_2)$	(16)
eQq_2	$2\zeta_3$	(16)

squares fit of the spectrum It was not necessary to introduce new coupling constants Unfortunately no improvement of the fit was obtained. For this reason we did not discuss here the explicit expressions for the fourth-order contribution of the hyperfine structure We did not find any other contribution which could explain the discrepancy between the experimental and theoretical frequencies.

No attempt was made to perform the very tedious fifth-order calculations

Comparison with previous experiments (2–5) is not simple, because the third-order hyperfine effects were always neglected. Especially the molecular fine-structure constants α_3 and α_7 include third order as well as second-order effects. However, if the third order effects in the hyperfine-structure constants are neglected, one can easily deduce relations between the hyperfine constants defined by Frosh and Foley (8), and by Dousmanis et al. (10), and the constants used in this work This is done in Table XVI

Neglecting third-order effects in the hyperfine structure, we calculated from Tables XVI and XIV the hyperfine coupling constants of Table XVII In this table are also listed the results of previous investigations It should be noted

Table XVII Values of the conventional constants obtained in the present work and by other investigations. In these constants third order effects are neglected. (All values in MHz).

Constant	Present value	Neumann (5)	Radford and Brown (4)	Favero et al (3)	Gallagher and Johnson (2)
a ($^{14}N^{16}O$)	84.195(2)	84.208 (2)	84.28(52)	83.82	83.40
b ($^{14}N^{16}O$)	41.79 (5)	41.508(75)	41.8 (6.3)	68.49	68.91
c ($^{14}N^{16}O$)	-58.66 (5)	-58.37 (7)	-58.8 (7.4)	-86.34	-87.60
d ($^{14}N^{16}O$)	112.600(1)	112.6196(3)	116 (30)	...	112.60
eQq_1($^{14}N^{16}O$)	-1.852(2)	-1.876 (8)	-1.81(30)	-2	-1.75
eQq_2($^{14}N^{16}O$)	24.23 (8)	23.04 (5)	23.1 (4)	33	27.9
a ($^{15}N^{16}O$)	-118.189(3)		-118.21(50)		-116.94
b ($^{15}N^{16}O$)	-59.78 (5)		-59.8 (5.8)		-96.63
c ($^{15}N^{16}O$)	83.51 (5)		83.4 (6.8)		122.82
d ($^{15}N^{16}O$)	-157.929(1)		-159 (33)		-157.88

that the accuracy of the molecular constants, especially a and d, claimed by Neumann (5) is too high, because he neglects the third-order hyperfine effects. Our calculated hyperfine-structure constants agree quite well with those of Neumann (5) and Brown and Radford (4).

APPENDIX

The molecular Hamiltonian $\mathbf{H}$ of a diatomic molecule is invariant under reflections σ_{xz} in a plane containing the molecular axis, so that

$$\sigma_{xz}^{-1}\,\mathbf{H}\,\sigma_{xz} = \mathbf{H} \tag{A1}$$

and the wavefunctions, which are used as basis for the calculation of the matrix elements of $\mathbf{H}$, must have the proper symmetry with respect to these reflections.

The zero-th-order molecular wavefunctions in a Hund case (a) can formally be written as $|\,J\Lambda\Sigma\Omega\rangle$. They can be split into a rotational and a rotationless part:

$$|\,J\Lambda\Sigma\Omega\rangle = |J\Omega\rangle\,|\,\Lambda\rangle\,|\,S\Sigma\rangle, \tag{A2}$$

where $|\,J\Omega\rangle$ is the rotational part. Under the reflections σ_{xz} the functions $|J\Lambda\Sigma\Omega\rangle$ behave as (6, 11–14)

$$\sigma_{xz}\,|\,J\Lambda\Sigma\Omega\rangle = (-1)^{s}(-1)^{J-\Omega+s-\Sigma+\Lambda}\,|\,J - \Lambda - \Sigma - \Omega\rangle. \tag{A3}$$

Herein s is even or odd for Σ^{+} or Σ^{-} states, respectively, and zero otherwise.

So functions with a proper symmetry can be defined as

$$|\,{}^{2S+1}\Gamma^{\pm}{}_{|\Omega|}J\rangle = (1/\sqrt{2})[|\,J\Lambda\Sigma\Omega\rangle \pm (-1)^{s}\,|\,J - \Lambda - \Sigma - \Omega\rangle], \tag{A4}$$

where Γ stands for $\Sigma^{s}, \Pi, \Delta, \cdots$.

The symmetry of these functions under the reflections σ_{xz} is $\pm(-1)^{J-S}$:

$$\sigma_{xz}\,|\,{}^{2S+1}\Gamma^{\pm}{}_{|\Omega|}\,J\rangle = \pm(-1)^{J-S}\,|{}^{2S+1}\Gamma^{\pm}{}_{|\Omega|}\,J\rangle. \tag{A5}$$

This is called the Kronig symmetry of the functions. These definitions of symmetry are in agreement with Herzberg (7), but differ slightly from those of Freed (1).

The symmetry considerations halve the number of matrix elements which must be calculated. From Eqs. (A1) and (A3) it follows.

$$\langle J\Lambda\Sigma\Omega\,|\,\mathbf{H}\,|\,J'\Lambda'\Sigma'\Omega'\rangle = \langle J\Lambda\Sigma\Omega\,|\,\sigma_{xz}^{-1}\,\mathbf{H}\sigma_{xz}\,|\,J'\Lambda'\Sigma'\Omega'\rangle$$
$$= f\,\langle J - \Lambda - \Sigma - \Omega\,|\,\mathbf{H}\,|\,J' - \Lambda' - \Sigma' - \Omega'\rangle, \tag{A6}$$

where

$$f = (-1)^{(s+s')+J+J'+s+s'+\Omega+\Omega' - (\Sigma+\Sigma') + (\Lambda+\Lambda')}. \tag{A7}$$

With

$$J = J',\ S = S',\ (-1)^{\Lambda+\Lambda'} = (-1)^{-(\Lambda+\Lambda')},$$

Eq.(A7) becomes

$$f = (-1)^{s+s'}. \tag{A8}$$

ACKNOWLEDGMENTS

REFERENCES

1. K. F. FREED, *J. Chem. Phys.* **45**, 4214 (1966).
2. J. J. GALLAGHER AND C. M. JOHNSON, *Phys. Rev.* **103**, 1727 (1956).
3. P. G. FAVERO, A. M. MIRRI, AND W. GORDY, *Phys. Rev.* **114**, 1534 (1959).
4. R. L. BROWN AND H. E. RADFORD, *Phys. Rev.* **147**, 6 (1966).
5. R. M. NEUMANN, *Astrophys. J.* **161**, 779 (1970).
6. J. H. VAN VLECK, *Phys. Rev.* **33**, 467 (1929).
7. G. HERZBERG, "Spectra of Diatomic Molecules," D. Van Nostrand Company, New York, 1950.
8. R. A. FROSH AND M. M. FOLEY, *Phys. Rev.* **88**, 1337 (1952).
9. F. H. DE LEEUW, Thesis, 1971, Nijmegen, The Netherlands.
10. G. C. DOUSMANIS, T. M. SANDERS, AND C. H. TOWNES, *Phys. Rev.* **100**, 1735 (1955).
11. J. T. HOUGEN, *J. Chem. Phys.* **37**, 1433 (1962); *J. Chem. Phys.* **39**, 358 (1963).
12. I. KOPP AND J. T. HOUGEN, *Can. J. Phys.* **45**, 2581 (1967).
13. J. H. VAN VLECK, *Phys. Rev.* **40**, 544 (1932).
14. D. W. LEPARD, *Can. J. Phys.* **48**, 1664 (1970).
15. T. C. JAMES AND R. J. THIBAULT, *J. Chem. Phys.* **41**, 2806 (1964).
16. C. C. LIN AND M. MIZUSHIMA, *Phys. Rev.* **100**, 1726 (1955).

ACCURATE FREQUENCIES BELOW 5 GHz OF THE LOWER *J* STATES OF OD

W. L. MEERTS AND A. DYMANUS

Department of Physics, University of Nijmegen, Nijmegen, The Netherlands
Received 1972 December 11

ABSTRACT

The hyperfine Λ-doubling transitions of the low-*J* states of OD were measured, using the molecular beam electric-resonance technique. These measurements are used to calculate some other transitions of OD, which might also be of interest for radio astrophysics.

Subject headings: hyperfine structure — molecules — radio lines

In 1955 Dousmanis, Sanders, and Townes (1955) reported the first measurements of the microwave Λ-doubling transition frequencies of OD. The observed frequencies were those belonging to the $\Delta F = 0$ transitions in the $^2\Pi_{3/2}$ and $^2\Pi_{1/2}$ electronic states. The hyperfine splitting of the transition was well resolved in the latter state but not in the $^2\Pi_{3/2}$ state. Consequently these lines contain almost no information about the hyperfine structure of OD. Some of the hyperfine-structure constants of OD can be predicted, however, from the corresponding values of OH reported by Radford (1962) and the ratio of the nuclear *g*-factors of proton and deuteron. Because of the rather large uncertainties of the frequencies measured by Dousmanis *et al.* (1955), it is not possible to predict the transitions in the low-lying *J*-states of OD with an accuracy better than 2 MHz, using this approach. It is felt that more precise transition frequencies are needed to increase chance of detecting the presence of the OD radical in interstellar space.

We measured all the hyperfine Λ-doubling transitions below 5 GHz originating in the lower *J* states of the electronic states $^2\Pi_{1/2}$ and $^2\Pi_{3/2}$. The measurements were performed using the molecular-beam electric-resonance method. The OD radicals are produced by the reaction $D + NO_2 \rightarrow OD + NO$ (Del Greco and Kaufman 1962). The atomic deuterium was produced by a 2.45-GHz microwave discharge in D_2O. The Earth's magnetic field is reduced by careful screening and compensation to about 5 milligauss. The signal-to-noise ratio of the observed transitions varied from 5 to 25 with an RC time of 3 s. The full line width at half-height was in the order of 10 kHz for most transitions. The experimental accuracy of the frequencies varied from 0.2 to 3 kHz and was mainly determined by the signal-to-noise ratio. The observed frequencies correspond to the $\Delta J = 0$; $\Delta F = 0, \pm 1$; Λ-doubling transitions between states with different Kronig symmetries. They are tabulated in table 1.

The theory developed in the previous paper (Meerts and Dymanus 1972) for a diatomic molecule in a $^2\Pi$ state is used to explain the observed spectrum. The molecular constants defined herein are calculated using a least-squares fit of our experimental frequencies and those of Dousmanis *et al.* (1955), weighted with their experimental uncertainties. As can be seen from table 1, the agreement is quite good. The molecular constants, which are varied in this fit, are those discussed in the previous paper (Meerts and Dymanus 1972); in addition, the spin-orbit coupling constant A_π is calculated. The values obtained for the hyperfine structure constants are given in table 2. Their definitions are those of Frosh and Foley (1952) and are also given by Meerts and Dymanus (1972). By using the molecular constants, obtained from the least squares fit, we calculated frequencies of a number of transitions of OD

TABLE 1

OBSERVED AND PREDICTED HYPERFINE Λ-DOUBLING TRANSITIONS OF THE OD RADICAL

Electronic State	J	F_+*	F_-	Observed Frequency (MHz)	Observed minus Predicted Frequency (kHz)
$^2\Pi_{1/2}$	0 5	0 5	0 5	3093 6057(10)	+0 4
		1 5	1 5	3111 1414(10)	+0 5
		0 5	1 5	3090 2163(10)	−0 3
		1 5	0 5	3114 5294(10)	−0.3
$^2\Pi_{3/2}$	1 5	0 5	0 5	310 1445(5)	+0 4
		1 5	1 5	310 2147(5)	+0 7
		2 5	2 5	310 3627(10)	+0 4
		1 5	0 5	303 0320(20)	+0 3
		0 5	1 5	317 3290(40)	+2.6
		2 5	1 5	298 0970(10)	0 0
		1 5	2.5	322 4800(20)	+0.6
$^2\Pi_{3/2}$	2 5	1 5	1 5	1190 5659(2)	0.0
		2 5	2 5	1190 7741(2)	0 0
		3 5	3 5	1191 1047(2)	+0 1
		1 5	2 5	1186 9986(30)	−1 5
		2.5	1.5	1194 3390(10)	−0 9
		2.5	3 5	1185 8712(10)	0 0
		3 5	2 5	1196 0060(30)	−1 4
$^2\Pi_{3/2}$	3 5	2 5	2 5	2822 0007(20)	+1.4
		3 5	3 5	2822 3883(20)	+2 0
		3 5	2 5	2820 8514(20)	−1 6
		2 5	3 5	2823 5328(20)	+0 2
		3 5	4 5	2821 0857(20)	−0 4
		4 5	3 5	2824 2276(20)	−0 2

* The subscript +(−) refers to the even (odd) Kronig symmetry (Meerts and Dymanus 1972).

in the range 5–10 GHz which might also be of interest to radio astronomy. The results can be found in table 3. The estimated accuracy is 20 kHz or less for the lower J states increasing to 200 kHz for the higher J states.

TABLE 2

HYPERFINE COUPLING CONSTANTS OF OD

Molecular Constant*	Value (MHz)
a	+13 297(2)
b	−17 962(6)
c	+20 234(6)
d	+8.768(1)
eQq_1	+0 143(2)
eQq_2	−0 122(6)

* For the convention of the constants see Meerts and Dymanus (1972)

TABLE 3

PREDICTED FREQUENCIES (in MHz) OF SOME HYPERFINE Λ-DOUBLING
TRANSITIONS OF OD

J	F_+	F_-	$^2\Pi_{1/2}$ Level	$^2\Pi_{3/2}$ Level
1.5	0.5	0.5	5887.720	
	1.5	1.5	5894.655	
	2.5	2.5	5906.189	
	1.5	0.5	5887.241	
	0.5	1.5	5895.134	
	2.5	1.5	5894.123	
	1.5	2.5	5906.721	
2.5	1.5	1.5	8110.631	
	2.5	2.5	8117.917	
	3.5	3.5	8128.085	
	1.5	2.5	8109.867	
	2.5	1.5	8118.681	
	2.5	3.5	8117.082	
	3.5	2.5	8128.920	
3.5	2.5	2.5	9578.721	
	3.5	3.5	9586.088	
	4.5	4.5	9595.526	
	3.5	2.5	9577.391	
	2.5	3.5	9587.419	
	4.5	3.5	9584.601	
	3.5	4.5	9597.014	
4.5	3.5	3.5	10191.845	5303.986
	4.5	4.5	10199.164	5304.575
	5.5	5.5	10208.077	5305.339
	3.5	4.5	10189.893	5304.645
	4.5	3.5	10201.116	5303.916
	4.5	5.5	10196.995	5305.585
	5.5	4.5	10210.246	5304.329

REFERENCES

Del Greco, F. P., and Kaufman, F. 1962, *Discussions Faraday Soc.*, **33**, 128.
Dousmanis, G. C., Sanders, T. M., and Townes, C. H. 1955, *Phys. Rev.*, **100**, 1735.
Frosh, R. A., and Foley, M. M. 1952, *Phys. Rev.*, **88**, 1337.
Meerts, W. L., and Dymanus, A. 1972, *J. Mol. Spectrosc.* (November issue).
Radford, H. E. 1962, *Phys. Rev.*, **126**, 1035.

ELECTRIC DIPOLE MOMENTS OF OH AND OD
BY MOLECULAR BEAM ELECTRIC RESONANCE

W.L. MEERTS and A. DYMANUS

Fysisch Laboratorium Katholieke Universiteit Nijmegen The Netherlands

The Stark shifts of hyperfine Λ doubling transitions originating from the $^2\Pi_{1/2}$ level of OH and OD are observed From these shifts we calculated the values of the electric dipole moments 1 6676(9) D for OH and 1 65312(14) D for OD

1 Introduction

The electric dipole moment of the hydroxyl radical (OH) has been investigated by several authors [1–3] The most accurate value is reported by Powell and Lide [4] $\mu = 1\ 660(10)$ D obtained from the Stark shifts of the microwave Λ-doublet transition of the $^2\Pi_{3/2}, J = 7/2$ level at 13438 MHz

After a molecular beam electric resonance study of the hyperfine Λ doubling spectrum of OD in zero external fields [5] we decided to investigate the Stark effect of OH and OD in order to obtain more accurate values of the dipole moments for both molecules as a first step in an investigation of their vibrational dependence

2 Theory

The hamiltonian used for the interpretation of the observed spectra is

$$H = H_\Gamma + H_{hf} - \mu\ E \qquad (1)$$

Herein H_F and H_{hf} describe the fine, hyperfine structure contributions, respectively, the last term gives the Stark effect, where μ is the permanent dipole moment of the molecule, and E the external electric field

For the interpretation of the spectra in zero electric field we used the theory developed in a previous paper [6] The lowest electronic state of the hydroxyl

radical is a $^2\Pi$ state The rotational wavefunctions can be formally written [6] as $|^2\Pi^p_{|\Omega|}J\rangle$, where $|\Omega|$ takes the values 1/2 and 3/2, and p stands for $\pm$ The nuclear spin I of the hydrogen or deuteron nucleus is coupled with the rotational angular momentum J to F in the conventional way $J + I = F$

The basic hyperfine wavefunctions take the form $|^2\Pi^p_{|\Omega|}JIFM_F\rangle$ Their Kronig symmetry is $p(-1)^{J-1/2}$

The matrix elements of H_I and H_{hf} on these basic wavefunctions are extensively discussed by Meerts and Dymanus [6] The matrix elements of the Stark contribution can easily be calculated (see also Freed [7]) The result is

$$\langle^2\Pi^p_{|\Omega|}JIFM_F|-\mu\ E|^2\Pi^p_{\Omega}J'I\Gamma'M'_F\rangle$$

$$= \delta(|\Omega|,\ |\Omega'|)f\mu F[(2J+1)(2J'+1)(2F+1)(2F'+1)]^{1/2}$$

$$\times \begin{Bmatrix} J & F & I \\ F' & J' & 1 \end{Bmatrix} \begin{pmatrix} F & 1 & F' \\ -M_F & 0 & M'_F \end{pmatrix} \begin{pmatrix} J & 1 & J' \\ -|\Omega| & 0 & |\Omega'| \end{pmatrix} \quad (2)$$

In this expression E is taken parallel to the z axis As the Stark effect operator has non zero matrix elements only between states with a different Kronig symmetry, the constant f takes the values

$$f = 0 \quad \text{if } |J - J'| = 0 \text{ and } p = p',$$

$$\text{or } |J - J'| = 1 \text{ and } p \neq p,$$

$$= (-1)^{2J+I+F+F'-M_F-|\Omega|} \quad \text{otherwise}$$

The energy matrix for the fine and hyperfine struc ture contributions involve a simple 2×2 secular equa tion The Stark effect enlarges the secular problem considerably because of the coupling between states with different symmetry and matrix elements off diagonal in J and F The only good quantum number of the hamiltonian (1) is M_F We calculated for each M_F value the total matrix of H including $\Delta J = \pm 1$ coupling terms The latter terms are responsible for second order contributions to the Stark energy Higher order terms turned out to be far below the experi mental accuracy The calculations were performed us ing a computer program which diagonalizes the com plete hamiltonian matrix

3 Results and discussion

The measurements were performed using a molec ular beam electric resonance spectrometer (MBER) described elsewhere [8] Initially attempts were made to measure the Stark splitting of the lowest rotational level ($J = 3/2$) of the $^2\Pi_{1\,2}$ state This state has a very strong Zeeman effect Although the earth's magnetic field has been compensated for with extreme care in ternal inconsistencies in the order of $1 \quad 10^3$ in the measured Stark splittings were observed These are caused probably by the component of the earth's mag netic field perpendicular to the electric field esti mated to be 15 30 mG As an alternative we decided to measure the Stark effect of the transitions belonging to the $^2\Pi_{1\,2}$ state which is essentially non magnetic However the conditions for MBER are not favourable because of the relatively high transition frequencies in zero external fields 4 7 GHz for OH [9] and 3 1 GHz for OD [5] respectively in their lowest rotational state $J = 1/2$ It turned out that the Stark splitting for OD could very well be observed at 3 1 GHz but the OH transition at 4 7 GHz could not be observed Fortunately the zero field transitions of the $J = 9/2$ $^2\Pi_{1\,2}$ state of OH are at easy MBER frequencies be tween 88 and 165 MHz So for OH the Stark splitting of these transitions is observed The zero field transi tion frequencies are given in table 1

The measurements are done at different electric field strengths and for different hyperfine transitions for both OH and OD The maximum Stark shift was 20 MHz and 15 MHz for OD and OH respectively

Table 1
Observed zero field Λ doubling transitions of the $^2\Pi_{1/2}$ $J = 9$ 2 level of OH

I_+[a]	I	Frequency (MHz)
4	4	164 7960(5)
5	5	117 1495(5)
4	5	192 9957(5)
5	4	88 9504(5)

[a] The subscript + ( ) refers to the even (odd) Kronig sym metry [6]

Using the theory discussed in the previous section the Stark shifts are calculated and values for the electric dipole moments for OH and OD are fitted to the ex perimental data The obtained dipole moments were 1 66758(10) D and 1 65312(14) D for OH and OD respectively The agreement between experimental and calculated Stark shifts was excellent within experi mental accuracy The quoted errors are based on the experimental uncertainties

However difficulties encountered in fitting the zero field spectrum force us to increase the inaccuracy in the reported value of the dipole moment of OH The nucleus of the difficulties is the high accuracy of the measurements and the rather strong centrifugal distor tion which has to be taken into account when fitting the zero field spectrum as well as the Stark spectrum

The OH molecule can be described by an interme diate Hund's case between (a) and (b) In the fit of the former spectrum we used an intermediate repre sentation starting from the case (a) basic wavefunc tions For the rotational constant (B_{II}) and the cen trifugal distortion constant (D_Π) of the $^2\Pi$ state we used the values reported by Dieke and Crosswhite [10] These constants were obtained from a fit of the observed ultraviolet band spectrum of OH to the the oretical spectrum calculated in an intermediate repre sentation starting from the Hund's case (b) wavefunc tions

This procedure is correct but problems are intro duced by an approximation in the expressions for the rotational energy (functions $f_{1\,2}(K)$ of ref [10]) the B_{II} part is in an intermediate case but the D_{II} part in pure (b) case This approximation is a good one for high J values for which OH is close to case (b) but not for low J values relevant to the present in vestigation For the correct treatment of the rotational

energy in our representation we had to transform the hamiltonian matrix of Dieke and Crosswhite Essentially this is a transformation from the Hund's (b) to the Hund's (a) representation However, when this is done an additional D_{11}-contribution [proportional to $J(J+1)$] appears for the rotational energy If Dieke and Crosswhite had used this approach their B_{11} and D_{11}-values would have been slightly different

The ratio between the rotational energy (including distortion effects) and the spin orbit energy is a measure for the mixing of the $^2\Pi_{1/2}$ and $^2\Pi_{3/2}$ levels As the Stark effect matrix elements are unequal for the two levels, the calculated Stark shifts depend on the mixing of the levels A slight change of the D_{11} constant will cause a very small variation in the mixing of both $^2\Pi$ levels and consequently in the Stark shifts The effect on the dipole moment can be $5 \cdot 10^4$ It is felt, that the error in the dipole moment of OH should reflect this uncertainty (0 0009 D), resulting in $\mu = 1\ 6676(9)$ D for OH

The observed Stark transitions are given in table 2 These transitions may be used to obtain a more accurate value of μ(OH), when the uncertainty of D_{11} is removed

There are no problems in the interpretation of the Stark spectrum of OD, because the lowest J-state, $J = 1/2$, is a pure $^2\Pi_{1/2}$-state, without any mixing with the $^2\Pi_{3/2}$ level The obtained dipole moment for OD is $1\ 65312(14)$ D For B_{11} and D_{11} of OD we used the values given by Dousmanis et al [11]

For Planck's constant the recent value of Taylor et al [12] is used $h = 6\ 626196(50) \times 10^{-34}$ J sec

The value of the anisotropy in the electric polariz-

Table 2
Observed transition frequencies of OH in electric field

				Frequency (MHz)	
F_+	M_{F_+}	F_-	M_{F_-}	$E = 157\ 157(5)$ V/cm	$E = 314\ 314(10)$ V/cm
5	5	5	5	121 2363(7)	132 7439(7)
4	4	4	4	167 6140(7)	175 7787(7)

ability for OH is not known, however, the value will lie between 0 2 and $1\ 0 \times 10^{-24}$ cm^3 The effect on the Stark shifts is estimated for an assumed value of $1\ 0 \times 10^{-24}$ cm^3 This causes shifts or 10 Hz or less, which is far below the experimental accuracy (700 Hz)

The value of the dipole moment of OH as reported by Powell and Lide [4] has to be corrected for the incorrect value of the dipole moment of OCS they used to calibrate the electric field strength [13, 14] The corrected value 1 667(10) D is in good agreement with the present more accurate value

The observed isotopic effect in the dipole moment of OH and OD is about 8×10^{-3}, which is quite an acceptable value This difference is caused by vibrational effects It is, however, not possible to discuss these effects quantitatively only on the basis of the dipole moments for OH and OD in the ground vibrational state, one also needs the values for other vibrational states

References

[1] R P Madden and W S Benedict J Chem Phys 23 (1955) 408
[2] R T Meyer and R J Myers J Chem Phys 34 (1961) 1074
[3] G Ehrenstein Phys Rev 130 (1963) 669
[4] I X Powell and D R Lide J Chem Phys 42 (1965) 4201
[5] W L Meerts and A Dymanus Astrophys J 180 (1973) 193
[6] W L Meerts and A Dymanus J Mol Spectry 44 (1972) 320
[7] K F Freed J Chem Phys 45 (1966) 4214
[8] I H de Leeuw, Ph D Thesis Katholieke Universiteit Nijmegen The Netherlands (1971)
[9] H I Radford Rev Sci Instr 39 (1968) 1687
[10] G H Dieke and H M Crosswhite J Quant Spectry Radiative Transfer 2 (1962) 97
[11] G C Dousmanis T M Sanders Jr and C H Townes Phys Rev 100 (1955) 1735
[12] B N Taylor W H Parker and D N Langenberg Rev Mod Phys 41 (1969) 375
[13] I H de Leeuw and A Dymanus Chem Phys Letters 7 (1970) 288
[14] S A Marshall and J Weber Phys Rev 105 (1957) 1502

CHAPTER 5.

THE HYPERFINE Λ-DOUBLING SPECTRUM OF SULFUR HYDRIDE IN THE ²Π₃/₂ STATE

W. L. MEERTS AND A. DYMANUS
Department of Physics, University of Nijmegen, The Netherlands
Received 1973 October 25

ABSTRACT

The hyperfine Λ-doubling spectrum of the five lowest rotational states of the ²Π₃/₂, $v = 0$ state is measured using the molecular-beam electric-resonance method. From the Stark splittings of the observed transitions the value of the electric dipole moment of SH is determined: $\mu = 0.7580(1)$ D.

Subject headings: molecules — hyperfine structure

A search for the emission lines of the sulfur hydride (SH) molecule in astronomical sources has been performed by Meeks, Gordon, and Litvak (1969) and by Heiles and Turner (1971). These attempts were unsuccessful, partly because of the inaccuracy of the Λ-doublet transition frequencies. The Λ-doublet transition of the lowest rotational states $J = 3/2$ and $J = 5/2$ of the ²Π₃/₂, $v = 0$ state of SH were investigated by several authors using paramagnetic resonance spectroscopy (Radford and Linzer 1963; Brown and Thistlethwaite 1972; Tanimoto and Uehara 1973). The accuracy of the predicted frequencies was of the order of 100–200 kHz. In order to check reliability of the ESR predictions and to obtain more accurate Λ-doublet transition frequencies for the SH radical we used the molecular-beam electric-resonance method for the five

lowest rotational states of the ²Π₃/₂ level. In addition the value of the electric dipole moment of SH is obtained.

The SH radical is produced by the reaction of hydrogen atoms with H_2S. The hydrogen atoms are produced by a 2.45-GHz microwave discharge in water. The signal-to-noise ratio of the SH transitions varied between 1 and 15 with a RC = 5 s. The observed frequencies correspond to the $\Delta J = 0$, $\Delta F = 0 \pm 1$, Λ-doubling transitions between states with different Kronig symmetry, originating in the five lowest J-states of the electronic ground state ²Π₃/₂. The lowest transition frequencies of the ²Π₁/₂ electronic state lie at about 8.4 GHz, beyond our present experimental possibilities. The observed transition frequencies are listed in table 1.

The theory discussed in an earlier paper (Meerts and

TABLE 1

OBSERVED Λ-DOUBLING TRANSITION FREQUENCIES (in MHz) OF THE ²Π₃/₂ ELECTRONIC STATE OF SH

J	F_+*	F_-	Present Observation	Predicted from ESR Measurements	
3/2	1	1	111.4862(5)	111.26(10)†	111.39(10)‡
	2	2	111.5452(5)	111.58(10)†	111.44(10)‡
	2	1	100.293(3)		
	1	2	122.737(3)		
5/2	2	2	442.4781(5)	440.4(2)§	440.8(2)¶
	3	3	442.6277(5)	441.2(2)§	440.9(2)‖
	2	3	437.9154(20)		
	3	2	447.1876(20)		
7/2	3	3	1094.1871(5)		
	4	4	1094.4596(10)		
	4	3	1093.5326(20)		
	3	4	1095.1179(20)		
9/2	4	4	2158.2986(10)		
	5	5	2158.7239(10)		
	4	5	2160.5318(10)		
	5	4	2156.4902(10)		
11/2	5	5	3714.8864(20)		
	6	6	3715.4892(20)		

* The subscript + (−) refers to the even (odd) Kronig symmetry (Meerts and Dymanus 1972).

† Radford and Linzer 1963.

‡ Tanimoto and Uehara 1973.

§ Brown and Thistlethwaite 1972.

¶ Correction by J. M. Brown added as note in the paper of Tanimoto and Uehara 1973.

77

Dymanus 1972) is used to explain the observed spectrum However, due to the lack of information about the $^2\Pi_{1\,2}$ state, the fine structure constants cannot be determined unambiguously The following hyperfine-structure constants are obtained from the observed spectrum $a + \frac{1}{2}(b + c)$, b, and d, a definition of these constants can be found in Meerts and Dymanus (1972) The obtained values for SH are given in table 2 In this table we also list the ESR results of Tanimoto and Uehara (1973) They are essentially in agreement with the present values The Λ doubling transition frequencies for the lowest J states predicted from ESR investigations are shown in table 1 It should be noted that there are rather strong deviations from the present direct measurements

From the observed Stark shifts of the $^2\Pi_{3/2}$, $J = 5/2$ state and the theory discussed by Meerts and Dymanus (1973), we calculated the electric dipole moment of SH

The value obtained is 0 7580(1) debye Previous measurements of this value by Byfleet, Carrington, and Russell (1971) yielded $\mu = 0\,62(1)$ debye This value is not in agreement with the present more accurate result The calculated dipole moment of SH by Cade and Huo (1966), $\mu = 0\,861$ debye, is in rather good agreement with the present experimental value

TABLE 2

HYPERFINE STRUCTURE CONSTANTS (in MHz) OF SH

Constant	Present Investigation	Tanimoto and Uehara (1973)
$a + \frac{1}{2}(b+c)$	$+17\ 075(6)$	$+17\ 0(2)$
b	$-63\ 540(40)$	$-60(2)$
d	$+27\ 386(60)$	$+29(17)$

REFERENCES

Brown, J M , and Thistlethwaite, P J 1972, *Mol Phys* , 23, 635
Byfleet, C R , Carrington, A and Russell, D K 1971, *Mol Phys* , 20, 271
Cade, P E , and Huo, W M 1966, *J Chem Phys* , 45, 1063
Heiles, C E , and Turner, B E 1971, *Ap Letters*, 8, 89

Meeks, M L , Gordon, M A , and Litvak, M M 1969, *Science*, 163, 173
Meerts, W L , and Dymanus, A 1972, *J Mol Spectrosc* , 44, 320
— 1973, *Chem Phys Letters* (to be published)
Radford, H F , and Linzer, M 1963, *Phys Rev Letters*, 10, 443
Tanimoto, M , and Uehara, H 1973, *Mol Phys* , 25, 1193

A Molecular Beam Electric Resonance Study of the Hyperfine
Λ-doubling Spectrum of OH, OD, SH and SD.[1]

W.L. Meerts and A. Dymanus

Abstract.

The molecular beam electric resonance method was
employed to obtain a complete set of hyperfine Λ-doubling
transitions of the free radicals OH, OD, SH, and SD. The
observed spectra could very well be explained by the degenerate
perturbation theory adapted to the $^2\Pi$ state. The experimental
results include fine and hyperfine coupling constants and the
electric dipole moments for all four molecules, and some
magnetic properties of SH. The deduced hyperfine coupling
constants agree well with the ab-initio calculations.

---

1. Introduction.

The structure and spectra of free radicals, here defined as molecules with one or more unpaired electrons, have been subject of a large number of theoretical studies and of experimental investigations using practically all available spectroscopic techniques. In contrast to the vast majority of stable molecules the ground electronic state of many free radicals is a state with a non-zero electronic orbital and/or spin angular momentum. Because of these angular momenta the energy levels of the radicals show fine structure and effects of the coupling between rotation and electronic motion, such as Λ-doubling in a $^2\Pi$ state and ρ-doubling in a $^2\Sigma$ state. The experimental investigations on the spectra of free radicals range from classical vacuum ultra violet (UV) spectroscopy to gas phase electron paramagnetic resonance (EPR) and microwave spectroscopy. The present communication describes a study of the OH, OD, SH, and SD radicals by the molecular beam electric resonance (MBER) technique. These radicals all have the $^2\Pi_{3/2}$ ground electronic state.

The most extensive measurements and analyses of the UV band spectra of OH were performed by Dieke and Crosswhite (1962). The UV spectrum of OD was measured recently by Clyne et al (1973). The first measurements of the microwave Λ-doubling spectra of OH and OD radicals were reported by Dousmanis et al (1955). The observed spectra originate from direct transitions between the Λ-doublet levels of rotational states in the $^2\Pi_{1/2}$ and the $^2\Pi_{3/2}$ electronic levels. The observed spectra are in the frequency range

80

from 7.7 to 37 GHz. The experimental accuracy of the observed frequencies of Dousmanis et al (1955) varied between 0.05 and 0.5 MHz. An extension (to the order of $(E_{rot}/E_{el})^2$ or $(E_{fine}/E_{el})^2$) of Van Vleck's theory (Van Vleck 1929) of molecular energies in the $^2\Pi$ states was employed to explain the observed spectra. Subsequent investigations on OH by Poynter and Beaudet (1968) on the $^2\Pi_{3/2}$, J = 7/2, 9/2 and 11/2 states, by Radford (1968) on the $^2\Pi_{1/2}$, J = 1/2 and $^2\Pi_{3/2}$, J = 5/2 states, and by Ball et al (1970; 1971) on the $^2\Pi_{1/2}$, J = 3/2 and 5/2 states, improved considerably the accuracy of the zero field transitions. Recently ter Meulen and Dymanus (1972) used a beam-maser spectrometer to obtain very accurate hyperfine Λ-doubling transitions frequencies of the $^2\Pi_{3/2}$, J = 3/2 state of OH. The magnetic properties of OH in the $^2\Pi_{1/2}$, J = 3/2 and 5/2 states and in the $^2\Pi_{3/2}$, J = 3/2, 5/2 and 7/2 states were investigated by Radford (1961; 1962) using the gas phase EPR technique. From the analysis of the EPR spectra Radford deduced the g_J values and the values for the hyperfine constants of OH, and the g_J factor for OD in the $^2\Pi_{3/2}$, J = 3/2 state. Accurate hyperfine Λ-doubling transition frequencies of OD in the $^2\Pi_{1/2}$, J = 1/2 state and in the $^2\Pi_{3/2}$, J = 3/2, 5/2 and 7/2 states were obtained by Meerts and Dymanus (1973a) from an MBER investigation. This investigation yielded also accurate values of the electric dipole moments of both radicals (Meerts and Dymanus 1973b).

The free radicals SH and SD have not been as extensively investigated as OH and OD. Ramsay (1952) obtained and analyzed the $A^2\Sigma \leftarrow X^2\Pi$ band spectra of SH and SD and determined the

rotational and vibrational constants of both radicals. The EPR techniques were used on SH by Radford and Linzer (1963) for the $^2\pi_{3/2}$, $J = 3/2$ state, by Tanimoto and Uehara (1973) for the $^2\pi_{3/2}$, $J = 3/2$ and $5/2$ states, and by Brown and Thistlethwaite (1972) for the $^2\pi_{3/2}$, $J = 5/2$ state. However, neither for SH nor for SD hyperfine Λ-doubling transitions were observed. Those of SH have recently been obtained by Meerts and Dymanus (1974) for the $^2\pi_{3/2}$, $J = 3/2$, $5/2$, $7/2$, $9/2$ and $11/2$ states using the MBER technique.

In the present investigation we used the molecular beam electric resonance technique on OH, OD, SH, and SD in order to obtain a complete as possible set of accurate experimental data on the $\Delta J = 0$ hyperfine Λ-doubling transitions in the lower rotational states of the ground vibrational state and the $^2\pi_{1/2}$ and $^2\pi_{3/2}$ electronic states of the four radicals. This was a logical step in a program on the hyperfine structure of open-shell molecules using the MBER method, which was started with a study of the only stable diatomic radical, NO (Meerts and Dymanus 1972). The MBER technique furnished high resolution hyperfine Λ-doubling spectra of the investigated radicals. The project was undertaken to investigate the feasibility of the MBER technique to short living radicals like OH and SH and to provide accurate hyperfine Λ-doubling spectra for a larger number of open-shell molecules. The experimental spectra could be used for a test of the current theories of the fine and hyperfine interactions in a molecule in a $^2\pi$ state.

82

A degenerate perturbation theory developed previously for the interpretation of the spectra of NO (Meerts and Dymanus 1972) was employed to explain the hyperfine Λ-doubling spectra of OH, OD, SH, and SD. It turned out that the theory extended to third order in fine and hyperfine structure was well capable of explaining the observed spectra for most transitions within the experimental accuracy. Only for the interpretation of the spectrum of OH we suspect that higher order hyperfine structure contributions should be included to improve the agreement between the experimental and the calculated spectrum.

From the analysis of the spectra the molecular properties, related specifically either to the properties of the unpaired π-electron or to the charge distribution of all the electrons in the molecules, could be determined. Ab-initio molecular orbital calculations are available only for the properties of OH and SH directly related to the π-electron distribution. It was found that the ab-initio results of Kayama (1963) for OH and of Kotake et al (1971) and Bendazzoli et al (1972) for OH and SH are in reasonably good agreement with the present experimental results.

The observed laboratory transition frequencies may be of help in the identification of observed spectra from interstellar radio sources and increase the chance of detecting the presence of the OD, the SH or may be even the SD radicals in space. Especially the chance of detecting the SH radical has been considerably improved by the reliable hyperfine Λ-doubling transition frequencies obtained in the present investigation. A search for the emission lines of the SH molecule has already been

83

undertaken by Meeks et al (1969) and by Heiles and Turner (1971).
The attempts were unsuccessful, partly because of the errors in
the Λ-doublet transition frequencies available at that time.

The values of the electric dipole moments of the four
radicals have been obtained from the observed Stark shifts of
some transitions. Significant isotopic effects were found.
Unfortunately, it is not possible to deduce reliable information
about vibrational and centrifugal effects on the electric dipole
moments from the isotopic dependence alone. Herefore measurements
in excited vibrational states are needed.

The SH radical in the $^2\Pi_{1/2}$, J = 1/2 state was also investi-
gated in a magnetic field. An analysis of the spectrum is given
and the g_J-factors of this state are reported. A large difference
of g_J values for the upper and the lower Λ-doublet levels is found.
This effect can be explained by breaking of the symmetry of the
electronic charge distribution around the molecular axis by the
rotation of the molecule.

2. Experimental Techniques.

The experiments were performed using a molecular beam elec-
tric resonance spectrometer described in detail elsewhere (de Leeuw
1971; de Leeuw and Dymanus 1973). Only the features pertinent to
the present investigation are discussed here. In the experi-
ments we used two types of C-fields: (1) a 20 cm long field for
high precision Stark measurements at low frequencies and (2) a
short (about 8 cm) transition field for measurements at frequencies

above about 2 GHz. The latter field, constructed of two flat copper plates, was unsuitable for Stark measurements because of poor DC-field homogeneity. Its small dimensions permitted good shielding of the earth's magnetic field for measurements of the zero-field transition frequencies. We succeeded in shielding the earth's magnetic field to about 5 mG, which was enough even for accurate measurements on the $\Delta F = \pm 1$ transitions (Meerts and Dymanus 1972). The long field consisted of two optically flat quartz plates, coated with a thin gold layer (de Leeuw 1971). The microwave power for inducing the transitions was obtained from a Hewlett-Packard 8660B synthesizer for frequencies below 1 GHz. Three Varian backward wave oscillators were used for the generation of frequencies in the GHz-range. These oscillators were frequency stabilized by phase locking techniques.

The beam was detected by an electron bombardment ionizer designed by Stolte (1972), followed by an electric quadrupole mass selector. The overall efficiency of the detection system was of the order of 2×10^{-3}.
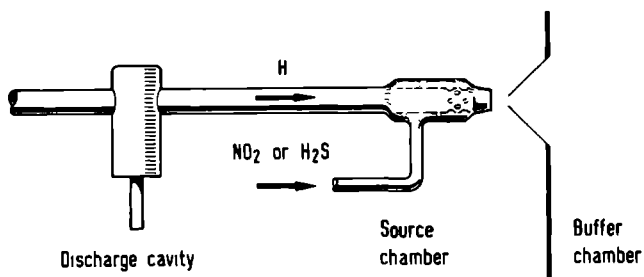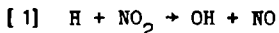

Fig. 6. Schematic diagram of the reaction source.

The beams of short-lived free radicals were produced in a reaction type source schematically shown in Fig. 6. The OH radicals were formed in the reaction between atomic hydrogen and NO_2 by (Del Greco and Kaufman 1962)

[1] $H + NO_2 \rightarrow OH + NO$

For the production of the OD radicals the hydrogen atoms were replaced by deuterium atoms. The SH and SD radicals were produced in the reaction of atomic hydrogen with H_2S and D_2S, respectively, by

[2] $H + H_2S \rightarrow SH + H_2$
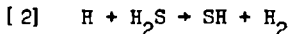
for SH and

[3] $H + D_2S \rightarrow SD + HD$
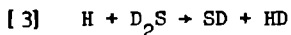
for SD. The atomic hydrogen was obtained from a microwave discharge at 2.45 GHz in water at the entrance of the tube. The power fed into the discharge was usually about 150 W. The deuterium atoms were obtained from a microwave discharge in D_2O. For D_2S we used a 98 % enriched sample. Because the D_2S sample had to be recovered, we also replaced H_2O by D_2O in the production of the SD radicals to reduce contamination of the D_2S sample by H_2S. A reaction of atomic deuterium and H_2S resulted in only a small number of SD radicals and almost the same number

86

of SH radicals as obtained in the reaction [2]. This indicates that the hydrogen atoms probably strip off one of the hydrogen atoms from the H_2S molecule forming H_2 and SH as proposed by McDonald (1963).

To handle the large gas flows, the source chamber was pumped by a mechanical pump system with a capacity of 500 m^3/h. The source chamber was separated from the resonance part of the machine by two buffer chambers, pumped by diffusion pumps. The beam was formed by a conical diaphragm 2 mm in diameter between the source chamber and the first buffer chamber. The distance between this diaphragm and the end of the reaction tube could be varied during the experiment, but was usually 5 to 20 mm.

The observed full linewidth at one half of the peak intensity varied between 3 and 25 kHz, depending on the type of C-field and on the observed transitions. The linewidths for the $\Delta F = 0$ transitions were determined essentially by the transit time of the molecules through the resonance region (C-field). However, the linewidths for the $\Delta F = \pm 1$ transitions were largely determined by the residual earth's magnetic field (Meerts and Dymanus 1972). The observed signal to noise ratio at RC = 5 s for the transitions of OH, OD, SH and SD was typically 100, 40, 20 and 6, respectively. A spectral line of a transition of SH in the $^2\Pi_{3/2}$, J = 3/2 state is shown in Fig. 8.

3. Theory.

The Hamiltonian for the interpretation of high-resolution spectra of the open-shell diatomic molecules can be written formally as

$$[4] \quad \underline{H} = \underline{H}_0 + \underline{H}_F + \underline{H}_{hf} + \underline{H}_{ST},$$

where $\underline{H}_0$ is the non-relativistic Hamiltonian for electronic energies in the Born-Oppenheimer approximation, $\underline{H}_F$ contains the spin-orbit and the rotational and gyroscopic terms which give rise to the Λ-splitting and the fine structure, $\underline{H}_{hf}$ describes the hyperfine contributions and the last term $\underline{H}_{ST} = -\underline{\mu}.\underline{E}$ gives the interaction of the electric dipole moment $\underline{\mu}$ of the molecule with an external electric field $\underline{E}$ (Stark effect). For $\underline{H}_F$ we used the expression of Van Vleck (1929)

$$[5] \quad \underline{H}_F = B(\underline{J}^2 - \underline{L}_z^2 + \underline{S}^2) + A\underline{L}_z\underline{S}_z - 2B\underline{J}.\underline{S}$$

$$+ (B + \tfrac{1}{2}A)(\underline{L}_+\underline{S}_- + \underline{L}_-\underline{S}_+) - B(\underline{J}_+\underline{L}_- + \underline{J}_-\underline{L}_+).$$

Herein A is the spin-orbit constant, B is the rotational constant; $\underline{L}$ and $\underline{S}$ represent the orbital and spin angular momentum of the electrons, respectively; $\underline{J}$ stands for the total rotational angular momentum including the rotation of the nuclear frame, but excluding the nuclear spins. The hyperfine Hamiltonian $\underline{H}_{hf}$ expressed in spherical tensor operators is (Freed 1966):

$$[6] \quad \underline{H}_{hf} = \zeta \sum_q (-1)^q T_q^{(1)}(\underline{I}) T_{-q}^{(1)}(\underline{L}_1)/r_{1I}^3 \; +$$

$$+ \; \zeta\sqrt{30} \sum_{q,\mu} \begin{pmatrix} 1 & 1 & 2 \\ \mu & q-\mu & -q \end{pmatrix} T_\mu^{(1)}(\underline{S}_1) T_{q-\mu}^{(1)}(\underline{I}) c_{-q}^{(2)}(\theta_{1I}, \phi_{1I})/r_{1I}^3 \; +$$

$$+ \; \frac{8}{3}\pi \zeta \sum_q (-1)^q T_q^{(1)}(\underline{I}) T_{-q}^{(1)}(\underline{S}_1) \delta(r_{1I}) \; +$$

$$+ \; \sum_q (-1)^q T_q^{(2)}(\underline{Q}) T_{-q}^{(2)}(\underline{V}_1) + C_{RS} \, \underline{I} \cdot \underline{J}$$

Herein $\zeta = g \, g_I \, \mu_o \, \mu_N$, where g, g_I, μ_o, and μ_N is the g value for the free electron, the nuclear g-factor, the Bohr magneton, and nuclear magneton, respectively; r_{1I} is the distance between electron 1 and the nucleus I, $T^{(1)}(\underline{M})$ is the spherical tensor of rank 1 constructed from the components of an angular momentum $\underline{M} = (\underline{I}, \underline{L}_1, \underline{S}_1)$, while:

$$[7] \quad T^{(2)}(\underline{Q}) = \sum_{\text{protons } p} e_p \, r_p^2 \, c^{(2)}(\theta_p, \phi_p)$$

$$[8] \quad T^{(2)}(\underline{V}_1) = - e \, c^{(2)}(\theta_{1I}, \phi_{1I})/r_{1I}^3 + Z_K \, c^{(2)}(\theta_{KI}, \phi_{KI})/R_{KI}^3$$

are spherical tensor operators of rank two describing the nuclear quadrupole moment (tensor) and the gradient of the electric field at the position of the nucleus I in the molecule. In expression [7] and [8] Z_K is the atom number of the second nucleus K ($K \neq I$) and R_{KI} is the distance between the two nuclei, $\theta_{1I}(\theta_{KI})$ is the angle between $\vec{r}_{1I}(\vec{R}_{KI})$ and the bond axis (z-axis) and $\phi_{1I}(\phi_{KI})$ is the azimuthal angle. The hyperfine interactions of Fq. [6] are written in one electron notation as used in the reduced density

matrix formulation (McWeeny 1960; McWeeny 1965).

The first contribution to the hyperfine Hamiltonian of Eq. [6] represents the interaction between the magnetic moment $\underline{\mu}_I$ associated with nuclear spin $\underline{I}$ and the orbital angular momentum $\underline{L}$ of the electrons. The second term describes the interaction of $\underline{\mu}_I$ with the spin angular momentum $\underline{S}$ of the electrons with zero density at the nucleus I. The third term is the Fermi contact term. The fourth contribution to $\underline{H}_{hf}$ is due to the nuclear electric quadrupole interaction. The last term represents the interaction between $\underline{\mu}_I$ and the orbital motion of the nuclei due to the rotation of the molecule (spin-rotation interaction); C_{RS} is the coupling constant of this interaction.

With the Hamiltonian of Eq. [5] and [6] the spectrum has been calculated using the degenerate perturbation theory described by Freed (1966) extended and adapted to a $^2\Pi$ state by Meerts and Dymanus (1972). Application of this theory to the Hamiltonians $\underline{H}_F$ and $\underline{H}_{hf}$ (zero external field) involves the solution of a 4 x 4 secular equation. However, these Hamiltonians are invariant under reflections of the coordinates and spins of all the particles in a plane containing the nuclei. Consequently if wavefunctions are used with the proper Kronig symmetry (Van Vleck 1929) with respect of these reflections, the secular determinant factors into two 2 x 2 determinants.

The coupling scheme for the electronic and rotational part of the wavefunction adopted in the calculations is the Hund's (a). Wavefunctions, $|{}^2\Pi^+_{|\Omega|}, J>$, including nuclear rotation are in this coupling scheme defined as:

[9] $|{}^2\Pi_{|\Omega|}^+$, $J> = \frac{1}{\sqrt{2}} \left[|J\Lambda\Sigma\Omega> \pm |J -\Lambda -\Sigma -\Omega> \right]$

with $\Omega = \Lambda + \Sigma$; Λ, Σ and Ω are the projections on the molecular
axis of $\underline{L}$, $\underline{S}$ and $\underline{J}$, respectively; $|\Omega|$ can take the values 1/2 and
3/2. The wavefunctions $|J\Lambda\Sigma\Omega>$ are given by Freed (1966). The total
wavefunction $|{}^2\Pi_{|\Omega|}^{\pm}$ $JIFM_F>$ of the molecule including the nuclear
part is obtained as a product of the electronic-rotational wave-
function $|{}^2\Pi_{|\Omega|}^{\pm}$, $J>$ and of the nuclear spin wavefunction $|I\ M_I>$
corresponding to the coupling scheme: $\underline{F} = \underline{J} + \underline{I}$, where $\underline{F}$ is the
total angular momentum of the molecule. These wavefunctions are
used as a basis for the degenerate perturbation calculation of
the energy matrix.

All molecules investigated can be described by a coupling
which is intermediate between the Hund's case (a) and (b). The
proper wavefunctions are obtained automatically by solving the
secular problem. The contributions of the fine and hyperfine
interactions to the energy are taken into account up to third
order. In the final expressions for the state energies we
separate terms with different dependence on the rotational
quantum number J, as only these terms can be determined from the
experimental data. The matrix elements of $\underline{H}_F$ and $\underline{H}_{hf}$ in terms of
J and a number of coupling constants were obtained using the
degenerate perturbation theory developed in a previous paper
(Meerts and Dymanus 1972). The results are

[10] $\langle {}^2\Pi^{\pm}_{\frac{1}{2}}|\underline{H}_F+\underline{H}_{hf}|{}^2\Pi^{\pm}_{\frac{1}{2}}\rangle$ =

$-\frac{1}{2}\alpha_1+\alpha_2(J+\frac{1}{2})^2+\alpha_{10}(J+\frac{1}{2})^4\pm\alpha_3(2J+1)\pm\alpha_4(J+\frac{1}{2})^3\pm\alpha_5(J+\frac{1}{2})z^2$

$+ y\{(\chi_1+z^2\chi_5)\pm(J+\frac{1}{2})(\chi_2+z^2\chi_6)\}+u\{(\frac{3}{4}-x)(\zeta_1+\zeta_4 J(J+1))\pm\zeta_5 z^2(J+\frac{1}{2})\}$,

[11] $\langle {}^2\Pi^{\pm}_{\frac{3}{2}}|\underline{H}_F+\underline{H}_{hf}|{}^2\Pi^{\pm}_{\frac{3}{2}}\rangle$ =

$\frac{1}{2}A_\Pi+B_\Pi(J(J+1)-\frac{7}{4})+\alpha_9 z^2+\alpha_{10}(J+\frac{1}{2})^2 z^2\pm\alpha_8(J+\frac{1}{2})z^2$

$+ y\{\chi_3+z^2\chi_7\}+u\{(\frac{27}{4}-x)(\zeta_2+\zeta_4 J(J+1))+(\zeta_7\pm\zeta_5(J+\frac{1}{2}))z^2\}$,

[12] $\langle {}^2\Pi^{\pm}_{\frac{1}{2}}|\underline{H}_F+\underline{H}_{hf}|{}^2\Pi^{\pm}_{\frac{3}{2}}\rangle$ =

$\alpha_6 z+\alpha_{11}z(J+\frac{1}{2})^2\pm\alpha_7 z(J+\frac{1}{2})\pm\alpha_8 z(J+\frac{1}{2})^3$

$+ zy\{(\chi_4+z^2\chi_8)\pm\chi_9(J+\frac{1}{2})\}+zu\{\pm(\zeta_3+\zeta_5 J(J+1))(J+\frac{1}{2})+(\zeta_6-\zeta_4 J(J+1))\}$.

Herein: $z = \sqrt{(J-\frac{1}{2})(J+\frac{3}{2})}$,

$x = J(J+1)$,

$y = (F(F+1)-J(J+1)-I(I+1))/(2J(J+1))$,

$u = \dfrac{\frac{3}{4}C(C-1)-J(J+1)I(I+1)}{2I(2I-1)J(J+1)(2J-1)(2J+3)}$,

$C = I(I+1)+J(J+1)-F(F+1)$.

The upper sign in Eq. [10], [11] and [12] is appropriate for the states with $(-1)^{J-\frac{1}{2}}$ Kronig symmetry, the lower sign for states with $(-1)^{J+\frac{1}{2}}$ Kronig symmetry.

92

The coupling constants A_Π, B_Π and α_i describe the contributions to the fine structure and the Λ-splitting in the various orders of approximation. In the first order α_1 can be approximated by A_Π, the spin orbit coupling constant of a Π state; α_2 and α_6 by B_Π the rotational constant of a Π state. In the second and third order all α_i's are essentially different, but to a good approximation $\alpha_1 \simeq A_\Pi$, $\alpha_2 \simeq B_\Pi + \alpha_7$, $\alpha_6 \simeq B_\Pi + \alpha_3$, $\alpha_9 \simeq \alpha_7$ and $\alpha_8 \simeq \alpha_5 (B_\Pi - B_\Sigma)/B_\Pi$, where B_Σ is the rotational constant of a Σ state. The coupling constants α_4, α_5, α_8, α_9, α_{10} and α_{11} contain only third order effects, but only α_4, α_5 and α_8 contribute directly to the Λ-splitting. The coupling constants α_{10} and α_{11} are set to zero because they do not contribute directly to the Λ-splitting and their effects are too small to be detected. The coupling constants χ_i are associated with the magnetic hyperfine interactions and ζ_i's with the electric quadrupole interaction. The coupling constant χ_5, χ_6, χ_7, χ_8, χ_9 and ζ_4, ζ_5, ζ_6, ζ_7 contain only third order effects, while the others contain second as well as third order contributions. From the observed spectra it was found that the contributions to the energy of χ_8, ζ_4, ζ_6 and ζ_7 were too small to be determined and the constants were taken equal to zero.

The coupling constants α_i, χ_i, ζ_i are rather complex expressions containing first, second as well as third order contributions. They are tabulated by Meerts and Dymanus (1972). A comparison of the present hyperfine coupling constants χ_i, ζ_i with those of the conventional theory (Dousmanis et al 1955; Radford 1961; Radford 1962; Lin and Mizushima 1955) can only be

made if the third order effects are neglected. In this approximation the relations between the present and the conventional hyperfine structure coupling constants are:

[13] $\chi_1 = \frac{1}{2}(a-\frac{1}{2}(b+c))$

[14] $\chi_2 = \frac{1}{2}d$

[15] $\chi_3 = \frac{3}{2}(a+\frac{1}{2}(b+c))$

[16] $\chi_4 = -\frac{1}{2}b$

[17] $\zeta_1 = \zeta_2 = eQq_1$

[18] $\zeta_3 = \frac{1}{2}eQq_2$

If third order effects are neglected the relations between the present Λ-splitting parameters and those used by other investigators are:

[19] $\alpha_3 = -\frac{1}{2}\alpha = \frac{1}{4}p + \frac{1}{2}q$

[20] $\alpha_7 = -\beta = \frac{1}{2}q$

α, β were used by Dousmanis et al (1955) and p, q were introduced by Mulliken and Christy (1931)

The contributions to the energy of the last term of the Hamiltonian [3], the Stark effect, is extensively discussed by Meerts and Dymanus (1973b) and the formulae are not reproduced here.

94

The observed spectra of OH, OD, SH and SD are analysed using the theory outlined above. However, in this theory developed primarily for NO, the centrifugal distortion effects are neglected. The neglect was fully justified for NO but such is not the case for the light molecules of the present investigation. A simple replacement of B_Π by $B_\Pi - D_\Pi J(J + 1)$ with D_Π the centrifugal distortion constant in the above equations is not correct. Problems arise because in the present calculations the values of B_Π, D_Π, accepted for all four molecules and for SH and SD also the values of A_Π are those obtained from analyses of rovibronic or electronic spectra. As these analyses are based on an effective Hamiltonian which is slightly different from the present one the spectroscopic constants derived are different. In order to obtain compatible constants A_Π, B_Π, and D_Π for the calculations of the state energies we have to use a Hamiltonian compatible with the one used in the analyses of the electronic or rovibronic spectra.

The electronic spectra of SH and SD were analysed by Ramsay (1952) using the expressions given by Almy and Horsfall (1937). These expressions are based on the Hund's case (a) representation, which we also used. So for the interpretation of the spectra of SH and SD our expressions [10], [11] and [12] are compatible (in this case identical) with those of Almy and Horsfall. The centrifugal distortion effects are taken care of simply by adding the contributions of D_Π in Eq. [10], [11] and [12] with the value of D_Π determined by Ramsay (1952). The rotational constants B_Π and D_Π of OH and OD were obtained by Dieke and Cross-white (1962) from a fit of the ultraviolet band spectrum to the

theoretical spectrum calculated using a Hund's case (b) represen-
tation. In order to take correctly into account the contri-
butions of B_Π and D_Π for OH and OD, we have to use the Dieke and
Crosswhite's expression for the rotational energy, or what comes
to the same, to transform the Hund's case (b) rotational Hamil-
tonian used by Dieke and Crosswhite to the case (a) representation.
The rotational energy of a $^2\Pi$ molecule in the Hund's case (b)
representation is given by $B(K(K+1)-1)$, where $B = B_\Pi(1-D_\Pi/B_\Pi K(K+1))$
and K can take the values $J + \frac{1}{2}$ and $J - \frac{1}{2}$. In this representation
the 2 x 2 rotational energy matrix can be written in the form

$$[21] \quad (\underline{H}_R)_b = \begin{bmatrix} B_1((J - \frac{1}{2})(J + \frac{1}{2}) - 1) & 0 \\ & \\ 0 & B_2((J + \frac{3}{2})(J + \frac{1}{2}) - 1) \end{bmatrix}$$

where $B_1 = B_\Pi - D_\Pi(J - \frac{1}{2})(J + \frac{1}{2})$ and $B_2 = B_\Pi - D_\Pi(J + \frac{1}{2})(J + \frac{3}{2})$.
This matrix can be transformed to the Hund's case (a) representa-
tion by the transformation:

$$[22] \quad (\underline{H}_R)_a = \underline{R}^+ (\underline{H}_R)_b (\underline{R})$$

where

$$[23] \quad \underline{R} = \frac{1}{\sqrt{2J + 1}} \begin{bmatrix} -\sqrt{J - \frac{1}{2}} & \sqrt{J + \frac{3}{2}} \\ & \\ \sqrt{J + \frac{3}{2}} & \sqrt{J - \frac{1}{2}} \end{bmatrix}$$

The matrix $(\underline{H}_R)_a$ contains the contributions of B_Π which are the
same as Eq. [10], [11] and [12].

All molecules discussed in this paper are properly des-

96

cribed in a Hund's case intermediate between (a) and (b). The ratio between the spin-orbit energy and the rotational energy (λ) is a measure for the mixing of the $^2\Pi_{1/2}$ and the $^2\Pi_{3/2}$ levels. The smaller the value of $|\lambda|$ is, the stronger is the effect of the mixing. This mixing also depends on D_Π. As pointed out by Mee⁻ts and Dymanus (1973b) the determination of molecular constants which are sensitive to this mixing, e.g. α_4, α_5, X_4, X_9, ζ_3 and the electric dipole moment μ, will be affected by the value of B_Π, D_Π and A_Π. However, only for $OH(\lambda = -7.5)$ these mixing effects do play a role in the determination of the molecular constants, and the values as obtained from the least squares fit of the spectra depend slightly on the choice of B_Π and D_Π. For OD $(\lambda = -14.0)$, SH $(\lambda = -39.8)$ and SD $(\lambda = -76.9)$ the effects of the mixing of the $^2\Pi_{1/2}$ ard $^2\Pi_{3/2}$ levels on the determination of the molecular constants can be neglected.

4. Experimental results and analysis of the spectra.

All the observed transitions involved the electric dipole transitions between hyperfine sublevels in zero magnetic field from a +Kronig symmetry level to a -Kronig symmetry level within one J-state of the $^2\Pi_{1/2}$ or the $^2\Pi_{3/2}$ electronic level. The molecular and hyperfine constants were obtained from the fit of the observed spectra to the spectra calculated using the theory outlined in the previous section. The values of the molecular constants taken from other sources and used in the analysis of the spectra are reproduced in Table 5. The physical constants

Table 1. Observed and calculated hyperfine Λ-doubling transitions of OH. PI stands for present investigations.

J	Ω	F_+	F_-[a]	Observed frequency (MHz)	Reference	Observed minus calculated frequency (kHz)
1/2	1/2	1	1	4750.656(3)	b.	27.5
		0	1	4660.242(3)	b.	24.7
		1	0	4765.562(3)	b.	19.3
3/2	1/2	1	1	7761.747(5)	c.	-7.5
		2	2	7820.125(5)	c.	0.3
		2	1	7749.909(5)	c.	-9.2
		1	2	7831.962(5)	c.	1.1
5/2	1/2	2	2	8135.870(5)	PI[d]	0.8
		3	3	8189.587(5)	PI[d]	4.6
		2	3	8118.051(5)	PI[d]	-4.5
		3	2	8207.402(5)	PI[d]	5.8
7/2	1/2	3	3	5473.045(5)	PI	-4.3
		4	4	5523.438(5)	PI	-12.6
		4	3	5449.436(5)	PI	-12.8
		3	4	5547.042(5)	PI	-9.1
9/2	1/2	4	4	164.7960(10)	PI[e]	-4.1
		5	5	117.1495(10)	PI[e]	-5.6
		4	5	192.9957(10)	PI[e]	-11.3
		5	4	88.9504(10)	PI[e]	2.1
3/2	3/2	1	1	1665.40184(20)	f.	26.0
		2	2	1667.35903(20)	f.	27.4
		2	1	1612.23101(20)	f.	28.0
		1	2	1720.52998(20)	f.	25.4
5/2	3/2	2	2	6030.747(5)	PI	-20.2
		3	3	6035.092(5)	PI	-18.2
		2	3	6016.746(5)	PI[b]	-25.7
		3	2	6049.084(8)	b.	-21.7
7/2	3/2	3	3	13434.62(1)	g.	-65
		4	4	13441.36(1)	g.	-100
9/2	3/2	4	4	23817.6153(20)	h.	6.3
		5	5	23826.6211(30)	h.	5.5
		4	5	23838.46(1)	g.	-480
		5	4	23805.13(1)	g.	-150
11/2	3/2	5	5	36983.47(3)	g.	-940
		6	6	36994.43(5)	g.	-910

a) The subscript + (-) refers to the even (odd) Kronig symmetry
b) Radford (1968)
c) Ball et al (1970)
d) Also reported by Ball et al (1971)
e) Reported by Meerts and Dymanus (1973b)
f) ter Meulen and Dymanus (1972)
g) Poynter and Beaudet (1968)
h) ter Meulen (1970)

were taken from Taylor et al (1969). The measurements and results
are reported below for the individual molecules.

4.1. The spectrum of the OH radical.

The first measurements of the Λ-doubling transitions of OH
were performed by Dousmanis et al (1955), on the $^2\Pi_{1/2}$, J = 3/2
and 5/2 states and on the $^2\Pi_{3/2}$, J = 7/2, 9/2 and 11/2 states. The
spectra of these transitions have been reinvestigated using impro-
ved experimental techniques by several investigators (Poynter and
Beaudet 1968; Radford 1968; Ball et al 1970; Ball et al 1971; ter
Meulen and Dynamus 1972, see also Table 1). We investigated the
J = 5/2 state of the $^2\Pi_{3/2}$ level, and the J = 5/2, 7/2 and 9/2
states of the $^2\Pi_{1/2}$ level to obtain a complete set of the zero
field transition frequencies of the lower J-states of the $^2\Pi_{1/2}$
and the $^2\Pi_{3/2}$ levels. The transition frequencies of the $^2\Pi_{1/2}$,
J = 9/2 state have already been reported in a previous communica-
tion (Meerts and Dymanus 1973b). A list of all the available data
and the references on the hyperfine Λ-doubling transitions of OH
is given in Table 1. A few remarks should be made about this Table.
The $\Delta F = 0$ transitions of the J = 9/2, $^2\Pi_{3/2}$ state have also been
measured by Poynter and Beaudet (1968), but only the much more
accurate frequencies obtained by ter Meulen (1970) with a beam
maser are reproduced in Table 1. We also remeasured the transi-
tions of the $^2\Pi_{3/2}$, J = 5/2 state and found that the $\Delta F = 0$
transitions slightly deviate from the results of Radford (1968).
The transitions observed in the J = 5/2 state of the $^2\Pi_{1/2}$ level

are in agreement with those of Ball et al (1971).

The transition frequencies of Table 1 were used in a least squares fit to the calculated spectrum. The fine structure contributions are determined by B_π, D_π, A_π, α_3, α_7, α_4, and α_5. The first two constants were taken from the results of Dieke and Crosswhite (1962) and the remaining five were varied in the fit. For the hyperfine contributions we essentially used the same approach as in the analysis of the spectra of NO (Meerts and Dymanus 1972) but with a modification for the hyperfine constants X_4, X_5 and X_7. As shown by Meerts and Dymanus (1972) these constants are related:

[24] $X_5' = X_5 - \alpha X_4$

[25] $X_7' = X_7 + \alpha X_4$

In a molecule, which can well be described by the Hund's case (a) approximation, α depends weakly on J. However, the OH radical belongs to the class intermediate between Hund's case (a) and (b). Because of the very strong coupling between the $^2\Pi_{1/2}$ and the $^2\Pi_{3/2}$ level (small absolute value of A_π/B_π) α varies by about 10 % for the investigated J states. So X_4, X_5 and X_7 can, in principle, be determined independently. Unfortunately the correlation between these three constants was still too large to calculate all of them from the observed spectra. We decided to choose for a variation of X_4 and of $X_5 + X_7$. The other hyperfine constants varied in the least squares fit were X_1, X_2, X_3, X_6 and X_0. The molecular constants of OH obtained in this way are given in

100

Table 4. A comparison between the experimental spectrum and the
spectrum calculated using the best fit constants is shown in
Table 1. The agreement between experimental and predicted fre-
quencies is satisfactory. However, the results are not as good as
we hoped, especially if compared with the results for OD (Table 2
and next section). The experimental results obtained by Poynter
and Beaudet (1968) deviate strongly from the calculated frequen-
cies. These results are not self consistent. The transitions of
the $J = 9/2$ state of the $^2\Pi_{3/2}$ level has to fulfil the following
sum rule

$$[26] \quad \nu(5_+ \rightarrow 4_-) = \nu(4_+ \rightarrow 4_-) + \nu(5_+ \rightarrow 5_-) - \nu(4_+ \rightarrow 5_-)$$

Herein $\nu(F_+ \rightarrow F'_-)$ is the frequency of the transition from F_+ to
F'_-. The observed transitions of Poynter and Beaudet violate this
rule by 670 kHz in spite of the claimed experimental accuracy of
10 kHz. As we used their results in the fit we decided to increase
the quoted errors to 200 kHz. Unfortunately, we are not able to
measure these transitions at this moment to check the reliability
of the calculations. However, in view of the results on the spectra
of the other radicals discussed in the next sections, we feel that
the employed theory is capable of predicting the transitions of
the $J = 7/2$, 9/2 and 11/2 states of the $^2\Pi_{3/2}$ level to within 30
kHz.

　　　　Recently Destombes et al (1974) reanalysed the spectrum of
OH by applying the theory of Poynter and Beaudet (1968) to the ob-
served Λ-doubling transitions of OH presented in Table 1 excluding

Table 2. Observed and calculated hyperfine Λ-doubling transitions of OD as obtained in the present experiments.

J	Ω	F_+[a]	F_-	Observed frequency (MHz)	Observed minus calculated frequency (kHz)
3/2	1/2	1/2	1/2	5887.741(5)	-0.3
		3/2	3/2	5894.680(5)	0.4
		5/2	5/2	5906.215(5)	1.8
		3/2	1/2	5887.282(5)	-2.1
		1/2	3/2	5895.135(5)	-1.8
		5/2	3/2	5894.179(5)	-1.5
		3/2	5/2	5906.712(5)	-0.3
5/2	1/2	3/2	3/2	8110.717(5)	2.8
		5/2	5/2	8118.013(5)	7.5
		7/2	7/2	8128.181(5)	7.0
		3/2	5/2	8109.994(5)	3.8
		5/2	3/2	8118.733(5)	3.5
		5/2	7/2	8117.228(5)	5.3
		7/2	5/2	8128.961(5)	4.2
9/2	3/2	7/2	7/2	5304.015(5)	-4.1
		9/2	9/2	5304.600(5)	-3.7
		11/2	11/2	5305.372(5)	-1.0
		7/2	9/2	5304.681(5)	3.1
		9/2	11/2	5305.619(5)	-0.4
		11/2	9/2	5304.359(5)	1.8

a) The subscript + (-) refers to the even (odd) Kronig symmetry.

those of the $^2\Pi_{1/2}$, $J = 7/2$ and $9/2$ states. The disagreement between the observed frequencies and those calculated by Destombes et al is an order of magnitude larger than obtained from the present calculations. This is due to the neglect of third order hyperfine structure contributions in the calculations of Destombes et al (1974).

4.2. The spectrum of the OD radical

In a previous investigation on the OD radical (Meerts and Dymanus 1973a) we reported the hyperfine Λ-doubling transitions in a number of rotational states of the $^2\Pi_{3/2}$ and $^2\Pi_{1/2}$ electronic state. In the latter state only the transitions in the rotational state $J = 1/2$ were measured from which only limited information about the fine and hyperfine structure of the $^2\Pi_{1/2}$ level could be obtained. So we decided to investigate also the $J = 3/2$ and $5/2$ rotational states of the $^2\Pi_{1/2}$ level, and also the $J = 9/2$ state of the $^2\Pi_{3/2}$ level. The observed transition frequencies are given in Table 2. A recalculation of the molecular constants in a least squares fit was performed using the new experimental transition frequencies $\nu_{ex}(i,w)$, and those obtained previously $\nu_{ex}(i,p)$ (Meerts and Dymanus 1973a). We used essentially the same theory as for OH, extended to include the electric quadrupole interaction due to the nuclear spin of the deuteron $(I = 1)$. The contributions of this interaction are described by ζ_1, ζ_2, ζ_3, and ζ_5. A comparison between $\nu_{ex}(i,w)$ and the calculated spectrum using the best fit constants is shown in Table 2. It is seen that the overall agree-

103

ENERGY SCHEME SH

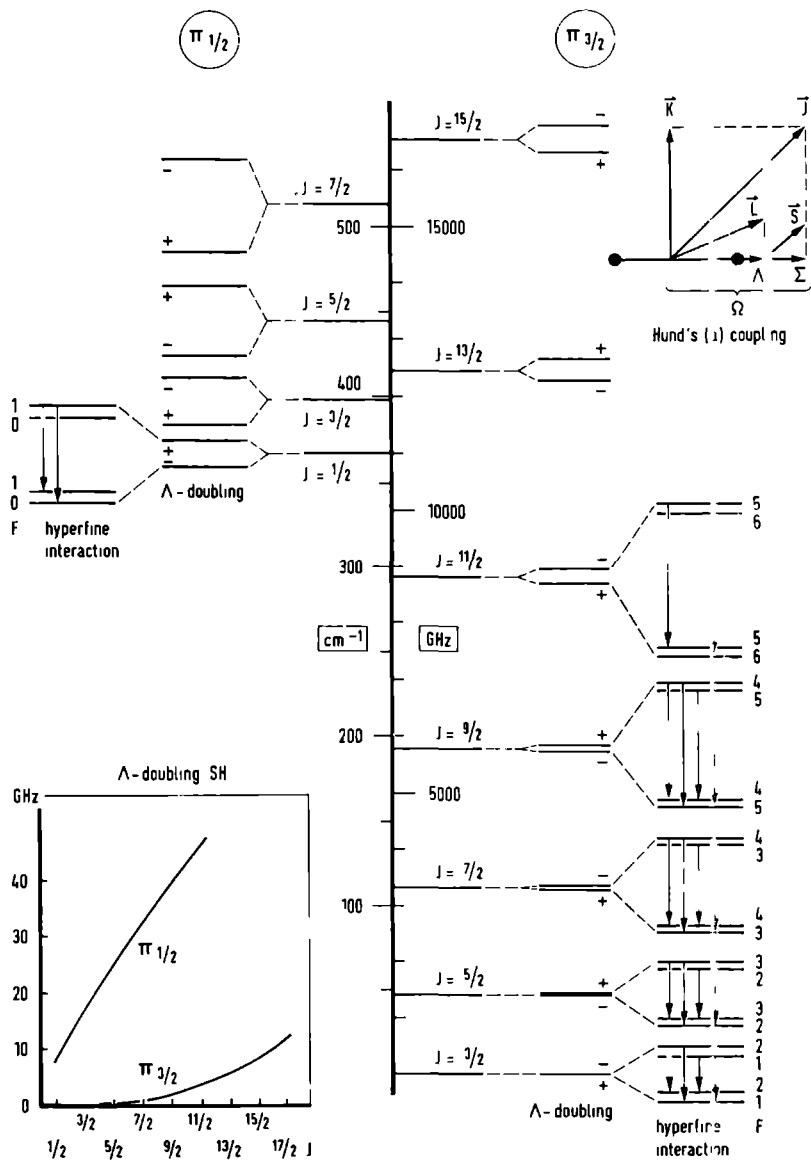**Fig. 7.** Energy level diagram of the lower rotational states of SH.

ment is quite good, while for $\nu_{ex}(i,p)$ the differences with the calculated frequencies are generally smaller than 1 kHz. So the $\nu_{ex}(i,p)$ values are not reproduced here. The molecular constants of OD obtained from the least squares fit of all the available transitions are given in Table 4.

4.3. The SH radical.

The Λ-doubling transitions in the lowest rotational states J = 3/2, 5/2, 7/2, 9/2 and 11/2 of the $^2\Pi_{3/2}$ level of SH were measured recently by Meerts and Dymanus (1974). In order to obtain information about the $^2\Pi_{1/2}$ level, we measured two transitions in the J = 1/2 state of the $^2\Pi_{1/2}$ level at about 8.4 GHz. The transitions could unambiguously be identified from the splittings in a magnetic field of 100 G. The transition frequency is 8445.211(5) MHz for the $F_+ \rightarrow F_- = 1_+ \rightarrow 1_-$ transition and 8459.034(5) MHz for the $F_+ \rightarrow F_- = 1_+ \rightarrow 0_-$ transition. The details of the procedure are given in an internal report (Meerts 1974). The observed magnetic spectrum of $^2\Pi_{1/2}$ level of SH is discussed in Sect. 4.6. The energy level scheme of the lowest rotational states of SH and the observed transitions of SH are shown in Fig. 7.

In the fit both the transition frequencies in the $^2\Pi_{1/2}$, J = 1/2 state obtained in the present investigation and those of the $^2\Pi_{3/2}$, J = 3/2, 5/2, 7/2, 9/2 and 11/2 states reported previously (Meerts and Dymanus 1974) were used. The least squares fit procedure differed slightly from that used in the analyses of the spectra of OH and OD. It was found that the spin-orbit coupling constant A_Π

105

Table 3. Observed and calculated hyperfine Λ-doubling transitions of SD in the $\Pi_{3/2}$ state obtained in the present measurements.

J	F_+ a)	F_-	Observed frequency (MHz)	Observed minus calculated frequency (kHz)
3/2	5/2	5/2	16.120(3)	−0.1
	3/2	1/2	14.719(5)	−2.1
	7/2	5/2	13.643(3)	−2.0
	5/2	7/2	18.591(3)	0.6
5/2	3/2	3/2	64.295(1)	0.3
	5/2	5/2	64.299(1)	0.5
	7/2	7/2	64.307(1)	−0.2
	3/2	5/2	63.410(5)	−2.1
	5/2	3/2	65.181(1)	−0.1
	5/2	7/2	63.096(3)	−2.0
	7/2	5/2	65.505(2)	−2.6
7/2	5/2	5/2	160.1546(10)	0.3
	7/2	7/2	160.1617(10)	−1.1
	9/2	9/2	160.1767(7)	−1.2
	7/2	5/2	159.635(2)	−0.8
	5/2	7/2	160.6807(10)	−0.6
	9/2	7/2	159.5752(10)	0.5
	7/2	9/2	160.7660(10)	0.0
9/2	7/2	7/2	318.8188(7)	−0.3
	9/2	9/2	318.8334(7)	−0.2
	11/2	11/2	318.8568(7)	0.2
	7/2	9/2	318.583(2)	0.9
	9/2	7/2	319.071(1)	0.5
	9/2	11/2	318.640(1)	0.6
	11/2	9/2	319.052(1)	1.2
11/2	13/2	13/2	554.8335(1)	0.5
13/2	11/2	11/2	881.757(2)	−0.3
	13/2	13/2	881.788(2)	−0.4
	15/2	15/2	881.831(1)	−0.2
	11/2	13/2	881.959(5)	−0.1

a) The subscript + (−) refers to the even (odd) Kronig symmetry.

could not be obtained from the observed SH spectrum and had to be kept constant. The value derived by Ramsay (1952) was used. As only one J-state of the $^2\Pi_{1/2}$ level was measured, only the hyperfine constants χ_1, χ_2, χ_3, and χ_4 could be deduced. The remaining constants $(\chi_5 + \chi_7, \chi_6,$ and $\chi_9)$ describe the third order hyperfine contributions and can only be obtained if also transitions in higher rotational states are measured. The molecular constants obtained for SH are given in Table 4. The differences between the calculated spectra using the best fit constants of Table 4 and the observed frequencies lie within the quoted experimental accuracy of 0.5 - 5 kHz for each transition in the $^2\Pi_{3/2}$ and $^2\Pi_{1/2}$ state. This indicates a very good agreement between theory and experiment for SH.

4.4. The SD radical.

Serious problems were encountered in obtaining the Λ-doubling spectrum of SD mainly because of the poor signal to noise ratio. The total number of SD radicals produced in the beam was the same as the number of SH radicals. However, the population of the rotational states for SD is lower than for SH by a factor of about two. Moreover the J-states of SD are split into more hyperfine levels than those of SH. The observed signal to noise ratio varied between 1 and 10 at RC = 5 s. The frequencies of the weakest transitions were obtained by applying signal averaging techniques. We investigated the J = 3/2 to J = 13/2 states of the $^2\Pi_{3/2}$ level of SD. An unsuccessful search was made for the transitions in the lowest rotational state J = 1/2 of $^2\Pi_{1/2}$. The observed transitions of the $^2\Pi_{3/2}$ level of SD are

Table 4. Molecular constants of OH, OD, SH, and SD obtained from a least squares fit of the observed spectra.

Quantity	Molecule			
	OH	OD	SH	SD
$A_\Pi^{a)}$ (cm^{-1})	-139.38(2)	-139.22(2)		
α_3 (MHz)	1184.407(2)	776.588(2)	2108.0(2)	
α_7 (MHz)	-582.61(2)	-164.69(2)	-141.9(1)	
α_4 (MHz)	-2.937(4)	-0.527(3)	2.1(4)	
α_5 (MHz)	2.813(4)	0.407(3)	0.50(4)	
X_1 (MHz)	39.497(8)	6.078(1)	24.04(6)	
X_2 (MHz)	28.311(9)	4.384(1)	13.68(6)	2.10(8)
X_3 (MHz)	139.55(4)	21.654(7)	25.617(8)	4.022(5)
X_4 (MHz)	59.04(4)	9.034(10)	31.72(2)	4.824(15)
$X_5 + X_7$ (kHz)	-201(8)	-16(3)		
X_6 (kHz)	-11(1)	-1.2(7)		
X_9 (kHz)	-16(3)	-1.2(7)		
ζ_1 (kHz)		284(7)		
ζ_2 (kHz)		286(7)		149(4)
ζ_3 (kHz)		-62(6)		-25(12)
ζ_4 (kHz)		0(2)		

a) The values of B_Π and D_Π were taken from Table 5.

108

given in Table 3. For the J = 11/2 state only one transition is
reported, because only this transition could be seen as a single
line. Calculations showed, that for the J = 11/2 state a number of
transitions have accidentally almost the same frequencies.

The transition frequencies of Table 3 of SD were used in a
least squares fit to obtain the molecular constants. Only some of
the molecular constants could be obtained, because no transitions of
the $^2\Pi_{1/2}$ level were available. The results are given in Table 4.
The agreement (Table 3) between the calculated and experimental
frequencies is excellent.

4.5. The electric dipole moment.

The electric dipole moments of the four radicals were
determined from the Stark shifts of transitions in a given rota-
tional state. The results for OH and OD were discussed by Meerts
and Dymanus (1973b) in a previous communication. In the present
investigation we observed the Stark shifts of the transitions
originating in the J = 5/2 state of the $^2\Pi_{3/2}$ level both of SH and
SD. The values obtained for the electric dipole moments are given
in Table 7 together with the values for OH and OD obtained pre-
viously by Meerts and Dymanus (1973b).

4.6. The magnetic spectrum of the $^2\Pi_{1/2}$, J = 1/2 state of SH.

The splitting of the Λ-doubling transitions of SH in the
J = 1/2 state of the $^2\Pi_{1/2}$ level at 8.4 GHz was investigated in a

109

Table 5. Molecular constants of OH, OD, SH and SD accepted in the fit of the MBER spectra (in cm^{-1}).

Quantity	Molecule			
	OH[a]	OD[b]	SH[c]	SD[c]
A_Π			-376.9_6	-376.7_5
B_Π	18.515	9.868	9.461_1	4.900_3
D_Π	0.00187	0.00052	0.00048_0	0.00013_5

a) Dieke and Crosswhite (1962).

b) Dousmanis et al (1955).

c) Ramsay (1952).

SH $\Pi_{3/2}$
J = 3/2
F = 2→2
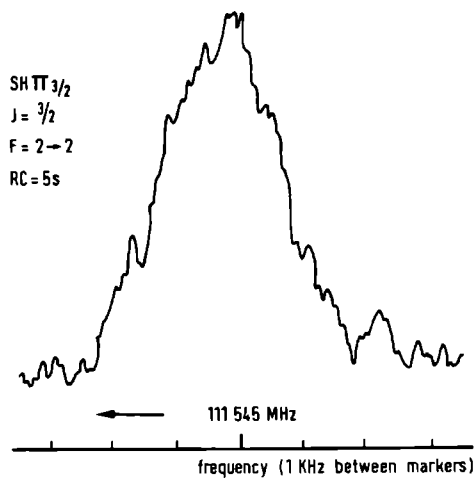RC = 5s

111 545 MHz

frequency (1 KHz between markers)

Fig. 8. Typical spectral line of SH.

weak external magnetic field. Although the primary object of the measurements was identification of the transitions some information about the magnetic properties of SH could be deduced from the observed splitting. A brief outline of the theory used for the interpretation of the splittings is given below.

The Zeeman Hamiltonian $\underline{H}_z$ of a diatomic molecule in a Π state in an external magnetic field is given by Carrington et al (1968)

$$[27] \quad \underline{H}_z = \mu_0 \, \underline{H} \cdot (\underline{L} + g\underline{S}) - g_N \, \mu_N \, \underline{H} \cdot \underline{I} - g_R \, \mu_0 \, \underline{H} \cdot (\underline{J} - \underline{L} - \underline{S})$$

The first and second term represents the electronic and nuclear Zeeman effect, respectively, while the last term describes the Zeeman effect of the rotating nuclei. For the rotational state $J = 1/2$ of the $^2\Pi_{1/2}$ level the paramagnetic contributions of the spin and orbital angular momentum almost cancel. At low (100 G) magnetic fields, $\underline{H}_z$ for this state can be treated as a first order perturbation of the hyperfine Λ-doublet levels. From the results of Carrington et al (1968) we obtain for the Zeeman energy:

$$
\begin{aligned}
[28] \quad <^2\Pi_{\frac{1}{2}}^{\pm} \, JIFM_F|\underline{H}_z|^2\Pi_{\frac{1}{2}}^{\pm} \, JIFM_F> &= (-1)^{F-M_F} \begin{pmatrix} F & 1 & F \\ -M_F & 0 & M_F \end{pmatrix}(2F+1) \; \times \\
&\times \left[\mu_0 H g_J^{\pm} \, (-1)^{J+I+F+1} \begin{Bmatrix} J & F & 1 \\ F & J & 1 \end{Bmatrix} [\,J(J+1)(2J+1)\,]^{\frac{1}{2}} + \right. \\
&\left. + \mu_N H g_N \, (-1)^{J+I+F} \begin{Bmatrix} I & F & J \\ F & I & 1 \end{Bmatrix} [\,I(I+1)(2I+1)\,]^{\frac{1}{2}} \right]
\end{aligned}
$$

111

In deriving Eq. [28] the interactions between the $^2\Pi_{3/2}$ and $^2\Pi_{1/2}$ states have been neglected. Consequently Eq. [28] is correct only for the lowest rotational state $J = 1/2$ for which this assumption is fully justified. The molecular g-factor $g_J^\pm$ is defined as

$$[29] \quad g_J^\pm = \frac{1}{2J(J+1)} \left\{ (1+g_R)<\Pi^\pm|T_0^{(1)}(\underline{L})|\Pi^\pm> - \tfrac{1}{2}(g+g_R) \right\} - g_R$$

The matrix element $<\Pi^\pm|T_0^{(1)}(\underline{L})|\Pi^\pm>$ can be obtained by a perturbation theory similar to that employed for the explanation of the Λ-splitting (Meerts and Dymanus 1972) and can be approximated by (Radford 1961)

$$[30] \quad <\Pi^\pm|T_0^{(1)}(\underline{L})|\Pi^\pm> = 1 \pm \Delta_1$$

where Δ_1 is a correction originating from the second and higher order interactions of the ground $^2\Pi$ state with the excited $^2\Sigma$ states. In this approximation the first term (1) is simply the first-order expectation value of $\underline{L}_z$ for a $^2\Pi$ state. The correction Δ_1 has the same origin as the Λ-splitting, breaking of the symmetry of the electronic charge distribution around the molecular axis by the rotation of the nuclear frame. This effect results in a different g_J-factor for the states with + and - symmetry. From the observed splittings of the transitions of SH at 8.4 GHz in a magnetic field of 100 G, we obtained: $\Delta_1 = -0.014(2)$ and $g_R = 6(2) \times 10^{-4}$ assuming $g = 2.00232$ and $g_N = 5.5856$, the g-factor of the electron and the proton, respectively. From Eq. [29] and [30] it follows

$$[31] \qquad g_J^+ - g_J^- = \frac{1 + g_R}{J(J+1)} \, \Delta_1$$

The g-factor of a diatomic molecule in a $^2\Pi$ state has been discussed by Radford (1961). Using his results the following expression is derived for $g_J^+ - g_J^-$:

$$[32] \qquad g_J^+ - g_J^- = \frac{\langle \Pi | L_y | \Sigma \rangle}{J(J+1)} \, \frac{4\theta}{E},$$

where E is the energy difference between the first excited $^2\Sigma$ state and the ground $^2\Pi$ state and $\theta = \langle \Pi | AL_y + 2BL_y | \Sigma \rangle$. This expression is correct only for the J = 1/2 state of the $^2\Pi_{1/2}$ level. The quantity θ/E can be expressed in the constants describing the Λ-splitting if only one excited $^2\Sigma$ state is assumed:

$$[33] \qquad \frac{\theta}{E} = - \frac{\alpha_3}{\sqrt{|\alpha_7 E|}}$$

With the results collected in Table 4 we obtain for SH: θ/E = -5.8×10^{-3}. With the derived values for Δ_1 and θ/E, we calculated the electronic matrix element $\langle \Pi | L_y | \Sigma \rangle$ using Eq. [31] and [32]. The result is $\langle \Pi | L_y | \Sigma \rangle = 0.60(8)$ for SH. In spite of the rather crude approximation performed in Eq. [32] and [33] this value compares well with that of OH found by Radford (1961) $\langle \Pi | L_y | \Sigma \rangle = 0.68(1)$, and the theoretical value of $\frac{1}{2}\sqrt{2}$ calculated from the pure precession approximation (Dousmanis et al 1955).

5. Discussion.

The analysis of the hyperfine Λ-doubling spectra yielded both the fine structure constants and the hyperfine coupling constants for all investigated molecules. From the least squares fit of the spectra of OH and OD a value for the ratio A_Π/B_Π ($= \lambda$) could be deduced, assuming fixed values for B_Π and D_Π (Table 5). An independent value for A_Π can only be obtained from transitions between $^2\Pi_{1/2}$ and $^2\Pi_{3/2}$ levels. The value of $|\lambda|$ for OH and OD is rather small, indicating a strong mixing between the $^2\Pi_{1/2}$ and $^2\Pi_{3/2}$ levels. This makes it possible to obtain a value for λ directly from the Λ-doubling spectra. In SH and SD the coupling between $^2\Pi_{1/2}$ and $^2\Pi_{3/2}$ is much weaker, and the value of A_Π had to be taken from other sources. The values of A_Π obtained in the present investigation for OH and OD, -139.38 cm^{-1} and -139.22 cm^{-1}, respectively, both in the ground vibrational state, lend strong support for the reliability of the applied theory. The present value of λ for OH is $-7.528(2)$; other reported values are: -7.547 (Dieke and Crosswhite 1962), $-7.444(17)$ (Dousmanis et al 1955), $-7.504(3)$ (Radford 1962) and -7.5086 (Mizushima 1972). For OD we found $\lambda = -14.108(4)$ while other investigators reported the values $-13.954(32)$ (Dousmanis et al 1955) and $-14.08(1)$ (Radford 1961). When comparing these values it should be noted that in all cases λ is obtained as a parameter, which describes the mixing between the $^2\Pi_{1/2}$ and $^2\Pi_{3/2}$ levels. The fact that this mixing is very strong in OH and OD makes it possible to determine λ, but the errors in the constants B_Π and D_Π affect strongly the value of λ. Especially the centrifugal dis-

di tortion has a significant effect on λ: a variation of +10 % in D_Π in OH results in a shift of +0.08 cm^{-1} in A_Π as obtained in the least squares fit of the spectrum.

A comparison between the α_3 and α_7 which describe the Λ-sp'itting and the values obtained by other investigators is not simple, because third order effects are absorbed in the parameters used in the present theory. A neglect of the third order contributions yields relations [19] and [20]. The result for the Λ-doubling constant obtained by various investigators for OH and OD are collected in Table 6. As can be seen from this table the present Λ-splitting constants deviate from those of Dousmanis et al (1955). Th deviation can partly be explained by the poor accuracy of the experimental results of Dousmanis et al (1955) which deviate for all transitions from the much more accurate present results. The deviations with the results of Mizushima (1972) for OH can be explained by the slight difference in the third order fine structure contributions to α_3 and α_7.

It is of interest to compare the experimentally determined Λ-splitting parameters α_3 and α_7 in the different isotopic species. If third order effects are neglected α_3 and α_7 can be written as (Meerts and Dymanus 1972)

$$[34] \quad \alpha_3 = \sum_i (-1)^s \frac{<^2\Sigma(i)||B\underline{L}_-||X^2\Pi><^2\Sigma(i)||(B+\tfrac{1}{2}A)\underline{L}_-||X^2\Pi>}{E_\Pi - E_{\Sigma}s}$$

$$[35] \quad \alpha_7 = \sum_i (-1)^s \frac{|<^2\Sigma(i)||B\underline{L}_-||X^2\Pi>|^2}{E_\Pi - E_{\Sigma}s}$$

Table 6. The Λ-doubling parameters for OH, OD, SH and SD as obtained from various investigations. (All values are in MHz.)

Quantity	Present investigation	Dousmanis et al. (1955)	Mizushima (1972)	Ramsay (1952)
α_3(OH)	1184.407	1180.7(1.5)	1183.128	
α_7(OH)	−582.61	−576.2(1.7)	−582.89	
α_3(OD)	776.588	774.5(1.1)		
α_7(OD)	−164.69	−161.9(1.7)		
α_3(SH)	2108.0			2100(50)[a]
α_7(SH)	−141.9			−180(40)
α_3(SD)	1127.3[b]			1150(50)
α_7(SD)	−38.07[b]			−50(40)

a) Estimated assuming uncertainties of 0.001 to 0.002 cm^{-1} in the constants p_0 and q_0 obtained by Ramsay (1952).

b) Obtained from the results for SH by isotopic substitution, see text.

116

where the sums are taken over all excited $^2\Sigma^s$ states; $s = \pm$ with $(-1)^s = 1$ for $s = +$, and $(-1)^s = -1$ for $s = -$. In the approximation that the reduced matrix elements in the above equations can be written as a product of the rotational constant B_Π and the matrix element $<^2\Sigma(i)||L_-||X^2\Pi>$, and that $<^2\Sigma(i)||AL_-||X^2\Pi>$ is the same for the two isotopes, $\alpha_3 - \alpha_7$ is proportional to B_Π whereas α_7 is proportional to B_Π^2. This is a part of the pure precession approximation (Dousmanis et al 1955). The experimental value for

$$[36] \quad R_1 \text{ (OH/OD)} = \frac{(\alpha_3 - \alpha_7)_{OH}}{(\alpha_3 - \alpha_7)_{OD}}$$

is 1.877 and the value for

$$[37] \quad R_2 \text{ (OH/OD)} = \sqrt{\frac{(\alpha_7)_{OH}}{(\alpha_7)_{OD}}}$$

is 1.881, while $(B_\Pi)_{OH}/(B_\Pi)_{OD} = 1.876$. It may be concluded from these values that the pure precession approximation allows a good prediction of the Λ-splitting parameters α_3 and α_7 from isotopic substitution in OH and OD. The relations [36] and [37] between R_1(SH/SD) and R_2(SH/SD) and the ratio between the B_Π values of isotopic species was applied to SH and SD in order to derive the values of α_3 and α_7 for SD from those of SH (Table 4). The value for $(B_\Pi)_{SH}/(B_\Pi)_{SD}$ is 1.931. Assuming that R_1(SH/SD) and R_2(SH/SD) are both equal to 1.931, the results for α_3 and α_7 of SD are: $(\alpha_3)_{SD} = 1127.3(3.0)$ MHz and $(\alpha_7)_{SD} = -38.07(20)$MHz. The errors are based on the estimated errors in R_1(SH/SD) and R_2(SH/SD). The values of α_3 and α_7 for SH and SD obtained in this way (Table 6)

agree quite well with the Λ-splitting parameters of Ramsay (1952).

If the third order effects are neglected we can deduce values for the hyperfine constants used in the low-order theories, using the values of Table 4 and the Eqs. [13] through [18]. The results are given in Table 7. In this work all the hyperfine constants have been obtained needed to describe the structure of the investigated transitions of OH, OD, SH and SD. Only for OH have these constants been obtained previously by Radford (1962) whose results are in agreement with the present more accurate values. The hyperfine constants $a + \frac{1}{2}$ (b + c), b and d of SH were deduced by Tanimoto and Uehara (1973) from EPR spectra, and their values agree with values obtained in this work. The electric quadrupole coupling constants for OD and SD were obtained in the present work for the first time. The ratios between the magnetic hyperfine structure constants of OH and OD and between those of SH and SD should be equal to the ratio of the nuclear g-factors of proton and deuteron. Small deviations are observed, which reflect probably the neglect of third and may be of even higher order effects in the present derivation of the constants a, b, c and d.

The hyperfine structure in radicals OH and SH is mainly determined by the unpaired π-electron. The fact that the hyperfine constants of OH are larger than those of SH may partly be explained by the larger average separation of the unpaired electron from the interacting hydrogen nucleus in SH.

The magnetic hyperfine constants a, b, c and d are related to expectation values of electronic operators:

Table 7. Values of the conventional constants for OH, OD, SH and SD as obtained in the present work.

Quantity	Molecule			
	OH	OD	SH	SD
a (MHz)	86.01(2)	13.296(3)	32.58(7)	$5.03(3)^{a)}$
b (MHz)	−118.08(8)	−18.07(2)	−63.44(4)	−9.65(3)
c (MHz)	132.12(9)	20.35(3)	32.44(14)	$4.95(4)^{a)}$
d (MHz)	56.62(2)	8.768(2)	27.36(12)	4.20(2)
eQq_1 (kHz)		$285(5)^{b)}$		149(4)
eQq_2 (kHz)		−124(12)		−50(24)
μ (D)	$1.6676(9)^{c)}$	$1.65312(14)^{c)}$	0.7580(1)	0.7571(1)
$g_J^+ - g_J^-$ (μ_0)			$-0.019(3)^{d)}$	
g_R (μ_0)			$6(2) \times 10^{-4}$	
$\langle \Pi | L_y | \Sigma \rangle$			0.60(8)	

a) Obtained from the results of SH from the ratio of the nuclear g-factors.

b) The value as given by Meerts and Dymanus (1973a) has to be multiplied by two.

c) Meerts and Dymanus (1973b)

d) Of the J = 1/2 state of $^2\Pi_{1/2}$

$$[38] \quad a = g g_I \mu_0 \mu_N \int \frac{1}{r_{1I}^3} D_L(\Lambda,\Lambda|\vec{r}_{1I}) d\vec{r}_{1I} = g g_I \mu_0 \mu_N <1/r^3>_U,$$

$$[39] \quad b = -\tfrac{1}{2} g g_I \mu_0 \mu_N \int \frac{3\cos^2\theta_{1I} - 1}{r_{1I}^3} D_S(\Sigma,\Sigma|\vec{r}_{1I}) d\vec{r}_{1I} +$$

$$+ \tfrac{8}{3} \pi \, g g_I \mu_0 \mu_N D_S(\Sigma,\Sigma|0) =$$

$$= -\tfrac{1}{2} g g_I \mu_0 \mu_N <(3\cos^2\theta - 1)/r^3>_U + \tfrac{8}{3} \pi \, g g_I \mu_0 \mu_N <\psi^2(0)>_U,$$

$$[40] \quad c = \tfrac{3}{2} g g_I \mu_0 \mu_N \int \frac{3\cos^2\theta_{1I} - 1}{r_{1I}^3} D_S(\Sigma,\Sigma|\vec{r}_{1I}) d\vec{r}_{1I} =$$

$$= \tfrac{3}{2} g g_I \mu_0 \mu_N <(3\cos^2\theta - 1)/r^3>_U,$$

$$[41] \quad d = \tfrac{3}{2} g g_I \mu_0 \mu_N \int \frac{\sin^2\theta_{1I}}{r_{1I}^3} e^{-2i\phi_{1I}} D_S(\Sigma,-\Sigma|\vec{r}_{1I}) d\vec{r}_{1I} =$$

$$= \tfrac{3}{2} g g_I \mu_0 \mu_N <\sin^2\theta/r^3>_U.$$

In these expressions $D_S(\Sigma,\Sigma'|\vec{r}_{1I})$ is the normalized spin density function of McWeeny (1960; 1965) and $D_L(\Lambda,\Lambda|\vec{r}_{1I})$ is its orbital analog with $\Lambda = 1$ and $\Sigma = \tfrac{1}{2}$, $\Sigma' = \Sigma$ or $-\Sigma$; the average values are the differences between the average values for the part of the electron density with spin "up" (α) and the part with the spin "down" (β). In the "spectroscopic approximation" it is assumed that the integrals in Eq. [38] through [41] are well approximated by averages only over the unpaired electron density as indicated by U. This approximation is only valid when the paired electrons have the same spatial density for the α and β spins. The electronic expectation values $<1/r^3>_U$, $<(3\cos^2\theta - 1)/r^3>_U$, $<\sin^2\theta/r^3>_U$ and $<\psi^2(0)>_U$

120

have been calculated from the present experimental magnetic hyper-
fine constants for all four molecules. The results for OH and OD are
almost equal as can be expected from the fact that the replacement
of hydrogen by deuterium in OH only slightly disturbs the electronic
distribution in the molecule. Consequently the corresponding results
for OH and OD were averaged. The indicated errors cover the values
obtained for OH as well as for OD. The same procedure was applied to
SH and SD and the results are given in Table 8.

Valuable information about the character of interactions and
about the electronic charge distribution in the molecule can be ob-
tained from the quantities $<1/r^3>_U$, $<(3 \cos^2\theta - 1)/r^3>_U$, $<\sin^2\theta/r^3>_U$
and $<\psi^2(0)>_U$. In an ab-initio molecular orbital calculation of OH
and SH the Fermi contact term can be used as a test of the quality
of the applied configuration interaction (CI). In a single configura-
tion MO-approximation the electronic configuration of OH is
$(1\sigma)^2(2\sigma)^2(3\sigma)^2(1\pi^+)^2(1\pi^-)$ and of SH
$(1\sigma)^2(2\sigma)^2(3\sigma)^2(1\pi)^4(4\sigma)^2(5\sigma)^2(2\pi^+)^2(2\pi^-)$. In the restricted
Hartree-Fock approximation the π^- orbital function vanishes on the
intermolecular axis and $<\psi^2(0)>_U = 0$. In the unrestricted Hartree-
Fock (UHF) theory each doubly occupied spatial orbital function
splits into two orbitals by the exchange polarization. The presence
of the π^- orbital has a different effect on the density of the α
and β core electrons. In the UHF-theory $<\psi^2(0)>_U$ no longer vanishes
due to polarization of the σ orbitals. Kayama (1963) used the UHF
approximation to show that $<\psi^2(0)>_U$ should be negative for OH. He
also performed an ab-initio MO-CI calculation using nine excited
configurations. The result of this calculation is shown in Table 8.

Table 8. Experimental and calculated molecular constants of OH (OD) and SH (SD) (in units of 10^{24} cm^{-3})

		$\langle 1/r^3\rangle_U$	$\langle(3\cos^2\theta - 1)/r^3\rangle_U$	$\langle\sin^2\theta/r^3\rangle_U$	$\langle\psi^2(0)\rangle_U$	$\langle(3\cos^2\theta -1)/r^3\rangle_T$	$\langle\sin^2\theta/r^3\rangle_T$
OH	Obsd	1.093(4)	1.117(2)	0.480(2)	−0.1115(5)		
	Calcd[a]	1.015	1.037	0.331	−0.103		
	Calcd[b]	1.064	1.165		−0.111[f]		
	Calcd[c]	1.014	1.018		−0.094[f]		
	Calcd[d]				−0.128		
	Calcd[e]				−0.115		
OD	Obsd					14.18(5)	0.43(5)
SH	Obsd	0.413(1)	0.274(1)	0.231(1)	−0.0795(5)		
	Calcd[b]	0.379	0.276		−0.035[f]		
	Calcd[c]	0.306	0.098		−0.009[f]		
	Calcd[d]				−0.047		
	Calcd[e]				−0.054		
SD	Obsd					11.53(5)	0.17(8)

a) Kayama (1963). b) Kotake et al (1971) for Slater type orbitals. c) Kotake et al (1971) for analytical Hartree Fock Orbitals. d) Bendazzoli et al (1972)UHF approximation. e) Bendazzoli et al (1972) RHF + CI.
f) Derived from the calculated values for $\langle 1/r^3\rangle_U$ and $\langle(3\cos^2\theta -1)/r^3\rangle_U$ and the experimental hyperfine constants.

Bendazzoli et al (1972) calculated $<\psi^2(0)>_U$ for OH and SH (1) with the UHF wavefunctions and (2) with CI-wavefunctions, denoted as RHF+CI since the one-electron functions used were molecular orbitals obtained in a restricted Hartree-Fock approximation. The results for $<\psi^2(0)>_U$ obtained by Bendazzoli et al with a set of contracted gaussian orbitals as basis set are reproduced in Table 8. The calculated values for $<\psi^2(0)>_U$ of Kayama (1963) and of Bendazzoli et al (1972) agree quite well with the experimental value.

Contrary to $<\psi^2(0)>_U$ the quantities $<1/r^3>_U$, $<(3\cos^2\theta - 1)/r^3>_U$ and $<\sin^2\theta/r^3>_U$ do not vanish in a single configuration approximation. In this approximation it is readily seen that each of them is simply given by the average value over the unpaired π-orbital ($1\pi^-$ for OH and $2\pi^-$ for SH). In the LCAO-MO approximation the unpaired electron is usually assigned to the np_x or to the np_y atomic orbital, both perpendicular to the molecular axis, with n = 2 for OH and n = 3 for SH. In ab-initio LCAO-MO calculations these atomic orbitals usually are Slater orbitals or analytical Hartree-Fock (AHF) orbitals, the latter consisting of a linear combination of Slater-type orbitals. The quantities $<1/r^3>_U$ and $<(3\cos^2\theta - 1)/r^3>_U$ were calculated for OH in the single-configuration approximation by Kayama (1963) using AHF orbitals, and by Kotake et al (1971) for OH and SH with Slater orbitals and with AHF orbitals. The authors used different AHF orbitals as basis in their calculations on OH. The results are summarized in Table 8. It is seen from this Table that the agreement between the experimental and calculated values for OH is quite good and that for SH the best results are obtained for Slater orbitals. The value

for $<(3 \cos^2\theta - 1)/r^3>_U$ for SH calculated with AHF orbitals differs markedly from the experimental value.

Tanimoto and Uehara (1973) observed the EPR spectra of SH in the $^2\Pi_{3/2}$, $J = 3/2$ and $5/2$ states, but were unable to deduce all the hyperfine constants independently from the experimental results. To solve this problem Tanimoto and Uehara used the approximation

[42] $<\sin^2\theta/r^3>_U$: $<(3 \cos^2\theta -1)/r^3>_U$: $<1/r^3>_U = \frac{4}{5}$: $-\frac{2}{5}$: 1

which is derived assuming that the unpaired electron occupies a 2p (in OH) or 3p (in SH) atomic orbital of oxygen or sulphur, respectively. However, the interacting nuclear spin is on the hydrogen atom, and this approximation fails completely; it predicts even the wrong sign for $<(3 \cos^2\theta - 1)/r^3>_U$.

The electric quadrupole coupling constants of OD and SD provide also information about the electronic charge distribution in the molecules. The coupling constants eQq_1 and eQq_2 can be expressed in the nuclear quadrupole moment Q and average values of $(3 \cos^2\theta -1)/r^3$ and $\sin^2\theta/r^3$:

[43] $q_1 = \dfrac{2Z_K}{R_{IK}} - \displaystyle\int \dfrac{3 \cos^2\theta_{1I} - 1}{r_{1I}^3} P_L(\Lambda,\Lambda|\vec{r}_{1I})d\vec{r}_{1I} =$

$$= \dfrac{2Z_K}{R_{IK}} - <(3 \cos^2\theta - 1)/r^3>_T,$$

[44] $q_2 = -3 \displaystyle\int \dfrac{\sin^2\theta_{1I}}{r_{1I}^3} e^{2i\phi_{1I}} P_L(\Lambda, -\Lambda|\vec{r}_{1I})d\vec{r}_{1I} = -3 <\sin^2\theta/r^3>_T,$

124

where $P_L(\Lambda,\Lambda'|\vec{r}_{1I})$ is the normalized electron density function of McWeeny (1969; 1965) with $\Lambda = 1$, and K stands for oxygen or sulphur for OD or SD, respectively. The averages of $(3\cos^2\theta - 1)/r^3$ and $\sin^2\theta/r^3$ marked with "T" are over all electrons and are different from the average values in Eq. [38] through [41].

The quantities q_1 and q_2 are proportional to the component along and perpendicular to the bond axis, respectively, of the gradient of the electric field produced at the deuteron nucleus by the electronic charge distribution and by the other nucleus (K). The average value q_1 is well known for molecules in a $^1\Sigma$ state, while q_2 is only observable in molecules with $|\Lambda| = 1$.

The nuclear part in Eq. [43] can easily be calculated from the known molecular geometries and the results are 17.17×10^{24} cm^{-3} and 13.09×10^{24} cm^{-3} for OD and SD, respectively. The electronic parts of q_1 and q_2 were obtained from the experimental quadrupole coupling constants of Table 7 and the value $Q = 0.002738 \times 10^{-24}$ cm^2 for the nuclear quadrupole moment of the deuteron (Ramsey 1956). The results are given in Table 8.

The average quantities $<(3\cos^2\theta - 1)/r^3>_T$ and $<\sin^2\theta/r^3>_T$ can only be determined for OD and SD. However, these quantities depend only on electronic distribution. Within the Born-Oppenheimer approximation assumed in the present theory, the charge distribution is the same in OD and OH. Consequently $<(3\cos^2\theta - 1)/r^3>_T$ and $<\sin^2\theta/r^3>_T$ should be the same for these molecules. The same arguments and conclusions apply also for SH and SD.

Unfortunately, no molecular orbital calculations are available of $<(3\cos^2\theta - 1)/r^3>_T$ and $<\sin^2\theta/r^3>_T$ for OH (OD) or SH (SD).

The values obtained in the present investigations may serve as a test for future calculations of the contributions of electrons occupying orbitals other than the unpaired π-orbital.

It is interesting to note that $\langle \sin^2\theta/r^3 \rangle_U$ and $\langle \sin^2\theta/r^3 \rangle_T$ are almost equal for both OH and SH. This can be understood by considering the contributions to $\langle \sin^2\theta/r^3 \rangle_U$ and to $\langle \sin^2\theta/r^3 \rangle_T$ as sums of one-electron contributions with each electron occupying a definite orbital. Electrons occupying σ-orbitals do not contribute because intergration over the azimutal angle ϕ yields zero. So contributions of electrons occupying a π-orbital remain. Electrons which can occupy an α state as well as a β state contribute to $\langle \sin^2\theta/r^3 \rangle_U$ because $D_S(\Sigma,-\Sigma|\vec{r}_{1I})$ connects electron states with different spin values. Consequently only an electron occupying an unpaired π-orbital contributes to $\langle \sin^2\theta/r^3 \rangle_U$. In the ground electronic states of OH and SH one π-orbital is singly occupied ($1\pi^-$ for OH and $2\pi^-$ for SH). So $\langle \sin^2\theta/r^3 \rangle_U$ contains effectively the contribution of one electron. The situation is quite similar for $\langle \sin^2\theta/r^3 \rangle_T$. If we assume that the azimutal dependence of a π^+-orbital is $(e^{i\phi} + e^{-i\phi})$ and of a π^--orbital $(e^{i\phi} - e^{-i\phi})$, then it is readily seen that the contributions to $\langle \sin^2\theta/r^3 \rangle_T$ of an electron in a $n\pi^+$-orbital cancels the contribution of an electron in a $n\pi^-$-orbital. So effectively only one electron contributes to $\langle \sin^2\theta/r^3 \rangle_T$ for OH $1\pi^-$ as well as for SH $2\pi^-$.

The observed isotopic effects in the dipole moments of OH and OD, and SH and SD are 8×10^{-3} and 1.5×10^{-3}, respectively. The order of magnitude agrees with the expectations, but the isotopic effect for SH and SD is smaller than expected from the effect

126

for OH and OD. Quantitative discussions have to await ab-initio calculation of the dipole moment function or accurate measurements of the dipole moment in higher vibrational states.

Results from previous measurements of the dipole moments of OH and OD have been already extensively discussed by Meerts and Dymanus (1973b). The dipole moment of SH has been determined by Byfleet et al (1971) using the gas-phase EPR with an external electric field. The result $\mu_{SH} = 0.62(1)$ D disagrees with the present more accurate value. In our opinion the origin of the discrepancy lies in the erroneous calibration of the electric field strength by Byfleet et al. This is supported by the fact that the value of the electric dipole moment of BrO obtained by Byfleet et al (1971) $\mu = 1.61(4)$ D, also deviates from recent value of Amano et al (1972)(1.765(23) D for ^{79}BrO and 1.794(49) D for ^{81}BrO).

The values for the electric dipole moments obtained by Cade and Huo (1966) from ab-initio calculations ($\mu = 1.780$ D for OH and $\mu = 0.861$ D for SH)are in a quite good agreement with the experimental values. The calculated values, however, are 7 and 13 % higher than the experimental values for OH and SH, respectively.

6. Conclusions.

The molecular beam electric resonance spectroscopy has proved to be a powerful technique in the investigation of spectra and properties of the free radicals OH, OD, SH, and SD via their Λ-doubling transitions. The radicals are produced quite efficiently to obtain signal to noise ratios of the order of 100 for the transi-

tions of OH and 20 for SH, respectively, at RC = 5 s.

The spectrum calculated using the third order degenerate perturbation theory gives a very good agreement with the experimental results for OD, SH, and SD. However, for SD no transitions in the $^2\Pi_{1/2}$ level could be observed and for SH transitions only in the J = 1/2 of the $^2\Pi_{1/2}$ level. Consequently the test of the theory is not complete for these molecules. For OH and OD we have measured transitions in a number of rotational states of both the $^2\Pi_{1/2}$ and the $^2\Pi_{3/2}$ level. The agreement for OD is excellent, but for OH the differences between the calculated and observed transitions are larger than the experimental errors. A similar situation was found previously in the analysis of the hyperfine Λ-doubling spectrum of ^{14}NO and ^{15}NO (Meerts and Dymanus 1972). The conclusions, based on the fact that the investigated molecules cover a large scale of different values of Λ-splitting, is that the disagreement cannot be eliminated by taking into account higher order contributions in fine structure. The OH and OD radicals can be described by a representation intermediate between the Hund's case (a) and (b) and the molecules SH, SD, ^{14}NO and ^{15}NO can be approximated by almost a pure Hund's case (a). The nature and the relative strength of the interactions responsible for the type of coupling apparently does not offer an explanation of the observed discrepancies between the experiment and the theory for ^{14}NO, ^{15}NO and OH. The only significant difference between the group ^{14}NO, ^{15}NO, OH and the group OD, SH, SD is the magnitude of the hyperfine contributions, which are about an order of magnitude larger for the first group than for the second. It is possible that taking into account of the fourth

128

or even higher order contributions due to hyperfine structure may lift the observed differences between calculated and experimental spectra in OH, ^{14}NO and ^{15}NO. However, this approach puts a heavy load both on the calculation of high order contributions and on the experiment to measure a sufficient number of transitions for the fit with increasing number of coupling constants. A possible solution of the problem is to replace the zero-order Hamiltonian [4] by an effective Hamiltonian which incorporates some of the lower-order contributions.

From the present investigations the fine and hyperfine structure constants of OH, OD, SH and SD were obtained. The relations between the fine structure parameters obtained by isotopic substitution of deuterium in OH could well be tested as well as their usefulness in deducing unknown molecular constants. The relevant relations (Eq. [36] and [37]) are actually based on the pure precession approximation (Dousmanis et al 1955). By applying this approximation the Λ-splitting parameters of SD could be obtained from the isotopic substitution of deuterium in SH. The hyperfine structure constants obtained from the experiment show a gratifying agreement with the ab-initio calculations.

Acknowledgement

References.

Almy, G.M. and Horsfall, R.B. 1973. Phys.Rev. 51, 491.

Amano, T., Yoshinaga, A. and Hirota, E. 1972. J.Mol.Spectrosc. 44, 594.

Ball, J.A., Dickinson, D.F., Gottlieb, C.A. and Radford, H.E. 1970. Astron.J. 75, 762.

Ball, J.A., Gottlieb, C.A., Meeks, M.L. and Radford, H.E. 1971. Astrophys.J. 163, L33.

Bendazzoli, G.L., Bernardi, F. and Palmieri, P. 1972. Mol.Phys. 23, 193.

Brown, J.M. and Thistlethwaite, P.J. 1972. Mol.Phys. 23, 635.

Byfleet, C.R., Carrington, A. and Russell, D.K. 1971. Mol.Phys. 20, 271.

Cade, P.E. and Huo, W.M. 1966. J.Chem.Phys. 45, 1063.

Carrington, A., Howard, B.J., Levy, D.H. and Robertson, J.C. 1968. Mol.Phys. 15, 187.

Clyne, M.A.A., Coxon, J.A. and Woon Fat, A.R. 1973. J.Mol. Spectrosc. 46, 146.

Del Greco, F.P. and Kaufman, F. 1962. Discussions Faraday Soc. 33, 128.

Destombes, J., Marlière, C., Rohart, F. and Burie, J. 1974. C.R.Hebd.Seances Acad.Sci.B, 278, 275.

Dieke, G.H. and Crosswhite, H.M. 1962. J.Quant.Spectrosc. Radiative Transfer 2, 97.

Dousmanis, G.C., Sanders Jr., T.M. and Townes, C.H. 1955. Phys.Rev. 100, 1735.

130

Freed, K.F. 1966. J.Chem.Phys. $\underline{45}$, 4214.

Heiles, C.E. and Turner, B.E. 1971. Astrophys.Letters $\underline{8}$, 89.

Kayama, K. 1963. J.Chem.Phys. $\underline{39}$, 1507.

Kotake, Y., Ono, M. and Kuwata, K. 1971. Bull.Chem.Soc.Japan
$\underline{44}$, 2056.

Leeuw, F.H. de. 1971. Ph.D. Thesis, Katholieke Universiteit,
Nijmegen, The Netherlands.

Leeuw, F.H. de and Dymanus, A. 1973. J.Mol.Spectrosc. $\underline{48}$, 427.

Lin, C.C. and Mizushima, M. 1955. Phys.Rev. $\underline{100}$, 1726.

McDonald, C.C. 1963. J.Chem.Phys. $\underline{39}$, 2587.

McWeeny, R. 1960. Rev.Mod.Phys. $\underline{32}$, 335.

McWeeny, R. 1965. J.Chem.Phys. $\underline{42}$, 1717.

Meeks, M.L., Gordon, M.A. and Litvak, M.M. 1969. Science $\underline{163}$, 173.

Meerts, W.L. and Dymanus, A. 1972. J.Mol.Spectrosc. $\underline{44}$, 320.

Meerts, W.L. and Dymanus, A. 1973a. Astrophys.J. $\underline{180}$, L93.

Meerts, W.L. and Dymanus, A. 1973b. Chem.Phys.Letters $\underline{23}$, 45.

Meerts, W.L. and Dymanus, A. 1974. Astrophys.J. $\underline{187}$, L45.

Meerts, W.L. 1974. Quarterly Report No. 45, Atomic and Molecular
Research Group, Katholieke Universiteit, Nijmegen, The Netherlands.

Meulen, J.J. ter. 1970. Quarterly Report No. 28, Atomic and
Molecular Research Group, Katholieke Universiteit, Nijmegen,
The Netherlands.

Meulen, J.J. ter and Dymanus, A. 1972. Astrophys.J. $\underline{172}$, L21.

Mizushima, M. 1972. Phys.Rev.A, $\underline{5}$, 143.

Mulliken, R.S. and Christy, A. 1931. Phys.Rev. $\underline{38}$, 87.

Poynter, R.L. and Beaudet, R.A. 1968. Phys.Rev.Letters, $\underline{21}$, 305.

Radford, H.E. 1961. Phys.Rev. $\underline{122}$, 114.

Radford, H.E. 1962. Phys.Rev. 126, 1035.

Radford, H.E. 1968. Rev.Sci.Instrum. 39, 1687.

Radford, H.E. and Linzer, M. 1963. Phys.Rev.Letters 10, 443.

Ramsay, D.A. 1952. J.Chem.Phys. 20, 1920.

Ramsey, N.F. 1956. Molecular Beams (Oxford University Press,

New York), p.172.

Stolte, S. 1972. Ph.D. Thesis, Katholieke Universiteit, Nijmegen,

The Netherlands.

Tanimoto, M. and Uehara, H. 1973. Mol.Phys. 25, 1193.

Taylor, B.N., Parker, W.H. and Langenberg, D.N. 1969. Rev.Mod.

Phys. 41, 375.

Van Vleck, J.H. 1929. Phys.Rev. 33, 467.

In dit proefschrift worden een aantal twee atomige molekulen met een open schil konfiguratie (OSK) onderzocht. Deze OSK is een gevolg van het feit dat deze molekulen of een netto elektron spin of een netto baan impuls moment hebben, of beide. Van de onderzochte molekulen ^{14}NO, ^{15}NO, OH, OD, SH, SD en SF is de elektronische grondtoestand een $^2\Pi$ toestand, terwijl de grondtoestand van CN een $^2\Sigma$ toestand is.

Deze molekulen, meestal vrije radikalen genoemd, zijn onderzocht met de molekulaire bundel elektrische resonantie (MBER) techniek. Deze methode bleek zeer geschikt voor het verkrijgen van de spectra en het bepalen van een aantal eigenschappen van deze radikalen. Aangezien deze molekulen, behalve NO, allen zeer kort levend zijn en snel rekombineren, was een speciale experimentele techniek vereist. De niet stabiele radikalen werden kontinu geproduceerd, meestal in een reaktie tussen een atoom en een tweede gas. OH en SH werden gevormd in een reaktie tussen atomair waterstof en NO_2 respektievelijk H_2S, en SF in een reaktie tussen atomair fluor en OCS. Er is geprobeerd CN te vormen in een reaktie tussen atomair stikstof en CH_2Cl_2 en door middel van dissociatie van C_2N_2. Atomair waterstof, stikstof en fluor werden verkregen uit een microgolf ontlading in respektievelijk H_2O of H_2, N_2 en CF_4. De toegepaste bron voor deze reaktie processen wordt beschreven en een schatting van het aantal geproduceerde OH, SH, SF en CN radikalen is gegeven. De vorming van een voldoende sterke bundel van CN radikalen is niet gelukt.

De frequenties van de toegestane $\Delta J = 0$ hyperfijn overgangen in veld nul zijn gemeten van ^{14}NO, ^{15}NO, OH, OD, SH, en SD in een aantal van de laagste rotatie toestanden. Uit metingen in elektrisch veld werd de waarde van het elektrisch dipool moment van OH, OD, SH en SD bepaald. Bovendien leverde een meting van SH in de $^2\Pi_{1/2}$, $J = \frac{1}{2}$ toestand in een magneetveld van 100 G de g faktoren van het onderste en bovenste Λ-niveau op. De signaal ruis verhouding van de MBER overgangen van SF bleek te klein te zijn om het spektrum van dit molekuul te kunnen analiseren.

Van Vleck (1929) introduceerde een theorie die een beschrij-

ving geeft van de Λ-splitsing in molekulen met een $^2\Pi$ toestand. Door
Frosh en Foley (1952) werd deze theorie uitgebreid met hyperfijn-
struktuur effecten in deze molekulen. Echter beide theorieën waren
slechts tot op eerste orde ontwikkeld.

De met de MBER techniek verkregen spektra van NO, OH (OD),
SH (SD) konden niet binnen de experimentele nauwkeurigheid (0.1 tot
5 kHz) verklaard worden met deze tot eerste orde ontwikkelde theo-
rie. De verschillen tussen het gemeten en berekende spektrum waren
200 tot 500 kHz. Een betere overeenstemming tussen de experimenteel
waargenomen en theoretisch voorspelde spektra werd verkregen met
behulp van een berekening met een in dit proefschrift ontwikkelde
ontaarde storingsrekening, die het mogelijk maakt bijdragen tot de
energie tot in derde orde van de Λ-splitsing en de hyperfijn struk-
tuur mee te nemen. Deze hogere orde bijdragen vereistten de invoe-
ring van een aantal nieuwe molekulaire konstanten om een volledige
beschrijving van het hyperfijn Λ-splitsings spektrum van $^2\Pi$ mole-
kulen mogelijk te maken. De met deze ontaarde storingsrekening be-
rekende spektra van OD, SH en SD waren binnen de experimentele nauw-
keurigheid in overeenstemming met de gemeten spektra; voor OH en
NO was de overeenstemming minder goed (afwijkingen van 5 tot 30
kHz). Een mogelijke verklaring voor dit laatste is gezocht in
het feit dat juist in NO en OH de hyperfijn struktuur bijdragen
erg groot zijn (100 MHz), zodat in de berekeningen zelfs vierde
orde hyperfijn bijdragen meegenomen dienen te worden om de spektra
van OH en NO binnen de experimentele nauwkeurigheid van de MBER
methode te kunnen verklaren. Het berekenen van deze vierde orde
bijdragen is echter binnen het raam van de toegepaste storingsre-
kening een uiterst gekompliceerde zaak.

De experimenteel bepaalde magnetische en elektrische hyper-
fijn struktuur grootheden van de molekulen OH, OD, SH en SD zijn
gebruikt als test van ab-initio molekulaire orbital berekeningen.
Speciaal de zogenaamde Fermi kontakt term is een goede test van
de toegepaste konfiguratie interaktie in de molekulaire bereke-
ningen. De molekulaire eigenschappen verkregen met de voorhanden
zijnde ab-initio berekeningen zijn redelijk goed in overeenstem-
ming met de experimenteel verkregen waardes.

134

<u>Curriculum Vitae.</u>

De auteur van dit proefschrift werd geboren op 5 februari 1948 te 's Gravenhage. Na afloop van de lagere school bezocht hij van 1960 tot en met 1965 de gemeente HBS b te Nijmegen en legde in 1965 met goed gevolg zijn eindexamen af. In 1965 ging hij wis- en natuurkunde studeren aan de Katholieke Universiteit te Nijmegen en legde in februari 1968 zijn kandidaats examen af, gevolgd door het doktoraal examen in de Wiskunde en Natuurwetenschappen op 18-6-1970. In zijn afstudeerperiode is hij werkzaam geweest in de werkgroep Atoom- en Molekuulfysika. Na het behalen van zijn doktoraal examen werd hij als wetenschappelijk medewerker in deze werkgroep aangesteld en verrichtte onder leiding van Prof.Dr. A. Dymanus onderzoek aan spectra van twee atomige molekulen met een open schil konfiguratie. Deze studie wordt afgesloten met de verdediging van dit proefschrift.

STELLINGEN

I

De verhouding tussen eQq_1 en eQq_2 van een molekuul in een $^2\Pi$ toestand heeft geen direkt verband met het karakter van de binding in het molekuul zoals door Freund e.a. gesuggereerd wordt.

S.M. Freund, E. Herbst, R.P. Mariella Jr. en W. Klemperer, J.Chem. Phys. 56 (1972) 1467.

II

Het gelijk nul stellen van de molekulaire grootheid ρ in de analyse van de Δ-vibratie toestand van OCS door Fabricant en Muenter leidt tot inkorrekte waardes van de andere molekulaire grootheden.

B. Fabricant en J.S. Muenter, J.Mol.Spectrosc. 53 (1974) 57.

III

Uit didaktisch oogpunt verdient het aanbeveling om bij de berekening van thermodynamische grootheden van kristallen (bv. de soortelijke warmte) eerst de algemene toestandssom zonder specifikatie van de trillingsmodi uit te rekenen, en vervolgens de Einstein respektievelijk Debye benadering hierop toe te passen.

F. Mandl, Statistical Physics (1971).

IV

Het zou fundamenteel juister zijn om uit de spektra van komplexen van H_2 en edelgassen een lineaire kombinatie van de "long-" en de "short-range" anisotropie koëfficienten (a_6 en a_{12}) van de intermolekulaire potentiaal tussen H_2 en het edelgas te bepalen, inplaats van zowel a_6 als a_{12}.

R.J. Le Roy en J. Van Kranendonk, J.Chem.Phys. 61 (1974) 4750.

De benadering van het RRKM formalisme voor lang levende botsings-komplexen met een groot baan impulsmoment door Safron e.a. leidt tot een te lage translatie energie van de produkten.

S.A. Safron, N.D. Weinstein, D.R. Herschbach en J.C. Tully, Chem.Phys.Letters 12 (1972) 564.

VI

De benadering $<1/r^3>$: $<(3 \cos^2\theta -1)/r^3>$: $<\sin^2\theta/r^3>$ = 1 : -0.4 : 0.8 is niet geldig voor OH en SH.

Dit Proefschrift.

VII

Regionalisering van het voortgezet buitengewoon onderwijs is nood-zakelijk om de kwaliteit van dit onderwijs te waarborgen.

VIII

Tussen de verschillende verschijningsvormen van muziek, bijvoor-beeld popmuziek en klassieke muziek bestaat geen fundamenteel verschil.

15 mei 1975   W.L. Meerts.